I.O.S.

THE DISTRIBUTION OF GLACIAL ERRATICS IN THE NORTHEAST ATLANTIC: FINAL REPORT

BY
Q. HUGGETT

REPORT NO. 213
1985

OCEAN DISPOSAL OF HIGH LEVEL RADIOACTIVE WASTE
A RESEARCH REPORT PREPARED FOR THE DEPARTMENT OF THE ENVIRONMENT

NATURAL ENVIRONMENT RESEARCH COUNCIL

INSTITUTE OF OCEANOGRAPHIC SCIENCES

INSTITUTE OF OCEANOGRAPHIC SCIENCES

Wormley, Godalming,
Surrey, GU8 5UB.
(0428 - 79 - 4141)

(Director: Dr. A.S. Laughton FRS)

Bidston Observatory,
Birkenhead,
Merseyside, L43 7RA.
(051 - 653 - 8633)

(Assistant Director: Dr. D.E. Cartwright FRS)

Crossway,
Taunton,
Somerset, TA1 2DW.
(0823 - 86211)

(Assistant Director: M.J. Tucker)

When citing this document in a bibliography the reference should be given as follows:-

HUGGETT, Q. 1985 The distribution of glacial erratics in the northeast Atlantic: Final Report. *Institute of Oceanographic Sciences, Report*, No. 213, 98pp.

INSTITUTE OF OCEANOGRAPHIC SCIENCES

WORMLEY

The distribution of glacial erratics in the northeast Atlantic: Final Report

by

Q. Huggett

I.O.S. Report No. 213

1985

DEPARTMENT OF THE ENVIRONMENT
RADIOACTIVE WASTE MANAGEMENT
RESEARCH PROGRAMME 1980/84

DoE Report No.: DoE/RW/85/056

Contract Title: Selection and Evaluation of Sites for the Disposal of High-level Radioactive Waste

DoE Reference: DGR481/179

Report Title: The Distribution of Glacial Erratics in the Northeast Atlantic: Final Report.

Author: QUENTIN HUGGETT

Date of submission to DoE: 1 April 1985

ABSTRACT

A detailed study of all the available information on glacial erratics has been carried out. This has included an examination of 288 dredge hauls, 1164 sediment cores and 176 camera runs.

Sufficient data have now been collected to provide an estimate of the impact risk of a point projectile with a glacial erratic, down to oxygen isotope stage 5 (127,000 years) in three areas of the North East Atlantic.

1. Porcupine seabight (50°N, 14°W)
   0.460%
2. King's Trough Flank (42°N, 24°W)
   0.502%
3. Great Meteor East (31°N, 25°W)
   0.015%

These estimates are for all erratics larger than 1.5 cm diameter and apply only down to oxygen isotope stage 5. If estimates are required at greater depths than this, it is proposed that a detailed study of a long core should be undertaken.

Keywords: 94 Disposal under the deep ocean bed
104 Site selection
131 Soils/sedimentation
299 DoE sponsored research

This work has been commissioned by the Department of the Environment as part of its radioactive waste management research programme. The results will be used in the formulation of Government policy but, at this stage, they do not necessarily represent Government policy.

CONTENTS

INTRODUCTION

The compaction of snow produces ice which, if it flows downhill, forms glaciers and ice sheets. The movement of the ice scrapes rock from the floor and walls of the enclosing or underlying valleys. This debris becomes frozen into the ice and protrudes in places, so increasing the scouring action of the glacier. In this way, glaciers and ice sheets erode bedrock to produce a sediment called glacial drift which is characteristically unsorted. It is composed of particles of rock which vary in size from rock flour to large boulders.

Depending upon climatic and geographic conditions, a glacier may terminate on land or at sea. If the termination occurs on land, rock material trapped in the ice is released at the toe of the glacier to produce a thick deposit of glacial material called a terminal moraine. When a glacier terminates in the sea, the toe is repeatedly broken off to form icebergs. These float oceanwards carrying glacial erratics frozen into them. This process is known to geologists as "ice rafting". Individual rocks may also become frozen into seasonal ice formed in shallow water, especially along beaches (Harland et al., 1966). This ice may also drift if broken into icebergs.

Calculations based upon the densities of rock and ice indicate that icebergs may carry up to 7.5% by volume of rock material before sinking. Generally, however, concentrations of around 1% have been observed in glacier ice (Ovenshine, 1966). Recent observations have shown that, even in more northerly latitudes, icebergs greater than 150 m thickness are rare (Sukhov, 1977). Other estimates, however, have suggested that icebergs up to 300 m draught do occur (Belderson et al., 1973). Assuming that icebergs up to 150 m thick would have been able to reach further south during glacial maxima, the largest spherical boulder that could have been transported would have a diameter of 78 m (assuming that the rock constitutes 7% of the iceberg).

Rock material may be continuously released from icebergs, either through their slow melting or in batches, as icebergs roll over and deposit material lying loose on their upper surfaces. Small fragments of ice containing more than 7.5% rock material may calve off from larger icebergs and sink to the seafloor before completely melting, so producing a characteristically clustered deposit of erratics on the seafloor (Heezen & Hollister, 1971).

For at least the past 2.4 million years, glaciers have been active in many areas around the North Atlantic Ocean (Shackleton et al., 1983; Kidd et al., 1983). An estimated 200,000 km^3 of glacial drift has been deposited in the

oceans by ice rafting alone (Ruddiman, 1977) During interglacial periods like the present, glacial activity is much reduced. Small icebergs (up to 10 m thick) have, nevertheless, been observed as far south as 31°N in the North Atlantic (USNOO, 1968).

Glacial erratics may, therefore, be expected to occur on and within deep sea sediment in the NE Atlantic Ocean. It is also expected that, as the frequency of iceberg sightings falls off to the south, so too should the density of ice-rafted material found on the sea floor. The Gulf Stream causes major longitudinal variations in ice rafting past and present, resulting in much lower input of glacial drift to the western North Atlantic compared with those in the east. Surface ocean currents may also affect input rates of glacial drift by channelling or spreading icebergs from their source areas to the north.

Variations in the distribution of ice-rafted material are also expected within the sediment. The main cause being changes in the rate of pelagic sedimentation which ultimately buries glacial erratics. These changes in pelagic sedimentation are caused by the major climatic changes that occur with and cause glaciation. Generally, an interglacial has a higher input of carbonate material with minor terrigenous clays, and a glacial period shows the reverse.

PROJECT OBJECTIVES

In the IOS report, "Guidelines for the selection of sites for disposal of radioactive waste on or beneath the ocean floor" (Searle, 1979), it was recognised that glacial erratics could obstruct the emplacement of waste canisters into the sediment. This project has, therefore, been conducted to collect data that would enable an assessment to be made of:

(1) The probability of a canister impacting with individual boulders; and,

(2) The southernmost limit of ice rafting in the NE Atlantic Ocean.

Prior to this project little work had been done on the distribution of glacial erratics. Data for such work has always been collected as a by product of other sampling programmes (such as for outcropping rock, ancient sediments and benthic biology).

The most detailed work to have been previously carried out was by Ruddiman (1977) who described layers of ice-rafted sands in sediment cores and used these to outline the changes in the distribution of Pleistocene glacial debris. However, that study was based on only 32 cores, covering the whole of the North Atlantic, and the maps produced are generalised. Other tentative suggestions

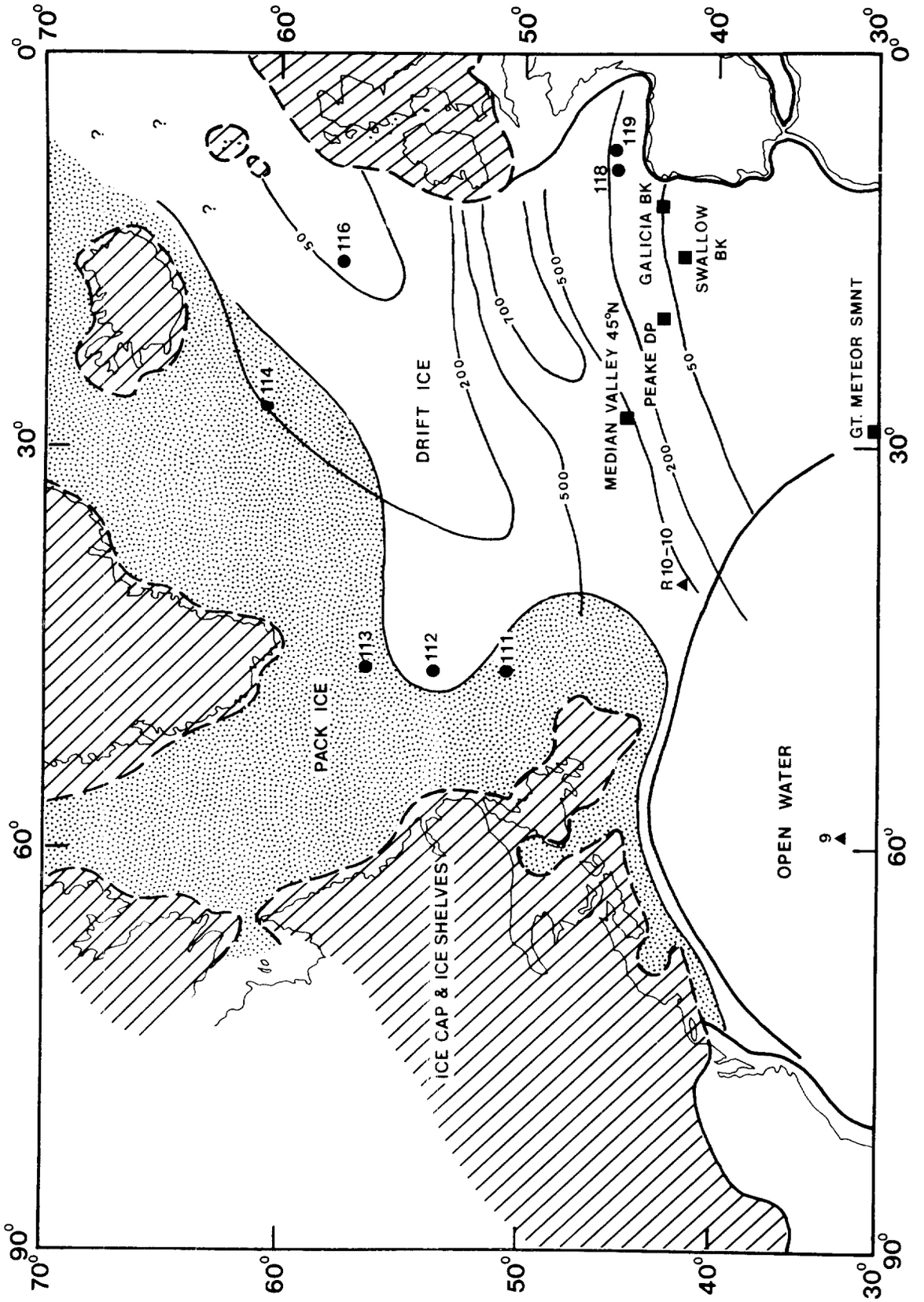

Figure 1 Occurrence of ice-rafted material in the North Atlantic reported in literature prior to this project on glacial erratics. Black squares indicate erratics in dredges and dots and triangles indicate erratics in DSDP and Lamont cores respectively. Contours indicate maximum rate of deposition of glacial sands in milligrams per square centimetre per thousand years (from Ruddiman, 1977); also shown are inferred limits of ice rafting (from Davies & Laughton, 1971).

have been made as to the nature of ice rafting (Il'In & Shurko, 1968) and the southern limits of glaciation have been inferred from findings of debris reported on seamounts and ridges and in isolated sediment cores (Davies & Laughton, 1972; Rawson et al., 1978; Fig. 1). Recently deposited ice-rafted material has been identified in bottom photographs in high latitudes (Kidd & Huggett, 1981) but, further south, Pleistocene rock accumulations are normally obscured by a thin veneer of sediment.

1. The first objective of this study was to examine the grain-size distributions of ice-rafted material. It was expected that the grain-size distributions of this material would be constant over the whole Atlantic. That distribution, once assessed, could then be used in the statistical calculations required to predict canister impact probabilities. To determine any lateral variation in grain-size distributions between areas of the N. Atlantic, dredge hauls have been examined from all the major repositories of such material in the UK, France, Germany and USA. A total of 288 dredge hauls have been examined (116 of which were taken from sediment surfaces and the remainder from rock outcrops). One hundred and twenty-one of the dredge hauls examined contained glacial erratics (Fig. 2, Appendix 1).
2. The second objective was to obtain quantitative data giving the distribution of ice-rafted material per unit area and ultimately per unit volume of sediment at or near the sediment surface. Ice-rafted material collected from rock outcrops could not be used to pursue this objective because such material cannot be collected in a controlled, quantitative manner. Therefore, material dredged from sediment surfaces alone was used and of the 116 dredge stations from such sites, 21 had been dredged with sufficient control to produce quantitative results.
3. The third objective was to obtain data to extend the surface distributions, which represent Holocene (Recent) deposition, back in time to cover the fluctuations in volume input of glacial drift which have occurred during past advances and retreats of the ice sheets. This would enable an estimate to be made of the probability of canister impact with erratics within the sediment. To this end, a general literature study of 1164 sediment cores was made, 72 of which contained pebbles likely to be of glacial origins. A further, more detailed, study was then carried out on IOS core No. D10333 which covers one complete glacial/interglacial cycle (Fig. 3, Appendix 2).

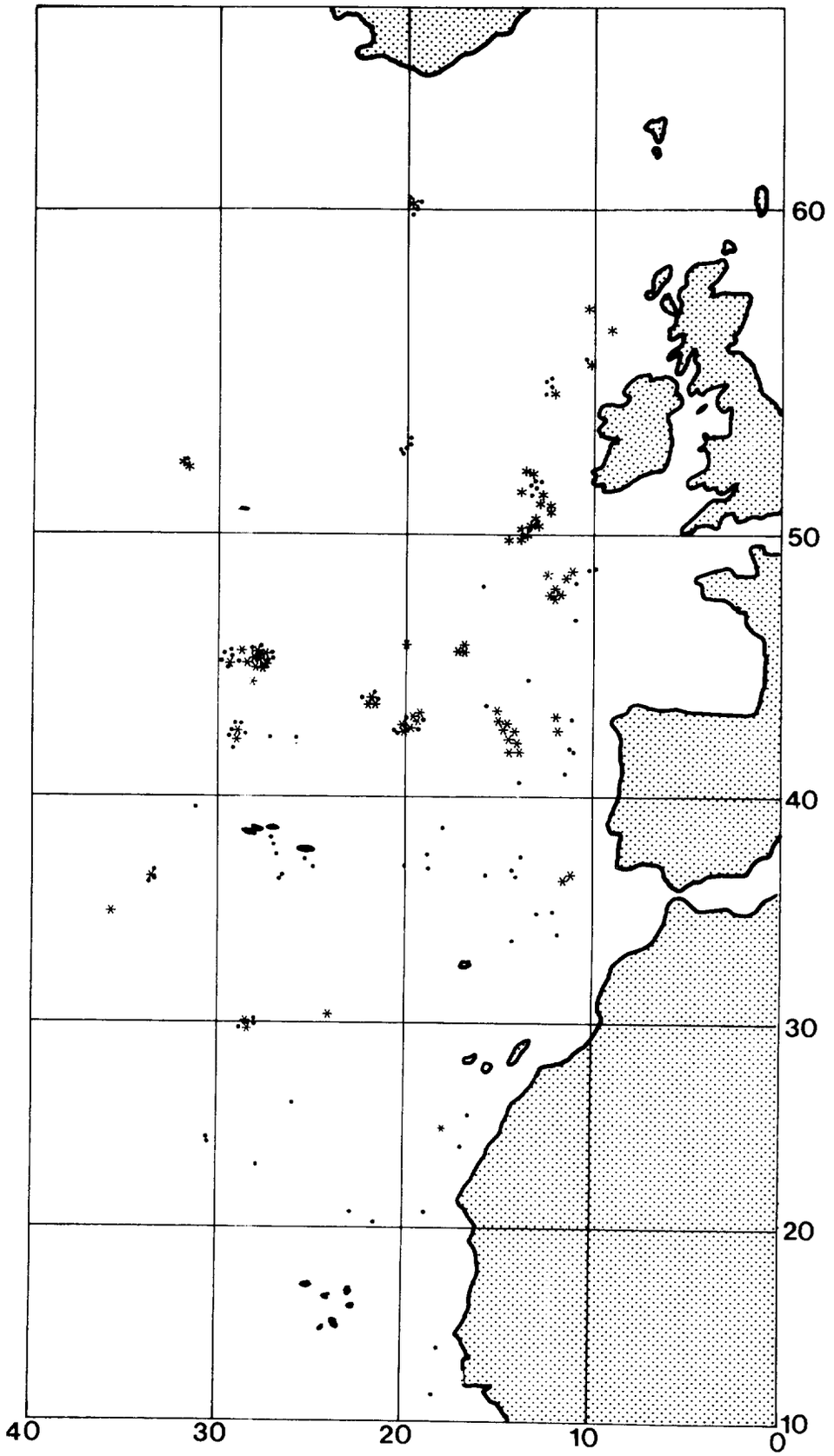

Figure 2. Chart showing the locations of the dredge hauls examined. Asterisks indicate that the dredge hauls contained ice-rafted material.

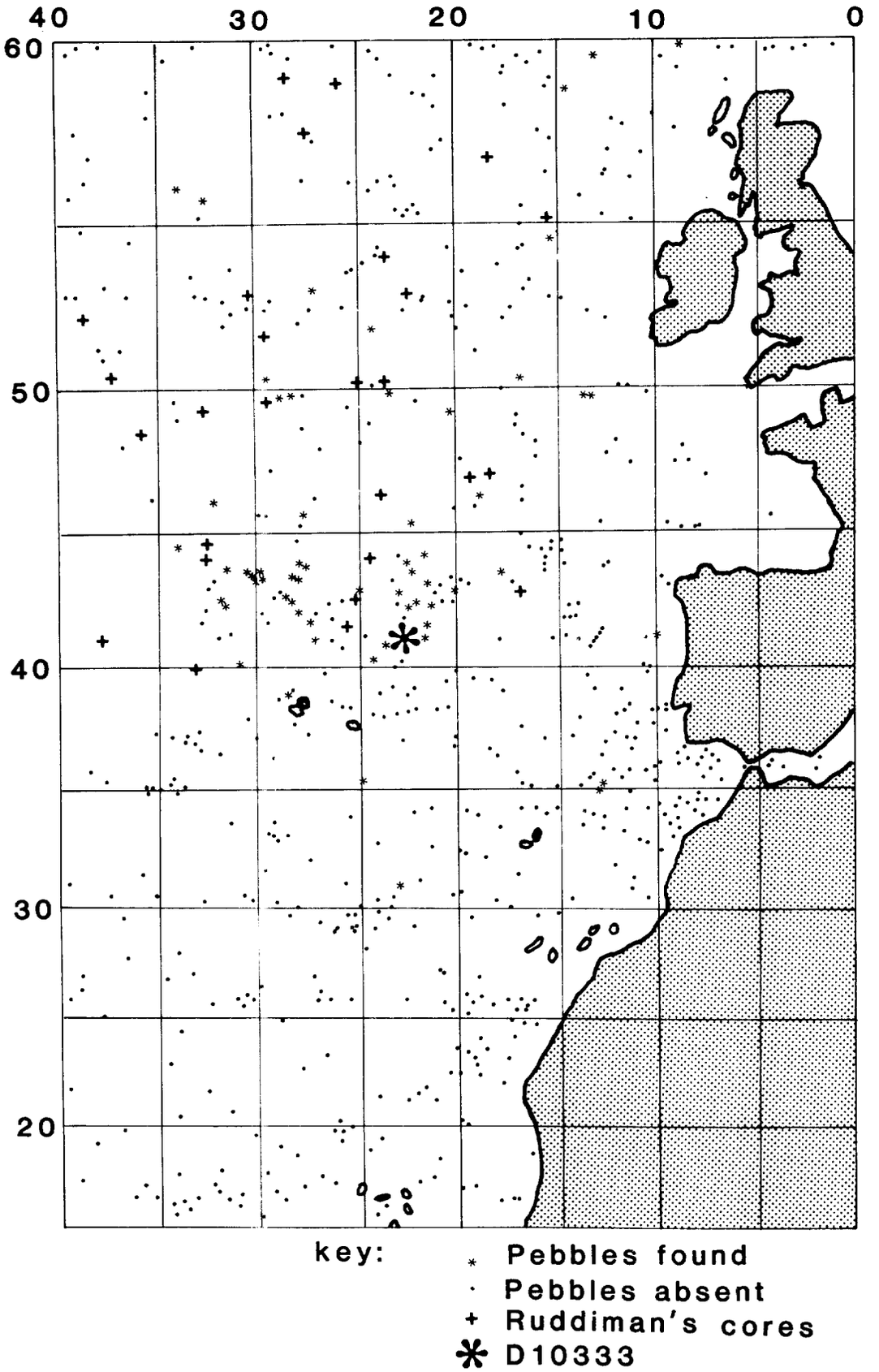

Figure 3. Chart showing the locations of the cores examined in the literature survey. Asterisks indicate that exotic pebbles were reported in the core descriptions. The cores used in Ruddiman's study (1977) and D10333 are indicated with triangles and an asterisk respectively.

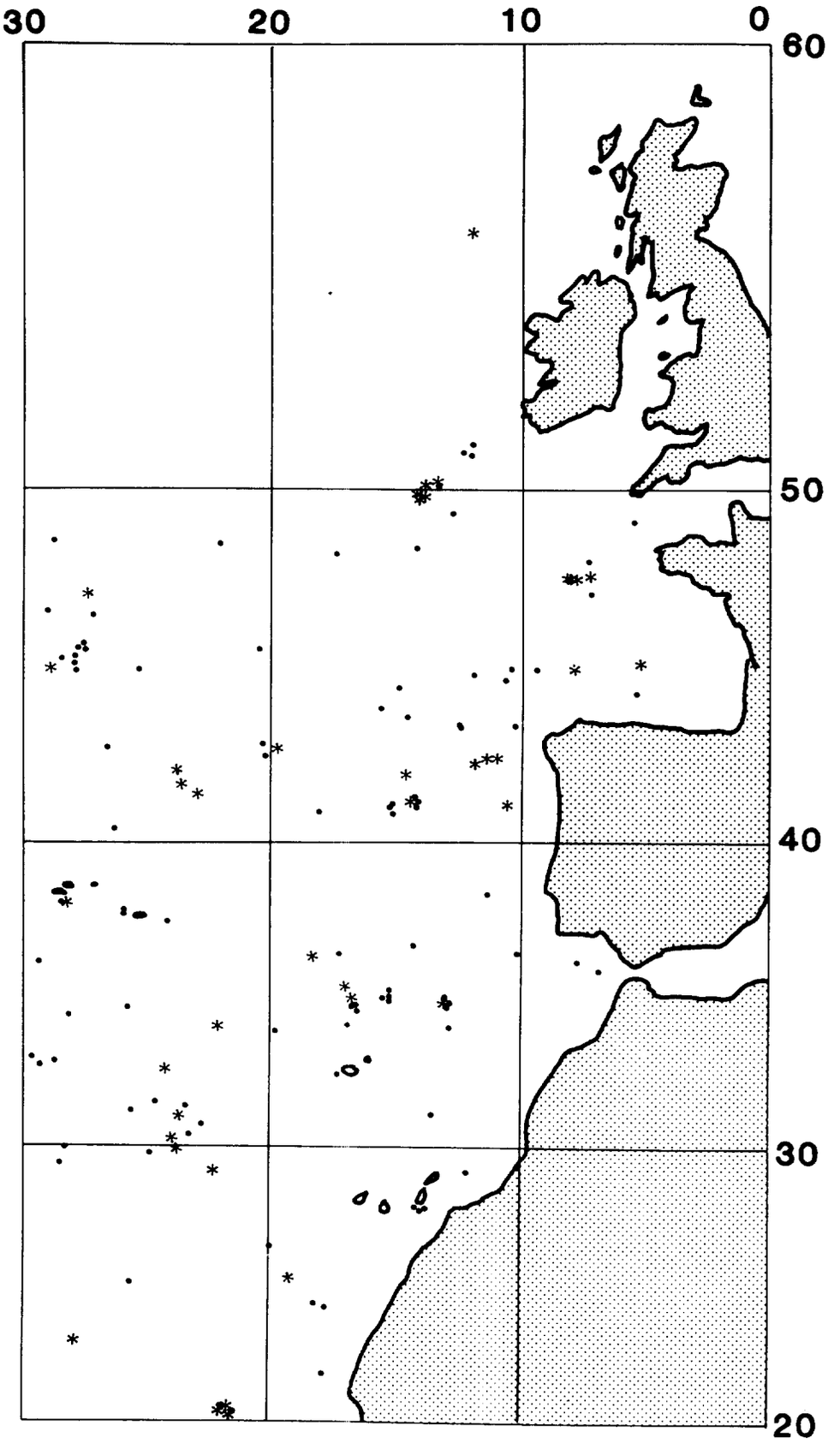

Figure 4. Chart showing the locations of all the camera stations examined. The asterisks indicate the stations at which exotic material was observed.

4. The final objective was to produce good statistical information for at least three latitudes so that impact probabilities could be interpolated for the whole of the NE Atlantic. In regions of low levels of ice-rafted material where large areas had to be sampled, surface distributions of ice-rafted material were estimated using a survey camera system. Photographs from 176 camera stations have been examined. Thirty-two of these were run with sufficient control to produce quantitative data (Fig. 4, Appendix 3).

This report has been split into three parts to describe the work carried out with dredges (objectives 1 and 2), cores (objective 3) and cameras (objective 4). In the discussion, the data are combined to achieve the objectives described above, and the limitations of these techniques will be discussed.

SECTION ONE: DREDGE DATA

Two types of dredging are carried out in the deep sea. Geological dredges are run over rock outcrops and biological dredges are run over sedimented surfaces.

(a) Geological Sampling.

Geological sampling is normally carried out over a position where the only information required is on rock or sediment type. Dredging carried out for this reason is a relatively crude operation; though it may sample a fixed, known point, the area of seafloor covered by the dredge is unknown. Two main types of dredge are used for this type of sampling:

(i) Pipe Dredge (PD) [Fig. 5(i)]. This has a mouth size of 15 cm diameter and length of 45 cm.

(ii) Rock Dredge (RD) [Fig. 5(ii)]. Many rock dredges approximate to the design of the Woods Hole Oceanographic Institution (WHOI) dredge (Nalwalk et al., 1961). This type of dredge rides over larger boulders and collects only smaller, pebble-sized material. The IOS version of this dredge is less selective and samples the full range of rock sizes that it can gather. Dredges of this kind are normally used in conjunction with nylon mesh liners in order to set the lower limit of grain sizes collected. The mouth width of this type of dredge is normally about 0.7 metres.

(b) Biological Sampling

Biological sampling is normally carried out in order to make quantitative

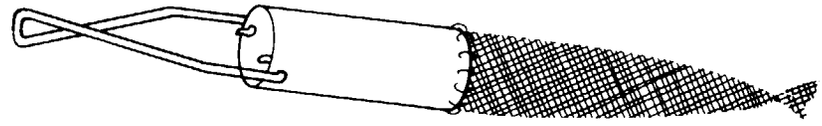

(i)

Figure 5(i) Pipe dredge. A type of rock dredge used until the early 1960s by many institutions. The mouth opening is 15 cm in diameter.

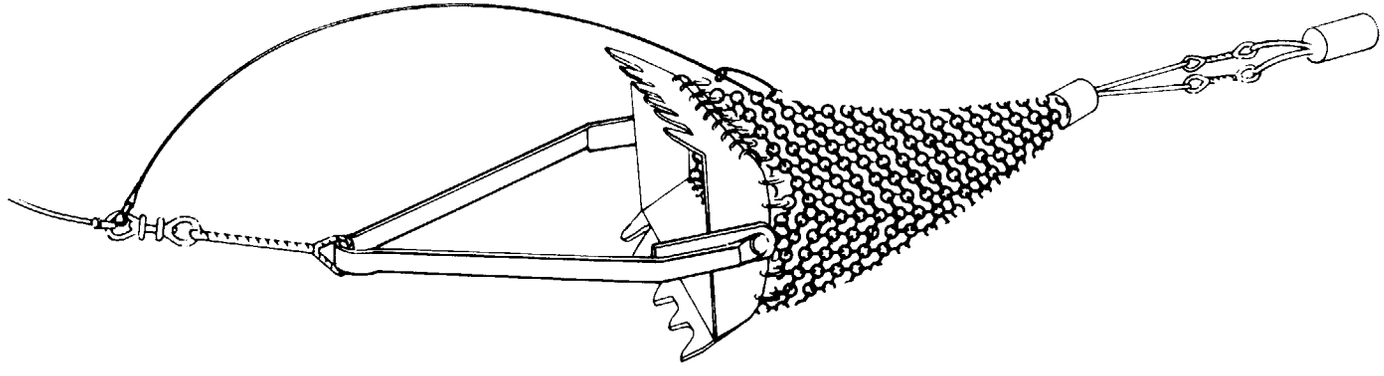

(ii)

Figure 5(ii) Rock dredge. A generalised picture of a rock dredge for use on rock outcrops. These, in various modified forms are used by most institutes and universities of the world. The mouth opening is usually around 1 m wide.

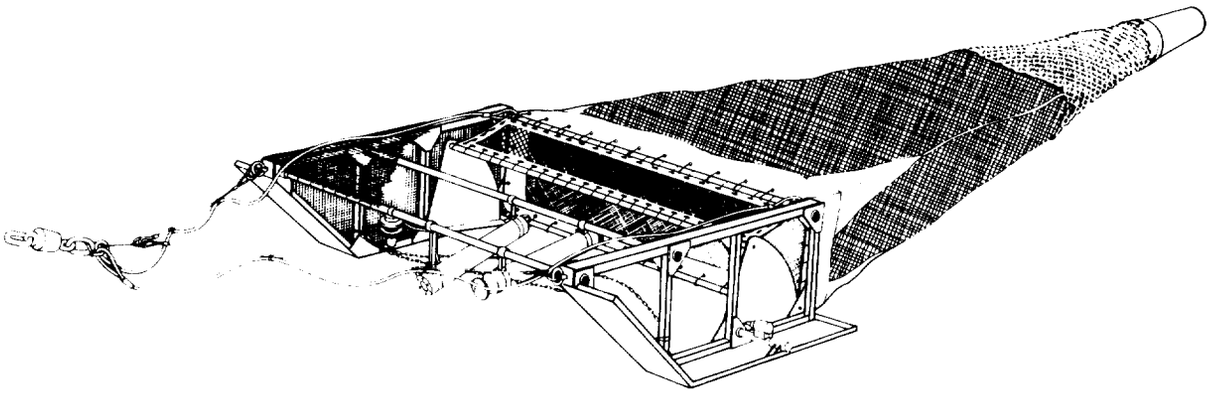

(i) IOS Epibenthic Sledge. A sampling device used by the IOS benthic biology group for sampling sedimented sea floors. The mouth opening is 1.2 m wide.

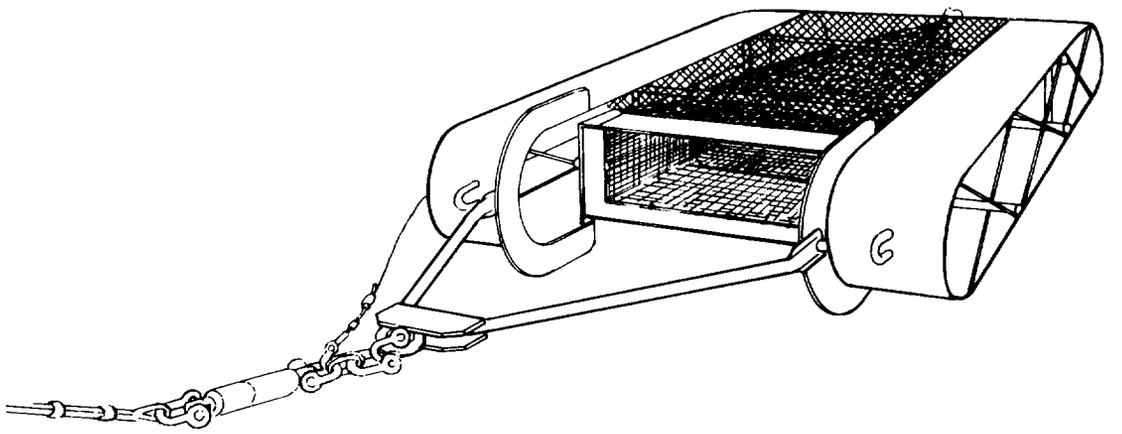

(ii) WHOI sampling sledge. Also used by marine biologists for sampling sedimented surfaces, this device has no camera or positive monitoring system and may be used either way up. It has a mouth opening of 1.2 m.

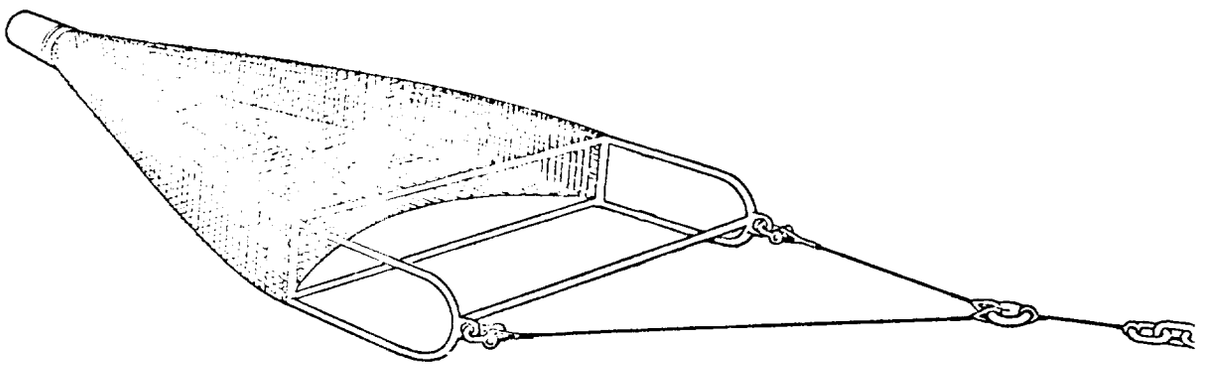

(iii) Agassiz trawl. This is the simplest dredge used on sediment surfaces. It has no positive monitoring system and may be used either way up. The mouth opening is adjustable and is usually set from 1-4 m wide.

Figure 6.

estimates of the biomass, and to collect specimens for morphological analysis. This type of sampling is, therefore, carried out under closely-controlled conditions using a relatively delicate instrument so that the area of seafloor sampled by the dredge may be estimated. In view of its relative fragility, this type of dredge may only be used on flat sedimented surfaces.

Four main types of biological dredge are used. These are:

(i) IOS Epibenthic sledge (BS) [Fig. 6(i)]. This is used for sampling sedimented seafloors. The skids (40 cm wide) are designed to prevent the sledge from sinking into the sediment. An odometer wheel measures the distance covered over the seafloor. The sledge also supports a 35-mm camera which photographs the sea bed immediately in front of the sledge mouth. The dredging operation is monitored by means of pinger telemetry which relays information to the ship on the depth, attitude and speed along the sea bed and indicates that the camera is functioning. The mouth is 1.2m wide by 0.7m high with mesh sizes usually less than 1 cm (Aldred et al., 1976).

(ii) WHOI Epibenthic sledge (WS) [Fig. 6(ii)]. This is similar to the IOS sledge, except that it has no camera or odometer wheel and is designed to operate either way up. It has a mouth size of 81 cm x 30 cm, with mesh sizes usually less than 1 cm (Hessler & Sanders, 1967).

(iii) Agassiz Trawl (AT) [Fig. 6(iii)]. The Agassiz trawl is similar to the WHOI sledge except that it is of a much simpler, more variable construction. The bottom bar is removeable enabling the mouth size to be set at any desired width. The Agassiz trawl used for this project had a mouth width of three metres.

(iv) Otter Trawl (OT). This is a modified fisherman's trawl collecting samples for qualitative work only.

Sample Treatment

During the examination of dredge hauls, care had to be taken to ensure that all the material studied was glacial drift and had not been deposited by some other agent. To this end, a set of criteria for identifying glacial erratics was developed and is fully described in Huggett and Kidd (1984).

Once identified, each ice-rafted specimen was examined to determine grain size (maximum diameter) and (in 25 locations) rock type. The lower size limit for material to be included was set at 1.5 cm; below this size little confidence

was placed in the criteria for identifying the ice-rafted proportions of dredge hauls (Huggett & Kidd, 1984).

Data quality varied considerably because of differing methods of sample storage and treatment used by the various institutions and repositories. Before this project, rock-dredging operations had only been carried out to collect in-situ bedrock. Grain size data were not always required and so material was often broken down for identification purposes; an example being rock dredge station number D9564 which was, unfortunately, one of the largest hauls examined. This, with the lack of data on mesh sizes, has meant that the control for producing grain size distribution curves for most dredge hauls is poor. At only one rock dredge station (D9825) was control good enough for grain-size distribution work to be done. The addition of data from biological sampling stations has proven vital in the generation of grain size statistics.

Results from dredging

The raw data of the rock size distributions from Station G21 (as an example) are illustrated in Figure 7. The percentage of particles smaller than a given size is plotted against a linear scale of particle diameter. Figure 8 shows the same data plotted on log-linear graph paper (exponential distribution) and in Figure 9 the same data are plotted on log-normal graph paper (log-normal distribution). The best (least squares) straight line fit is obtained using the log-normal distribution. This function is commonly used to describe particle size distributions which involve physical breakage processes whereby a particle is repeatedly diminished by the breaking off of random proportions (Barndorff-Nielsen, 1977).

Figure 10 (drawn from Table 1) shows the grain-size data from all the useable dredge stations, plotted on log-normal graph paper. These stations are taken from three main areas at 41°N, 46°N and 51°N (see Appendix 1). At every station except G21, curvature of lines drawn through the data can be seen. This phenomenon may be the result of a number of causes, the first and most obvious being that the deposit has been sorted and may not represent a log-normal distribution. Considering the processes that produce glacial drift, it seems unlikely that any sorting can have occurred during either its formation or deposition. In the one dredge station run over rock outcrop (IOS dredge No. D9825), however, the dredging operation itself may have sorted the glacial drift. This can arise from the roughness of the rock outcrop obscuring the glacial erratics from the dredge, resulting in the larger material being

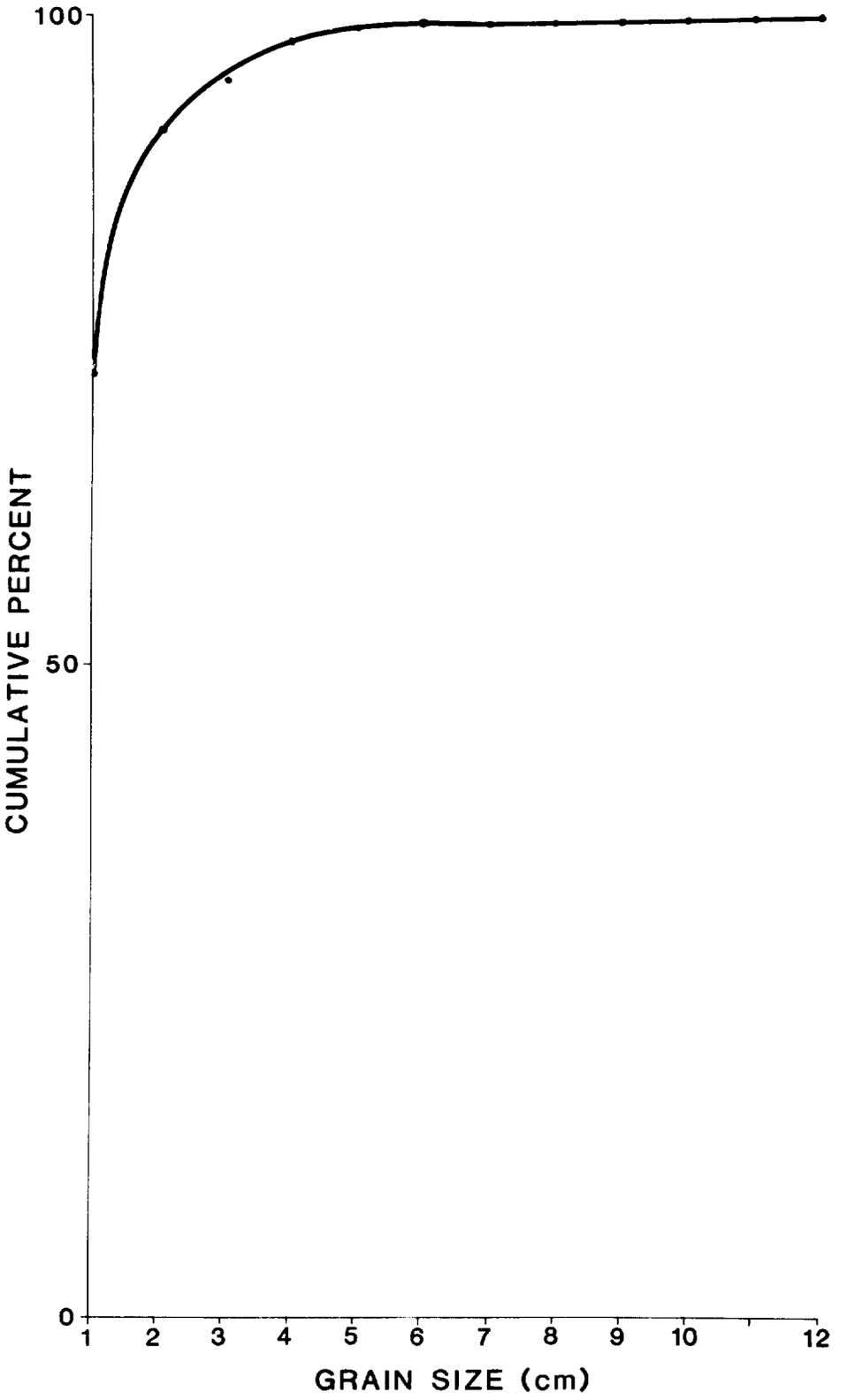

Figure 7 Linear plot of cumulative size data from Station G21.

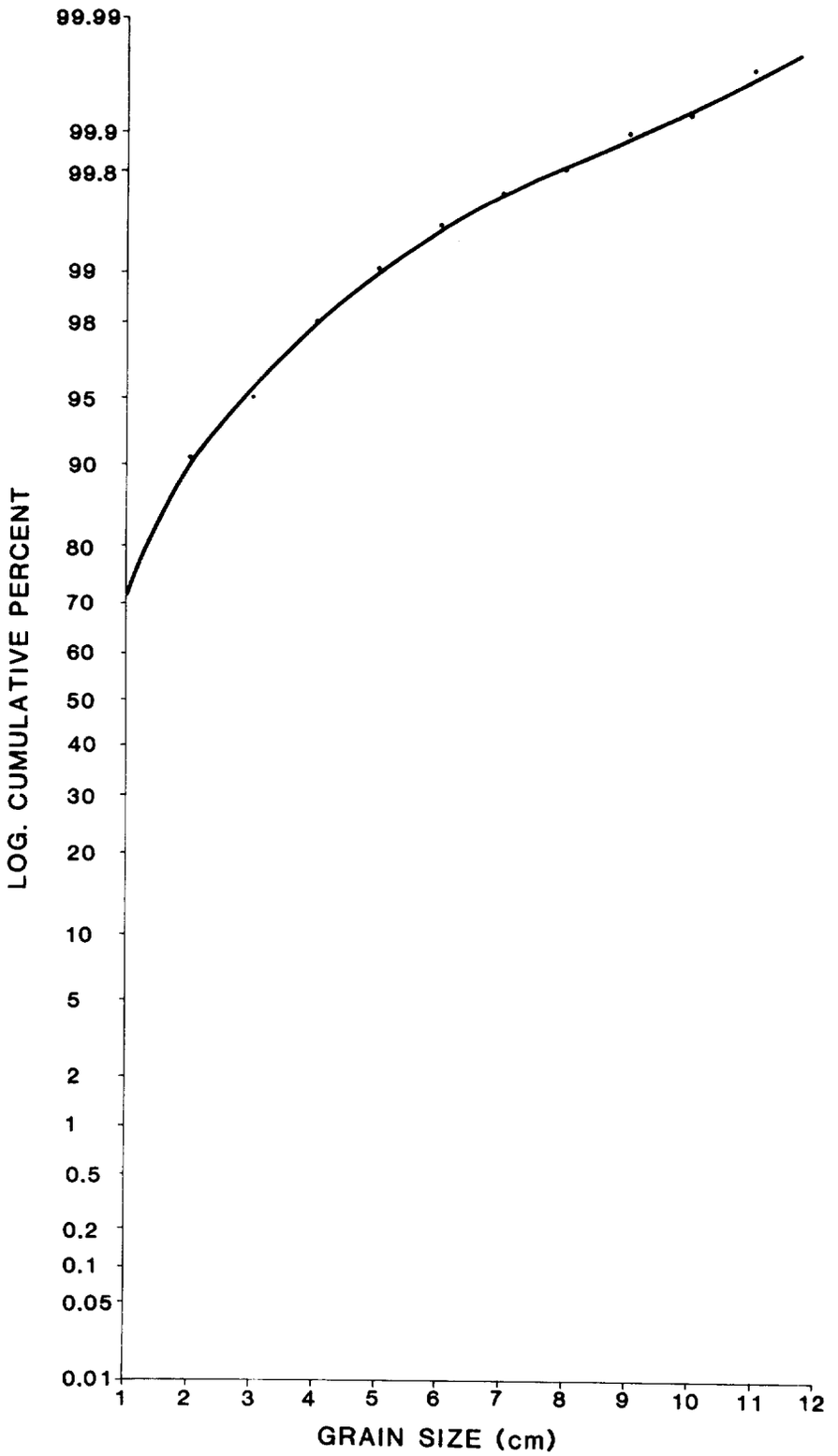

Figure 8 Log-linear plot of cumulative size data from Station G21.

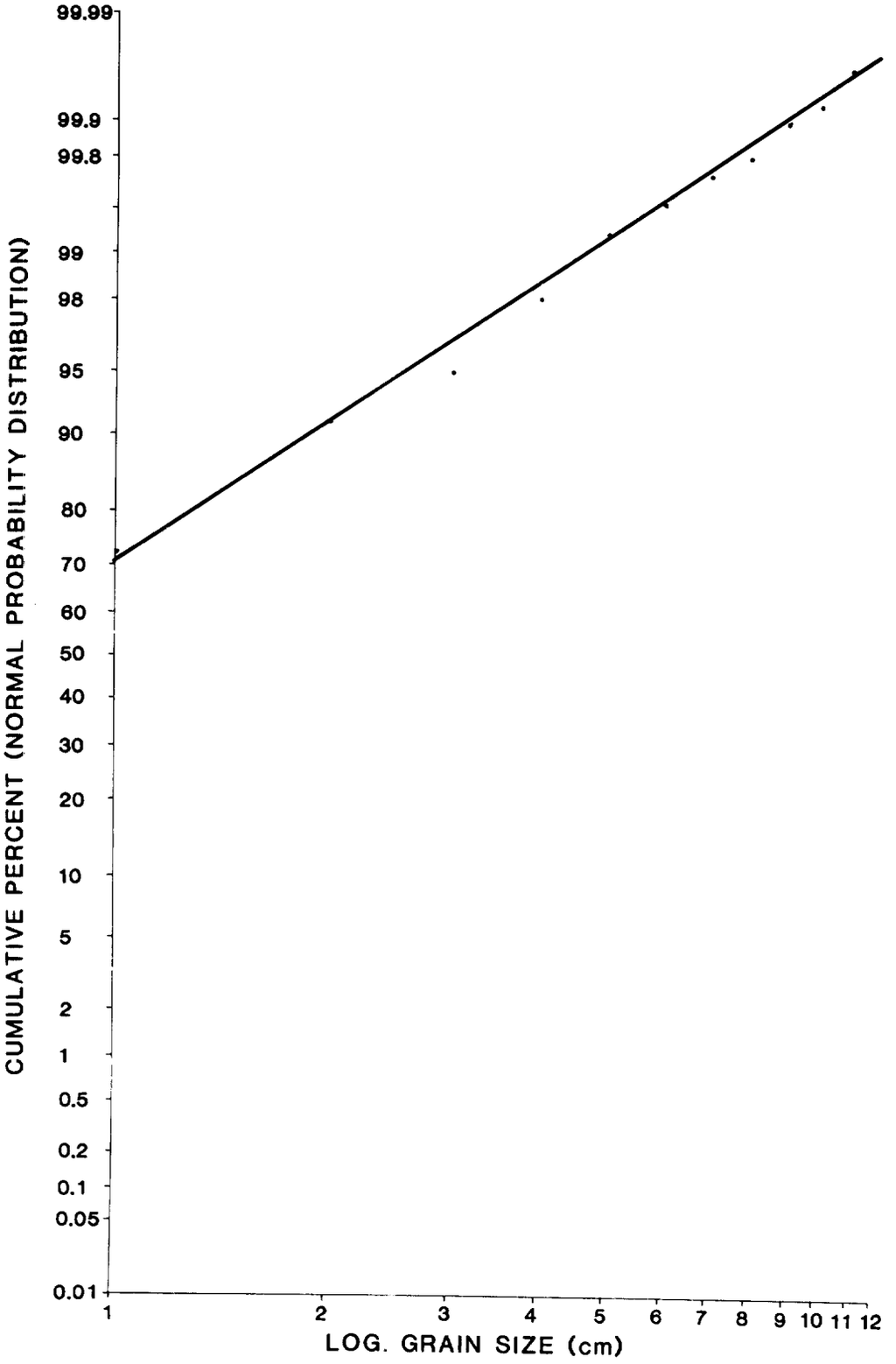

Figure 9 Log-normal plot of cumulative size data from Station G21.

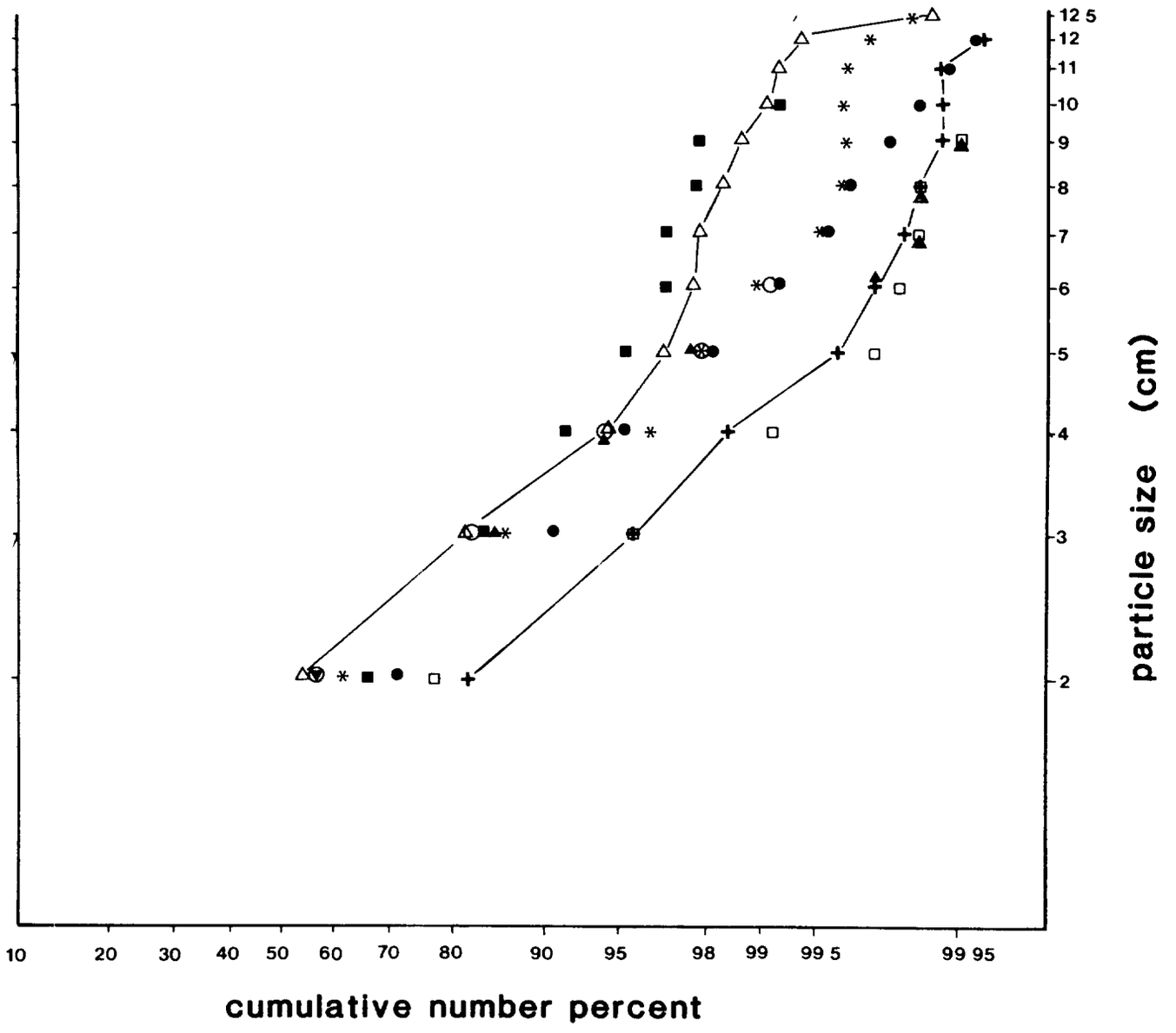

Figure 10 Log-normal plot of all stations from which size data could be obtained.

preferentially collected. The rest of the dredges were run over sediment surfaces, so another explanation will need to be sought for the curvature in their grain-size plots. Table 1 shows that there is a rapid fall-off in the number of particles recovered as one moves into the larger particle sizes. The paucity of data at this tail-end (large grain size) of the distribution renders the plots in Figure 8 susceptible to curvature by the occurrence or omission of a single rock. Bearing this in mind, straight-line fits to these plots were produced by omitting the curved tail-ends of the plots, as these sections of the data are not statistically significant. At the foot of Table 1, the mean and variance of the plotted data have been noted. The mean is, therefore, between 0.2 and 0.68 and the variance between 0.48 and 0.64.

Knowing the area of sediment surface covered by the dredges, estimates of the distribution of glacial erratics (larger than 1.5 cm) per unit area can be made. These estimates vary from the maximum of 120,250 pebbles/km^2 calculated for Station G5 to the minimum of 40,657 pebbles/km^2 for Station D9756#9K14. These estimates apply to ice-rafted material ranging in size from 1.5 cm diameter (mesh size of the dredge bag) to 70 cm diameter (height of the dredge mouth). The largest glacial erratic that was examined had a maximum diameter of 54 cm and was collected at Station D9564 (44°N, 22°W).

SECTION TWO: CORE DATA

Data from two different types of corer have been used for this project.

(a) Piston/gravity/pilot corers

These are corers with round barrels, usually fitted with a plastic liner which may be pulled out of the corer and split, so reducing handling disturbance to a minimum. These cores are forced into the seafloor by their own weight and momentum, either at the end of a coring wire or by free fall. The liners are normally between four and seven centimetres internal diameter. Such corers are not very efficient at sampling the uppermost layers of sediment of which up to 1 m may be absent from the sample.

(b) Kastenlot corer

The Kastenlot corer is used in the same way as a gravity corer and is forced into the seafloor by its own weight and momentum. It differs from the gravity corer only in that it has an unlined square-section barrel which is split lengthways in order to expose the sample. It is 15 cm square and has taken

samples up to 4 m long. For studying glacial erratics, this corer has two distinct advantages. Firstly, it samples a greater volume of sediment; secondly, it samples the upper sediment layers more efficiently than other corers because of the nature of its core catcher and the greater barrel volume.

Sample Treatment and Data Processing

Initially, core samples were used qualitatively to assess the latitudinal limits of ice rafting, past and present. For this, copies of core descriptions of 1164 cores were obtained and those containing pebbles (not identified as pumice) were separated and plotted (Fig. 3; Appendix 2).

A more detailed study was then carried out along the lines of Ruddiman's work (Ruddiman, 1977; Fig. 11) on IOS core No. D10333. This was a 1.7m long Kastenlot core taken in the King's Trough Flank area (KTF) (Kidd et al., 1983), and is a complete core with very little disturbance or loss of surface material. The core was divided into 8-cm layers which were sub-sampled to produce samples weighing approximately 200 gms. These were weighed, dried, weighed again and washed through a 63μ sieve to remove the clay and silt fraction. The residue was then dried and passed through a stack of six sieves and each fraction weighed. The residues were then examined under a microscope and particles counted to estimate the number of ice-rafted particles/cc for particles > 63μ . In order to extrapolate the particle counts over the whole core, use was made of bulk density measurements carried out on the core for each 8 cm layer.

Figure 12 shows the downcore variations in ice rafting from which one can deduce the last glacial/interglacial boundary; this correlates well with micropalaeontological observations (Kidd et al., 1983). This curve has been drawn from particle counts per unit volume and so it represents real variations in ice-rafted deposition assuming pelagic sedimentation to be constant.

SECTION THREE: CAMERA DATA

Photographs from 176 stations (Appendix 3) were examined and these could be split into three different types:

(a) Close-up photography from epibenthic sledges

The epibenthic sledge illustrated in Figure 6(i) has a camera which is capable of photographing 2.6 m^2 of the seafloor per frame. The design of the system only allows the camera to operate while it is horizontal; objects lying on the seafloor may, therefore, be measured using a simple scale grid.

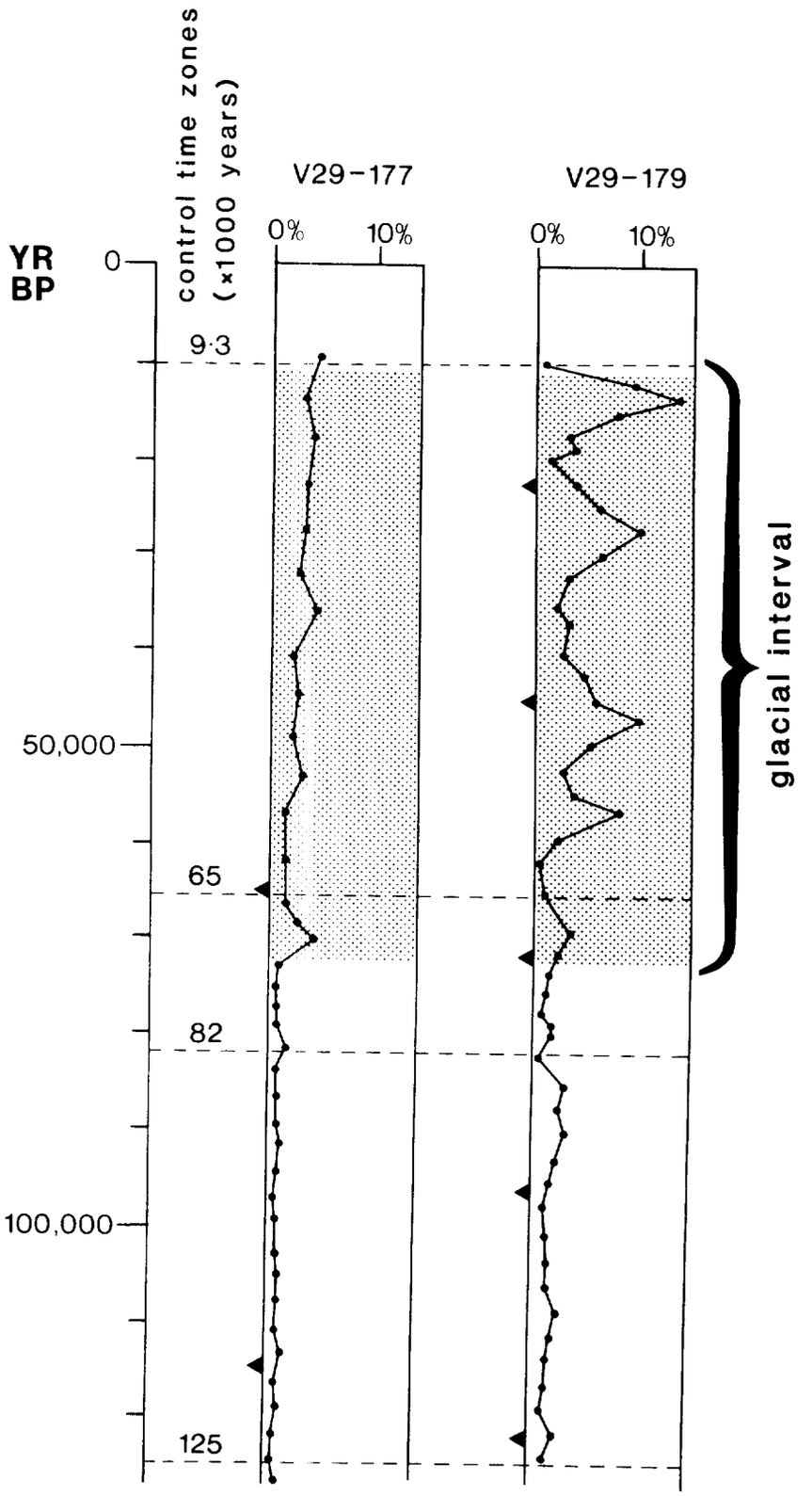

Figure 11 Downcore estimates of ice-rafted input taken from two of Ruddiman's (1977) cores: V29-177 (at 41.5°N) and V29-179 (at 44°N).

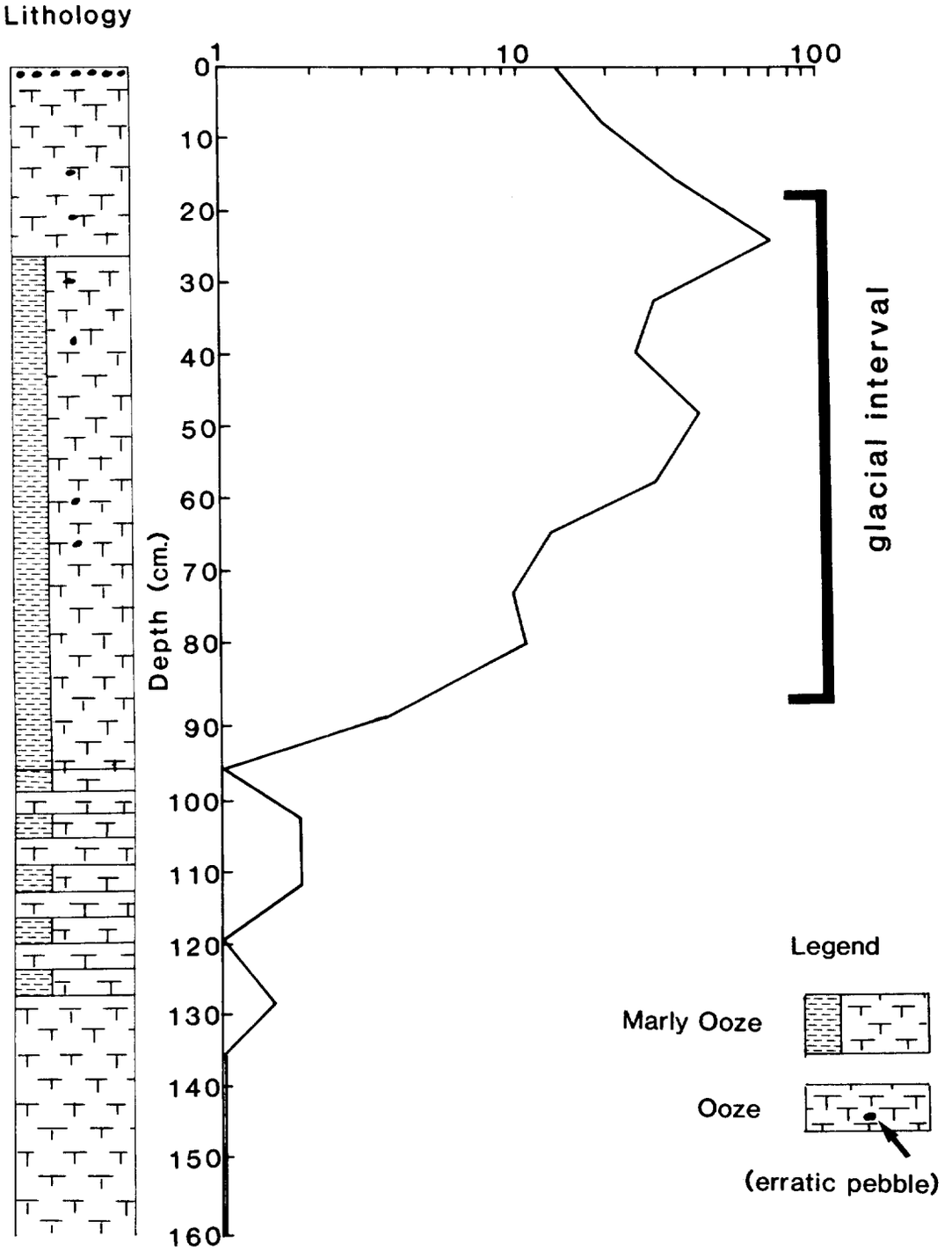

Figure 12 Downcore variations in ice-rafted input for core D10333. The estimates have been made at 8 cm intervals and have been normalised to produce numbers of ice-rafted particles per 100 cc.

(b) Wide-area survey photography

An underwater camera system, recently developed at the IOS, was used to photograph large areas of the seafloor (Fig. 13). The camera is suspended approximately 10m from the seafloor and towed at 0.5 knots (0.25 m/s). The height of the camera above the seafloor is monitored using a Near-Bottom Echo Sounder and controlled with the ship's main winch. Using this configuration, the camera photographs 80m^2 of the seafloor per frame and adjacent frames overlap by approximately 40%. In principle, adjacent photographs could be used to produce stereo images. However, as a result of the towing instabilities of the camera frame, the stereo pairs are unsuitable for accurate photogrammetry.

(c) Qualitative photography

Photographs held in collections at Lamont-Doherty Geological Observatory (LDGO) and IOS and some of those printed in Heezen & Hollister (1971) were examined for a simple qualitative estimate of the occurrence of ice-rafted material (Appendix 3; Fig. 4).

Sample Treatment and Data Processing

(a) Close-up photography from epibenthic sledges

Photographs taken with this instrument were all taken from the same position on the frame and did not overlap. Therefore, the distributions produced are taken from the sum of the area covered by each photograph. Up until August 1979 the area covered was 2.6 m^2 per frame; after that date the area changed to 1.5 m^2 per frame. At the start of this study, photographs from benthic dredge stations at which no clastic material (including clinker and pumice) was recovered were examined. In this way, experience in the identification of the benthic community and the lebenspurren that they produce was gained. Clastic material seen at other stations was then identified in photographs. In cases where doubt existed over the identity of an object, it was not included in the counts. Using this instrument, objects down to 1.5 cm (maximum diameter) were identified.

(b) Wide-area Survey Photography

On average, the WASP camera system took 850 useable frames per run. For each run the acoustic telemetry records were analysed with the help of a computer programmed to produce a record of the total area covered and the average height (which we try to maintain at 10 m) during the run. When an object of interest

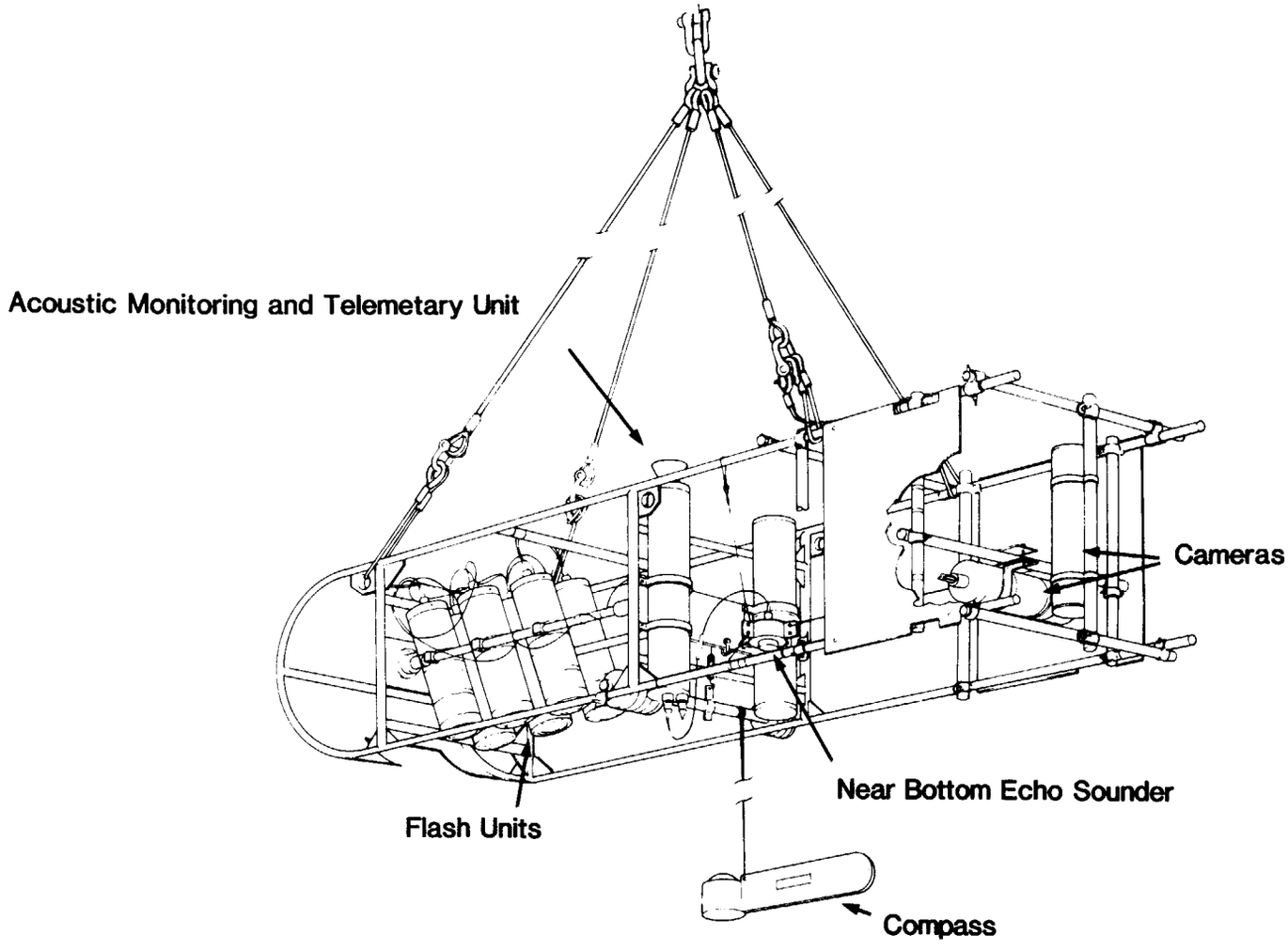

Figure 13 WASP (Wide Area Survey Photography) camera system. This system has six flash units illuminating an area of the seafloor from approximately 10m which is photographed by one or two cameras. At least 1600 frames may be photographed per run, covering a maximum area of 100,000 m^2 of seafloor per run. The height of the camera from the seafloor is monitored using a near-bottom echo sounder, the output of which is displayed both on board the ship and in the corner of the frame being photographed.

is identified on a photograph, the height of the camera from the seafloor is used to give a scale factor which allows the size of the object to be measured. In some cases (e.g. D10664) so much clastic material was observed that only selected photographs could be examined in detail and the data were extrapolated from these. For the purposes of calculation, two "domains" of data were collected. Domain L was for photographs taken from 8 metres or less and domain U contained photographs between 8 and 18 m. This approach was taken because the size of the smallest resolveable object changes with height. Eight metres was chosen as the domain boundary because this is the minimum height that the altimeter can measure. Domain L is, therefore, a domain of qualitative data only, in which no measurements can be made. The smallest resolveable object at maximum altitude in Domain L is 1.5 cm and in Domain U, 10 cm. In some areas with abundant clastics, objects less than 10 cm were recorded to give qualitative data on sediment type, etc.

Results from photography

The eight WASP camera stations examined for this project have covered a total of 0.4 km^2 of seafloor. They are spread over three latitudes: 26°N, 31°N and 42°N; and over three types of sediment: pelagic clays, turbidites and pelagic oozes respectively. Table 2(a) shows the distributions of ice-rafted material observed over three latitudes. The sedimentation rates have been included in order that simple comparisons may be made between the areas, bearing in mind that surface distributions are a function of both latitude and sedimentation rate.

The close-up photography taken from the benthic sledges has been revealing in that it indicates a discrepancy between photographed and sampled distributions. Table 2(b) (taken from Kidd & Huggett, 1981) shows that clinker from coal-burning ships (which was deposited within the last 200 years) has been buried out of sight of the camera at one station (No. 9775#3) whereas glacial erratics deposited within the last 2000 years) may still be photographed at another (Station 9756#14). The conclusion here is that there are some localised processes that may bury pebble-sized material lying on the sediment surface. Kidd & Huggett (1981) suggested that this process may be bioturbation or sediment slumping.

DISCUSSION

CALCULATION OF IMPACT PROBABILITY

The probability of a canister impacting with a glacial erratic depends upon two variables; the distribution of glacial erratics and the canister diameter. Assuming, for the time being, that the canister is a point projectile of infinitely small radius, the impact probability will depend only upon the distribution of glacial erratics. As, at this stage, we are only considering a point projectile, its impact probability is the same as the probability of encountering a glacial erratic in a given area of seafloor or, more simply, the proportion of that area of seafloor covered by glacial erratics.

The dredges used to sample sediment surfaces sample the top 3 cm of sediment over which they run. Assuming that they do not overlap, the probability of encountering any erratics may be expressed as the sum of the projected areas of the glacial erratics per unit surface area of sediment. For example, Station G21 in Table 1 covered 35,320 m^2 of sediment. In Table 3, the size classes have been altered to express projected area (rather than diameter) and totalled to produce the sum of the areas which is 1.6 m^2. This value represents the total projected area of glacial erratics observed over a dredge run which covered 35,320 m^2. Therefore, for the top 3 cm of sediment at 45°N (i.e. Station G21) the likelihood of encountering a glacial erratic is 1.6/35,320 = 0.0045%. From this first approximation three points should be raised:

1. As previously shown, the largest possible glacial erratic would have a diameter of 78 m, well out of range of our sampling techniques! This approximation also uses grain sizes down to 1.5 cm. The smallest erratic considered hazardous to canister emplacement may be larger than 1.5 cm. Some flexibility must, therefore, be introduced into the calculations in order that we may consider a variety of grain-size ranges.
2. This calculation applies only to the latitude or even area from which the samples were taken (i.e. Station G21, 42°N). For some areas to the north of this there is no problem as we have good data at 50°N. To the south, however, the fall-off in the bulk quantity of ice-rafted material makes sampling problematical, as not enough specimens have been collected for observing grain-size distributions.
3. The third point is that this approximation only applies to the top 3 cm of sediment whereas the base case scenario is for canisters to be emplaced at a depth of 30 m below the surface (Anderson, 1981). Impact probabilities must therefore, be extrapolated from a combination of dredge and core data.

Bearing these points in mind, a mathematical approach must be taken in order to give the flexibility needed to address three problems:

1. Calculate impact risks for different size ranges of glacial erratics.
2. Calculate impact risks for different latitudes or regions.
3. Calculate subsurface impact risks.

From the analysis of the grain sizes of glacial erratics a log-normal function may be used to describe the grain-size distribution thus:

$$f(x) = \frac{1}{x\sqrt{2\pi} \cdot \sigma} \cdot \exp\left\{-\frac{[\log x - \zeta]^2}{\sigma^2}\right\}$$

where x = grain size

σ = variance

ζ = mean

[N.B. All logarithms used in this manuscript are Log_e.]

Values for the mean and variance of the grain-size data are shown in Table 1. This function may now be integrated to produce two equations. The first calculates the average particle cross-sectional area between two particle size limits (x_1, x_2). The second calculates the total number of particles to be found between limits x_1 and x_2 over the dredge run being considered.

Equation 1. Calculation of average area ($\overline{A}$) between two size limits, x_1, x_2 (cm diameter) where $x_1 < x_2$ (e.g. $x_1 = 1.5$ and $x_2 = 7800$ cm diameter).

$$\overline{A} = \overline{A}(x_1, x_2) = \frac{\frac{\pi}{4} \exp\left[\frac{4\sigma^2 + 4\zeta}{2}\right] \cdot \left[\Phi(Z_2) - \Phi(Z_1)\right]}{\Phi(y_2) - \Phi(y_1)}$$

where:

$\overline{A}$ = average particle area for particles between grain-size limits x_1 and x_2

σ = variance

ζ = mean

$Z_i = (\log x_i - \zeta - 2\sigma^2)/\sigma$

$y_i = (\log x_i - \zeta)/\sigma$

Φ is derived from the function:

$$\Phi(x) = \frac{1}{\sqrt{2\pi}} \int_{-\infty}^{x} e^{-\frac{1}{2}t^2} dt$$

This is the standard function for estimating the area under the normal probability curve.

Equation 2: This equation gives the total number of particles, N, between the size limits x_1 and x_2 at a station where P particles were sampled between size limits P_1 and P_2.

$$N = N(x_1,x_2) = P(p_1,p_2) \frac{\Phi\left[(\log_e(x_2) - \zeta)/\sigma\right] - \Phi\left[(\log_e(x_1) - \zeta)/\sigma\right]}{\Phi\left[\frac{\log p_2 - \zeta}{\sigma}\right] - \Phi\left[\frac{\log p_1 - \zeta}{\sigma}\right]}$$

where: $P(p_1,p_2)$ = Number of particles between size limits p_1 and p_2

ζ = mean

σ = variance

$p_1 = 1.5$ Grain-size limits over which ζ, σ and P were

$p_2 = 7.5$ established

x_i = grain size limits as in equation 1

Part of this equation may be calculated as a general case for this project:

$$\Phi\left[\frac{\log p_2 - \zeta}{\sigma}\right] - \Phi\left[\frac{\log p_1 - \zeta}{\sigma}\right] = 0.4316$$

The value $P(p_1, p_2)$ is specific to each dredge run or combination of runs considered since the area of seafloor covered by each run is different.

1. Calculation of impact risks for different size-ranges of glacial erratics

The value $N(x_1, x_2)$ is the number of particles of average area $\overline{A}$ to be found over the area covered by the dredge. The product of $N(x_1, x_2) \cdot \overline{A}$ gives the total projected area of glacial erratics over the area covered by the dredge. The ratio of these is the probability of encountering a glacial erratic of any size between x_1 and x_2 down to 3 cm in the sediment which is the sampling depth of the instrument. Equations 1 and 2 may therefore be used to answer the first problem to be addressed.

2. Calculation of surface impact probabilities in areas of scarce data

On examination, there appears to be no significant variation in the grain-size distributions plotted in Figure 10. This confirms the view that in the open ocean ice rafting mixes material from different sources to such an extent that no trends or provenance can be observed from whole dredge collections. The size distributions are, therefore, all derived from the same population which exhibits a log-normal distribution. The only difference between stations is in the number of particles/km^2 on the sea bed which is a function of distance from source (latitude). Thus, it is argued that the log-normal distribution derived from stations in the North Atlantic can be

applied for all the abyssal areas where ice-rafting has taken place. Only one dredge station (D10328) over sedimented surfaces was run in the Great Meteor East (GME) region at 30°N. This dredge haul contained only six glacial erratics even though it covered 4,444 m^2 of seafloor. Having made the assumption that these six specimens came from the same population as all the data in Table 1, the mean and variance of the grain-size distribution may be established from that table. $\overline{A}$ (Equation 1) is, therefore, calculated without reference to Station D10328 whereas $N(x_1, x_2)$ (Equation 2) is (i.e. $P(p_1, p_2) = 6$). Therefore, one can still calculate the total projected area A ($= \overline{A} \cdot N(x_1, x_2)$) of glacial erratics to be found over the area covered by the dredge run.

3. Calculation of sub-surface impact probabilities

At this stage, we need to make use of the study made of the core D10333 and of Ruddiman's work (Ruddiman, 1977). The downcore variations in ice-rafted input in core D10333 (Fig. 12) may be redrawn to show how subsurface distributions of ice-rafted material vary according to glacial and interglacial cycles (Fig. 14, Table 4). The curve in Figure 14 has been drawn to represent the ratio between the present day input and ancient input rates. This curve depends upon good recovery of the surface sediments in order to provide the ratio of past and present-day input rates. From Ruddiman's cores (Fig. 11) one can see that there are no data for the surface sediments. It should be noted, therefore, that if core D10333 has undergone any winnowing or other post-depositional processes, the whole core is affected for these calculations. For this reason care was taken to examine the integrity of this core to ensure that the surface sediments were recovered in good order. The study of core constant over each 8 cm segment, the cumulative impact risk becomes:

Equation 3:

$$R_i = \sum_{i=1}^{n} \left[\frac{8}{3} \; r \; \cdot \frac{E_i}{E_1} \right]$$

where: r = the surface impact risk (down to 3 cm depth in sediment)

R_i = the total cumulative risk down to depth i

$\frac{E_i}{E_1}$ = the ratio of the input rate at depth i, E_i to the present day input rate E_1

For the top two metres, therefore, a curve may now be drawn to show the cumulative risk of canister impact with depth for all the grain sizes examined at 42°N (Line A, Fig. 15) (assuming that no particles overlap). The cumulative risk has been estimated from the sum of the risks in each 8-cm layer.

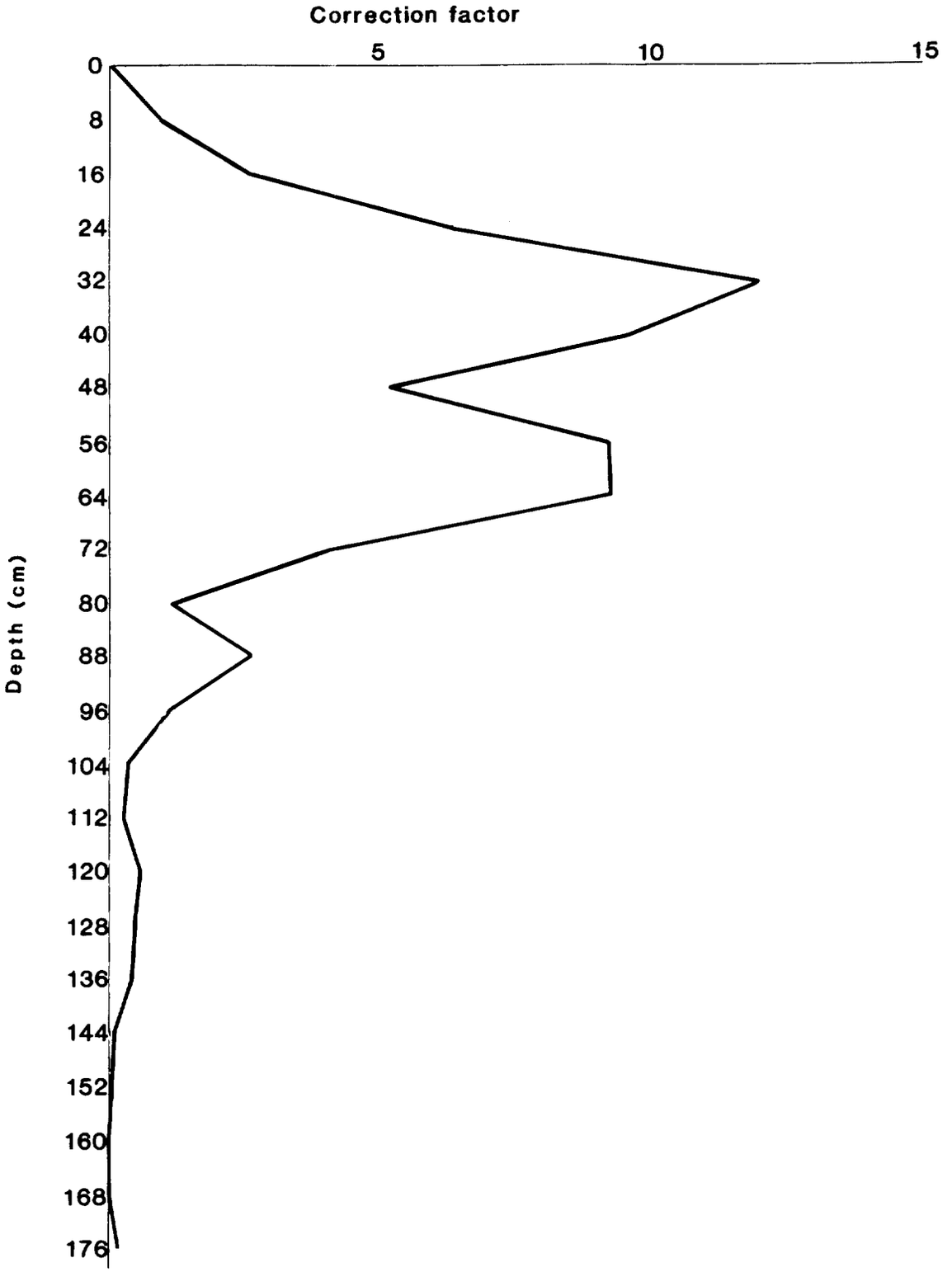

Figure 14 Downcore graph of D10333 showing correction factors to be applied to impact risk data at surface when accumulating the risk downcore.

The results from this work depend upon two natural variables; latitude and the lower size limit. Figure 15 shows the graph of cumulative risk of impact with depth (for all grain sizes) with different lines being drawn to show the three areas sampled and the affect of latitude. For the purposes of detailed calculation, the corresponding values for ζ, σ, N and P can be found in Table 5.

The lowest size limit considered here is 1.5 cm diameter; this being the smallest ice-rafted material that was examined. Figure 16 uses the same data as Figure 15 [line A] except that different lines have been drawn to show how a change in the lower size limit changes the cumulative impact risk. A direct and more detailed analysis can be made using the Equations 1-3 in conjunction with Tables 4 and 5. The values for $\Phi(x)$ can be obtained from any compilation of statistical tables. Figure 16 was drawn assuming the same sedimentation rates for all areas considered. Pelagic sedimentation rates do vary slightly and minor corrections can be made by fixing the curve in Figure 16 to oxygen isotope stages identified in cores from the different latitudes. The main differences are brought about by turbidite sedimentation, however. Figure 17 shows the same curve (for latitude 31°N) as Figure 15 except that it has been altered to include the turbidites identified by Weaver & Kuijpers (1983). These turbidites do not carry glacial erratics so they merely vertically stretch the record.

The use of core D10333 has provided data down through one glacial/interglacial cycle. Although an accurate estimate of ice-rafted input cannot be derived for sediments below this, one can draw a curve to show all the major glacial/interglacial cycles back to oxygen isotope stage 19. Figure 18 has been drawn as a rough illustration only to demonstrate the likely occurrence of ice-rafted material below 2 m in the sediment. It has been drawn assuming that the input of ice-rafted material has been the same for each glacial/interglacial cycle. Oxygen isotope stage 19 is approximately 712,000 years BP (Shackleton, 1977; Pisias & Moore, 1980). This corresponds to 16 m depth in the King's Trough Flank region (i.e. at core D10333) (Kidd & Ruddiman, in press).

SOURCES OF ERROR

There are two major sources of error: those introduced by the sampling method and errors from assumptions made in the interpretation of the data.

(a) Errors introduced by sampling techniques

Various aspects of the sampling method introduce a bias to rock dredge data. These are:

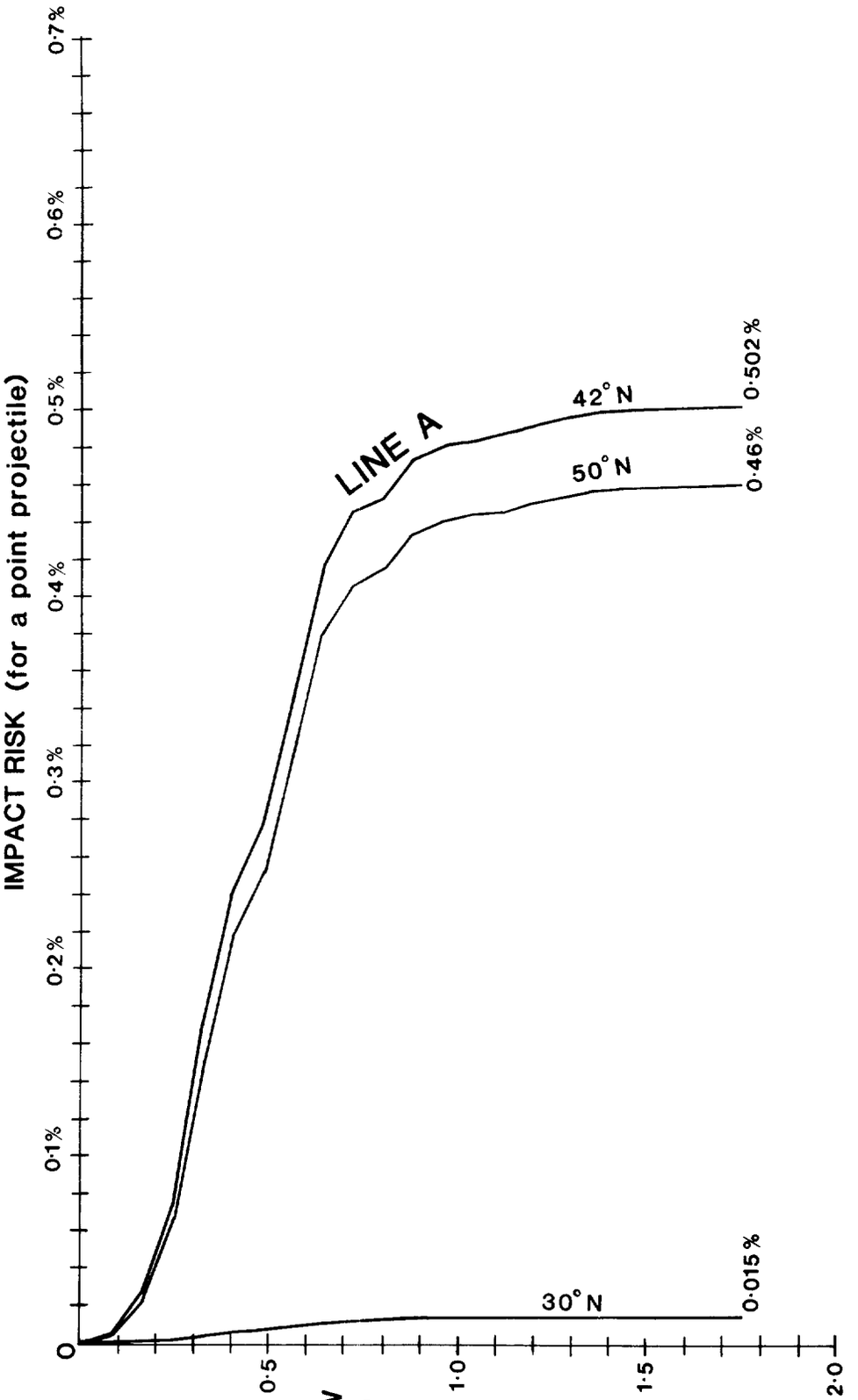

Figure 15

Graph showing risk of encountering ice-rafted material for all material between 1.5 and 7800 cm diameter downcore. Three lines have been drawn to show the differences between the risks calculated in the three areas for which there are data.

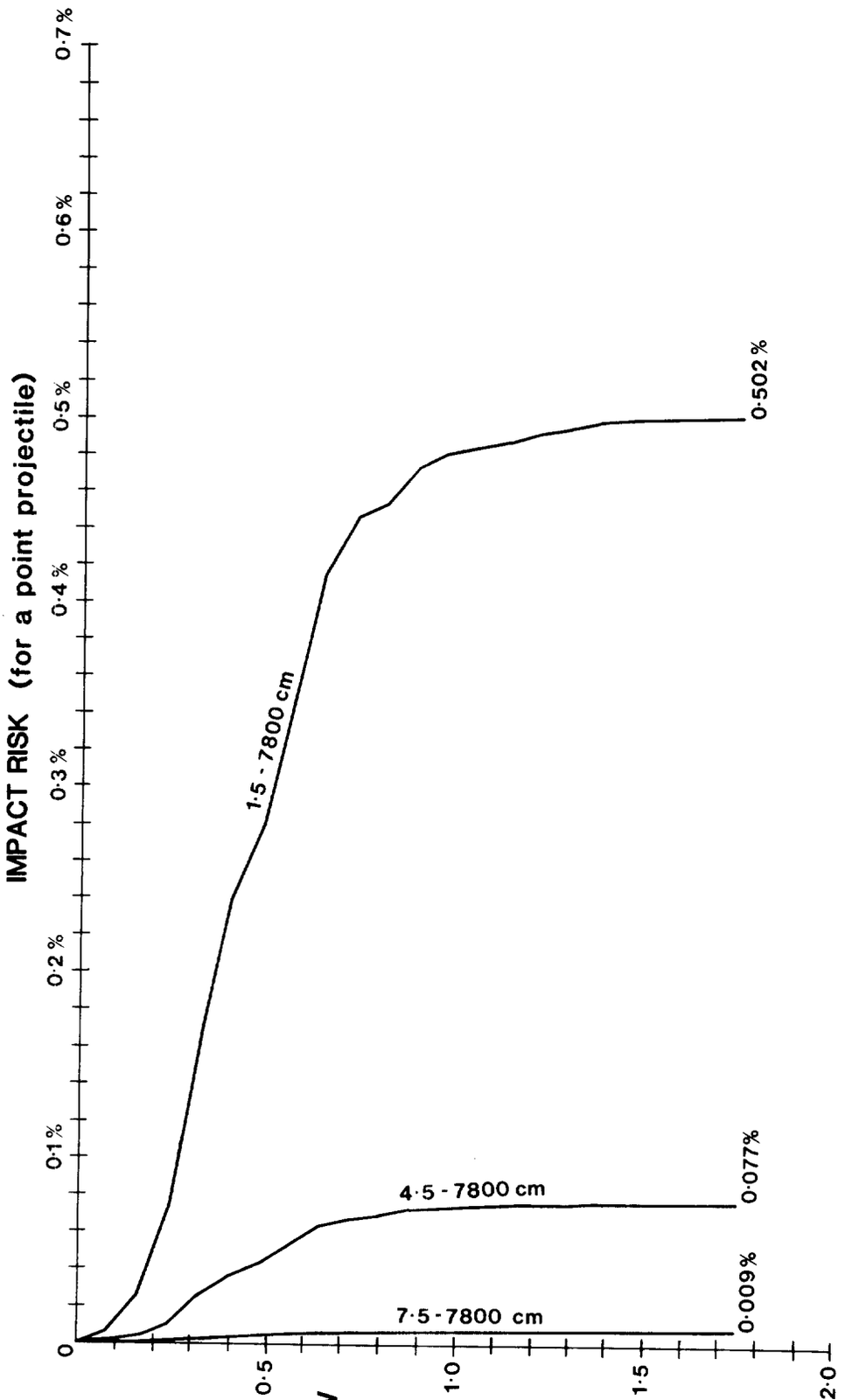

Figure 16 Graph showing risk of encountering ice-rafted material at 42°N. Three lines have been drawn to show the risk for different ranges of grain sizes.

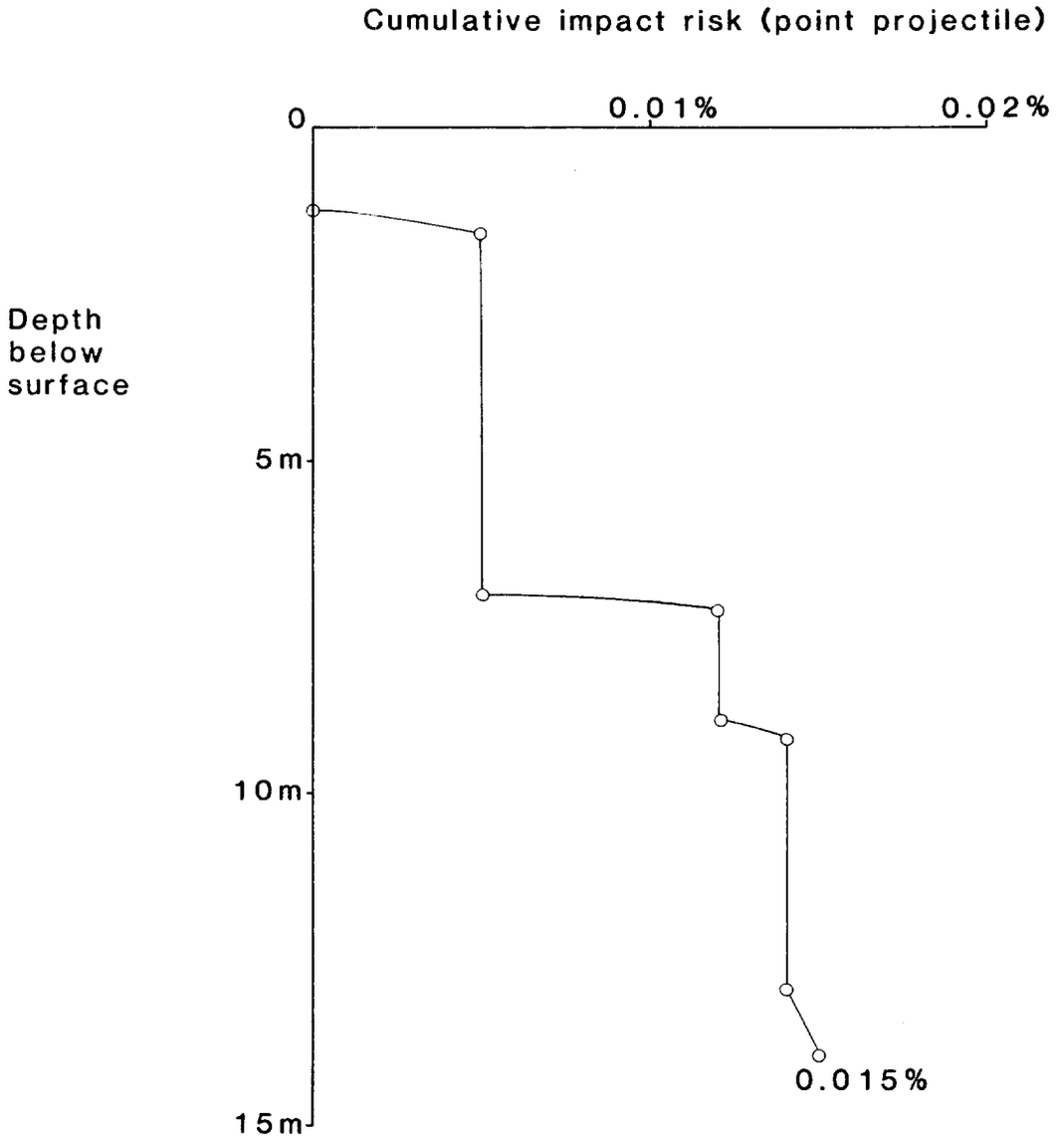

Figure 17 Graph showing effect of turbidite sedimentation on risk of encountering ice-rafted material between 1.5 cm and 7,800 cm diameter. This graph is based upon Line A (Fig. 15) and core 82PCS13 from the Great Meteor East area.

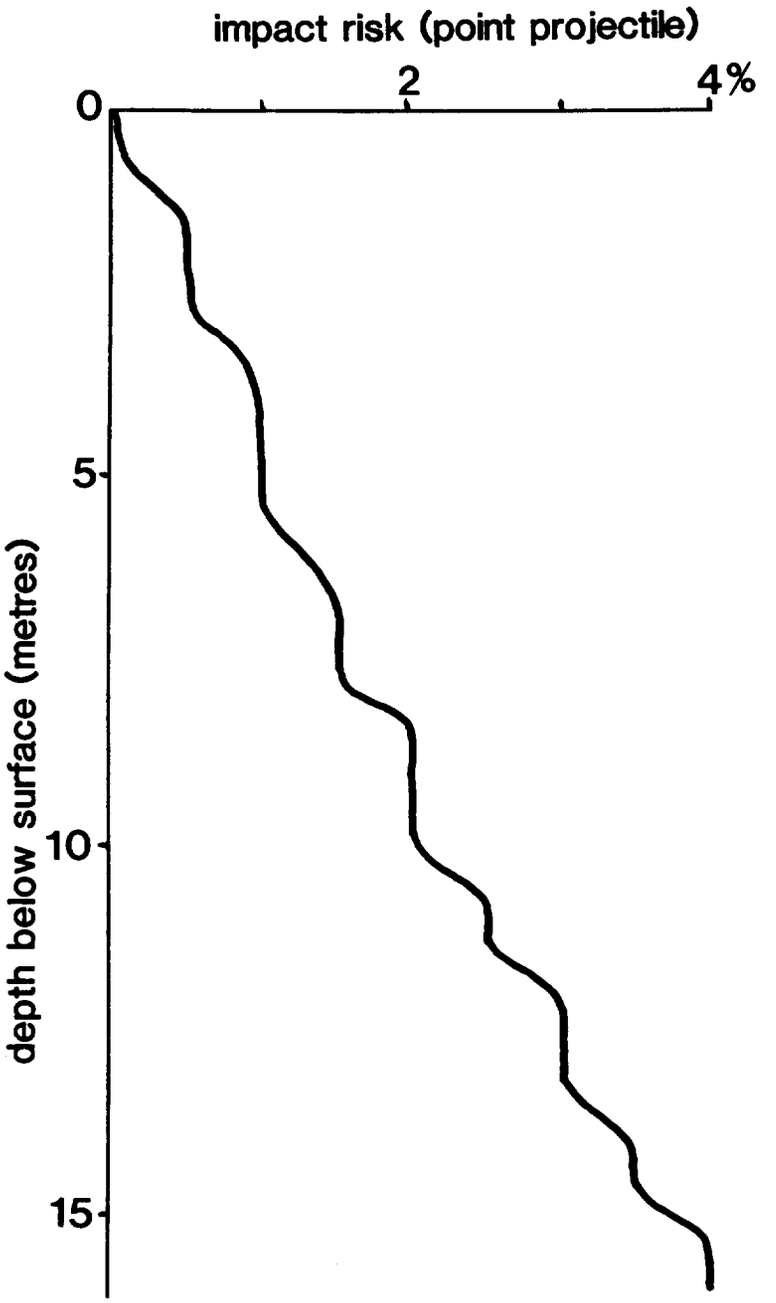

Figure 18 Graph illustrating possible risks of encountering ice-rafted material down to a depth of 20 m. TO BE USED AS A ROUGH GUIDE ONLY.

Dredge Design

In most cases, rock dredges with chain bags were used in conjunction with fine mesh liners, the precise mesh sizes of which were never recorded. The mouth sizes of the dredges were not always recorded either. However, in all cases of geological sampling (except RD 9564), in-situ material, larger than the largest erratic collected, was always seen in the dredge hauls. Thus, the upper grain-size limit seen in those hauls was probably defined by the natural distribution of erratics on the sea bed rather than the ability of the dredges to collect large erratics.

Dredging Operations

In estimating grain size distributions, it is assumed that the dredge collects all the material in its path that is small enough to enter it. The populations that we observe from the material collected may be biased because the dredge rides over large boulders (as some dredges are designed to do; Nalwalk et al., 1961). Other errors can be introduced by the dredge lifting off or even, in the case of exceptionally large hauls, spilling some of its load. Some of these effects could explain the curvature of some of the distributions plotted in Figure 10.

Ship's Track

In areas of rock outcrop, scientists have used their knowledge of the structure of the sea floor to improve the quality of dredge hauls. Scree-like accumulations of material at the foot of submarine slopes commonly produce high proportions of glacial erratics in dredge hauls (up to 45% in D9561). Precise dredging with acoustic navigation in the King's Trough area during Discovery Cruise 84 (Kidd et al., 1982) has highlighted the importance of the ship's track during dredging operations. Hauls taken along and across strike produced different yields of glacial erratics. This effect negates the use of such dredge hauls in the production of normalised data. Data from these hauls may be used in the examination of grain-size distributions, however.

Mistaken identity in photographs

On sediment surfaces, as outlined in Huggett & Kidd (1984), pebble material may be derived from six sources. Boiler scale from ships and pumice are fairly distinct, even in deep sea photographs, and may be distinguished from other pebble-sized material. As a matter of interest, however, both may be confused

with the benthic foraminifera Xenophyrophora.

Ballast and coal shale are indistinguishable from ice-rafted debris. Figure 19 shows the results of an analysis carried out in 1980 of the IOS benthic Biology Group's collection of material dredged from sediment surfaces (Kidd et al., 1980). The most striking result is clearly the amount of clinker and even unburnt coal that is to be found on the seafloor. Figure 20 is a photograph of a whole coal briquette dredged from 46°N, 17°W! The results of this work have shown that, in searching for glacial erratics, the use of deep-sea photography alone is insufficient. Control samples of the seafloor must also be collected in order to estimate the input of coal debris over the area of seafloor covered. As a general guide, Figure 21 illustrates the major steamship routes of the NE Atlantic (Somerville, 1950). Ballast is regarded as insignificant as, except in the cases of whaling ships and ships in distress, ballast is normally unloaded close to port, prior to taking on cargo.

Carbonate erratics

Previous attempts to estimate ice-rafted inputs downcore (Ruddiman, 1977) were made using an acid leach technique whereby insoluble residues are weighed and compared with the original sample. The lengthier process of making particle counts was chosen because of the input of calcareous ice-rafted detritus. This was shown firstly during the analysis of rock types of dredged rock material which showed that 6.7% of all erratics collected were soluble in HCL (Figure 22). Secondly, a short survey of washed residues used for the study of foraminifera revealed that, in some cases, soluble material comprised 100% of the lithic residues (or glacial drift) (Table 6).

(b) Errors introduced by natural fluctuations of the distributions observed

In undertaking this study, it has been assumed that between sampling sites there is lateral and vertical homogeneity, or that changes occur according to some predetermined pattern. With ice rafting, there are some processes that affect the validity of these assumptions:

Iceberg grounding

Iceberg ploughmarks have been recorded on both sides of the Atlantic Ocean as far south as latitude 43°N. Figure 23 is a chart of the northeast Atlantic Ocean showing the 500 m isobath. The deepest known ploughmarks were observed in 500 m water depth (Belderson et al., 1973). It is conceivable, therefore, that

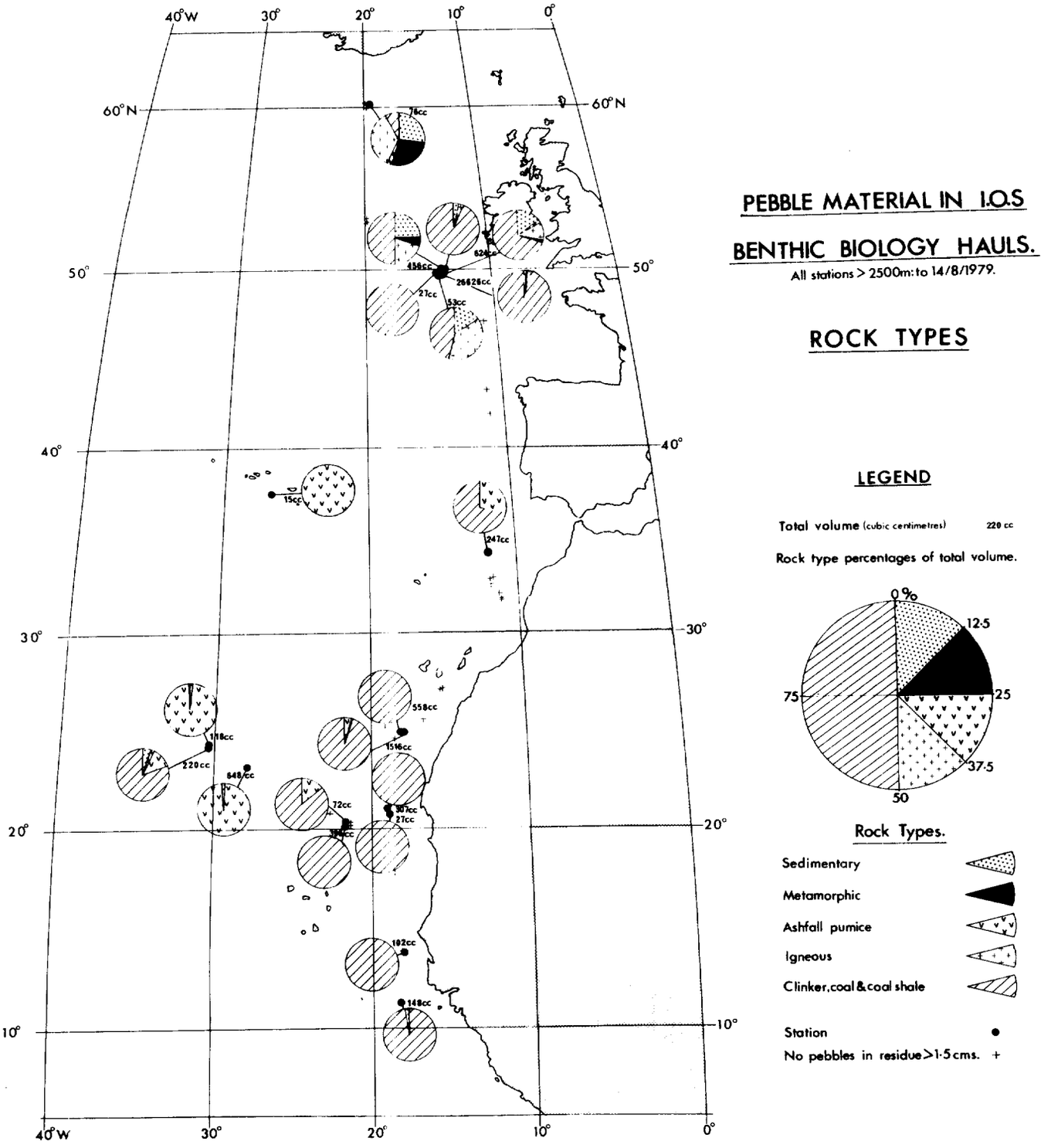

Figure 19 Chart showing rock-type distribution for all the IOS sediment surface dredges.

Figure 20 Coal briquette dredged from sediments at 46°N, 17°W with its provenance clearly marked! [PATENTS CARDIFF].

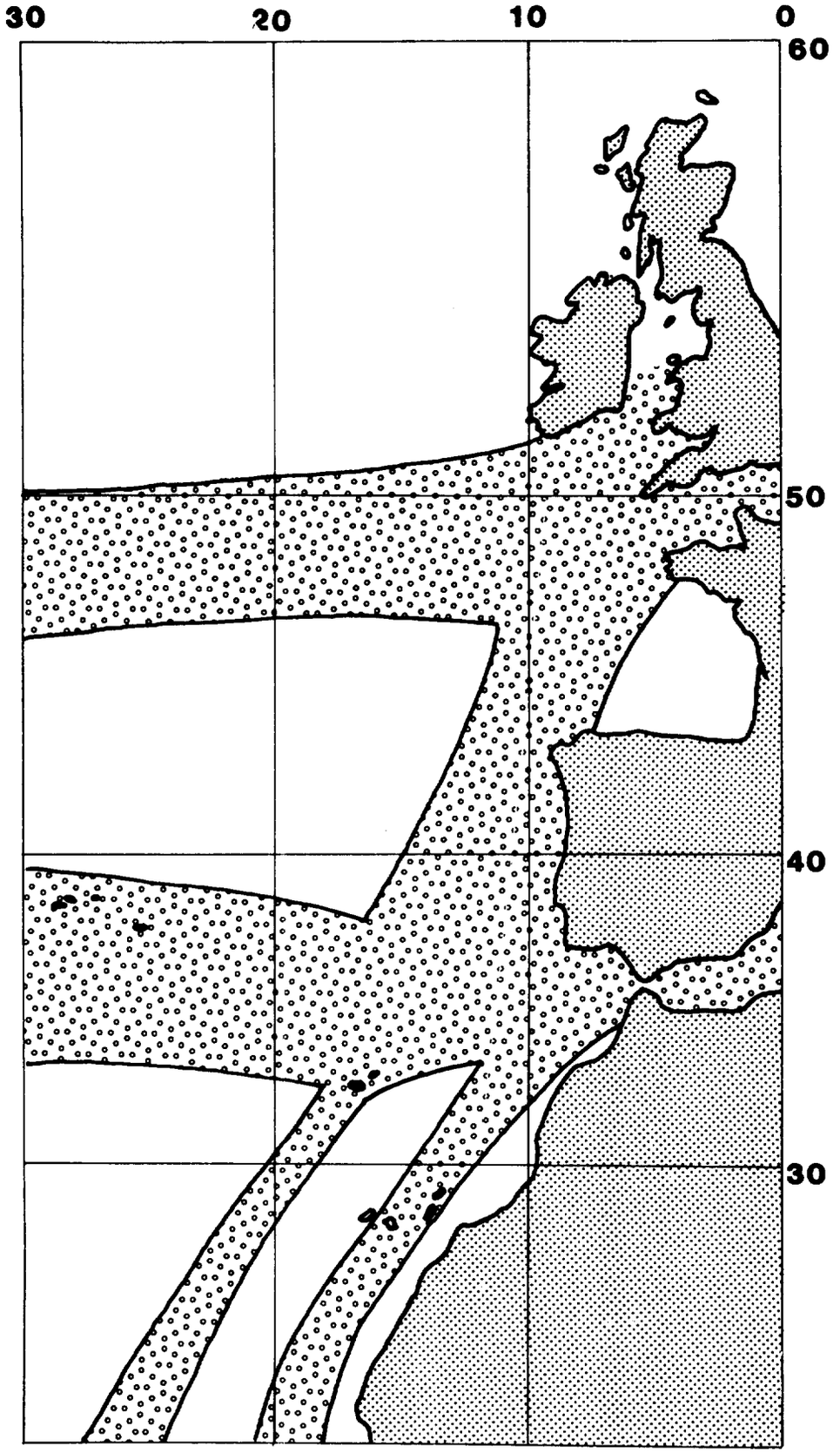

Figure 21 Chart showing major steamship routes where deposits of clinker are likely to be found (taken from Somerville, 1950).

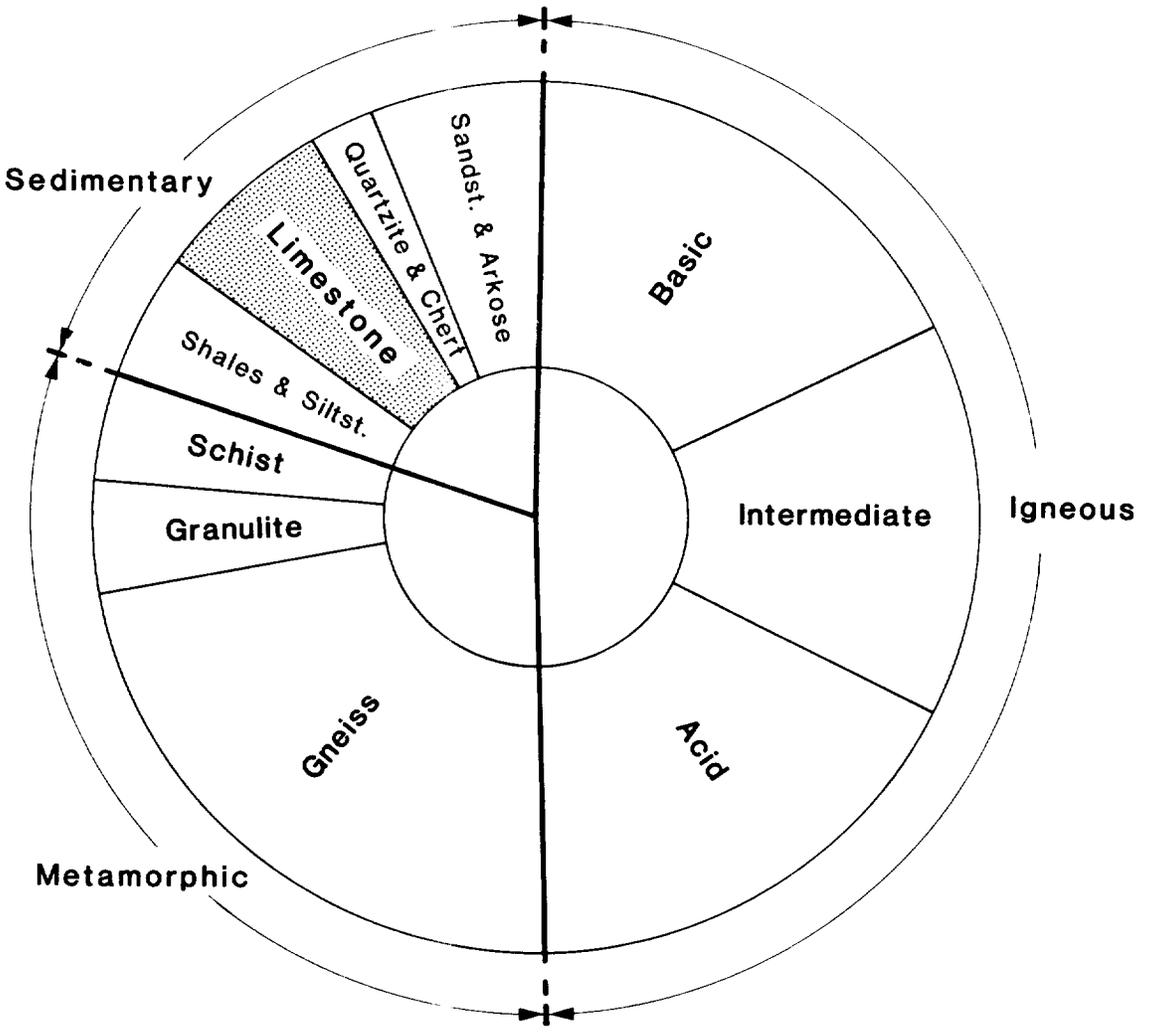

Figure 22 Pie chart showing the distribution of rock types in ice-rafted material in the King's Trough region (44°N, 22°W) (dredge hauls D9561-D9566).

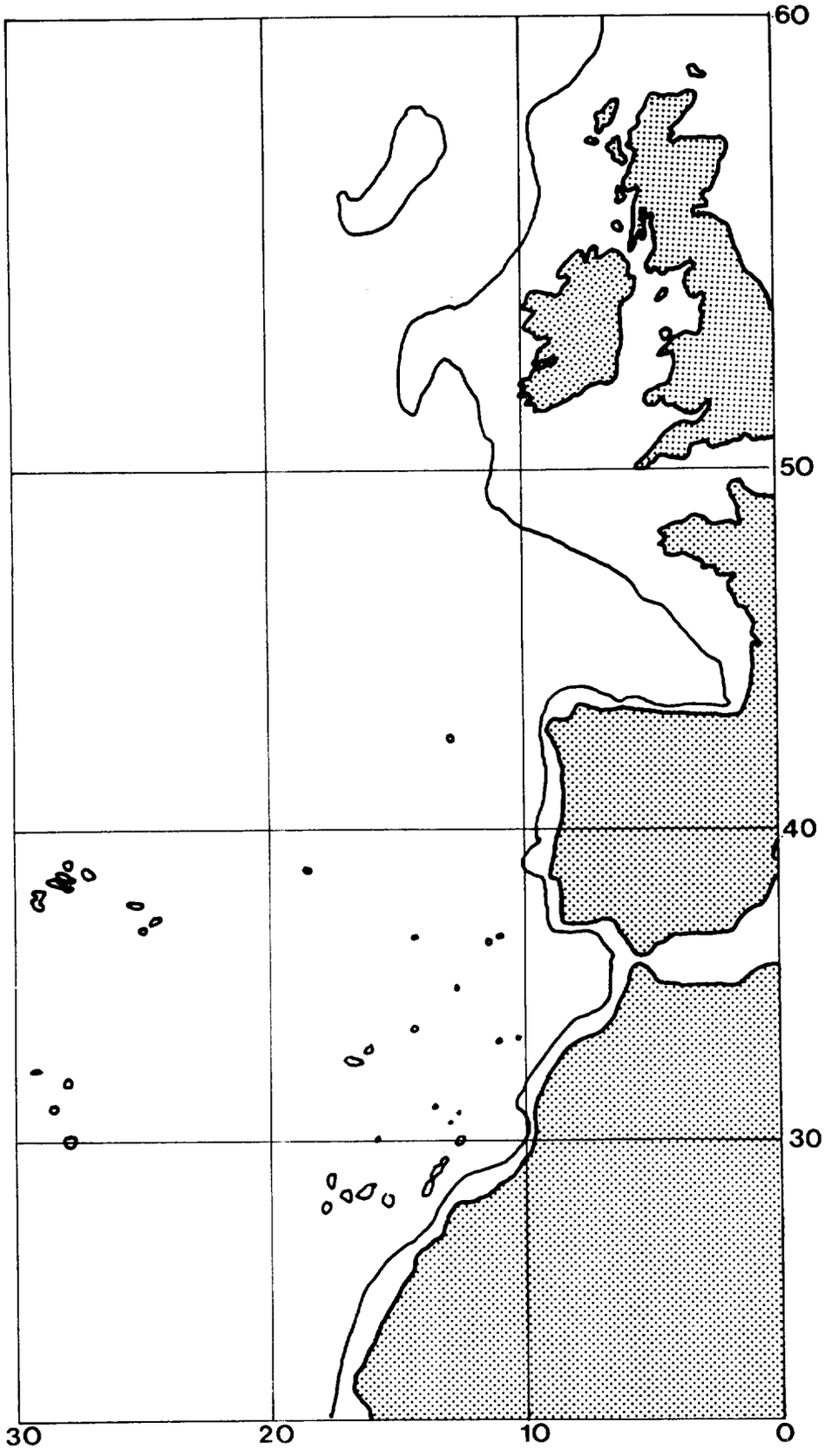

Figure 23 Chart showing 500 m isobath.

some of the seamounts in the NE Atlantic ocean have trapped passing icebergs, so experiencing a greater than normal input of ice-rafted debris.

Surface eddy currents

Studies of individual icebergs tracked by satellite have shown that they often divert from their course for short periods of time to complete a small circle before continuing (Tchernia & Jeannin, 1983). This behaviour is a way of slowing the progress of the iceberg and increasing deposition of material on to the seafloor over which it is taking place.

Satellite-tracked buoys are used to plot surface water movements. In the centre of large water masses, satellite-tracked buoys follow relatively straight paths. At the fronts between water masses, however, the buoys are caught by eddies forming at the front and they have been seen to cross the same point up to three times (Gould, in press). In his analysis of ice-rafted sand in deep-sea cores, Ruddiman (1977) drew a chart (Figure 1) showing deposition rates for ice-rafted material. This axis of increased deposition is believed to coincide with the position of the polar front where ice reaches water warm enough in which to melt. Following the study of satellite-tracked buoys, it would appear that the eddying of icebergs would provide a significant process by which increased deposition of ice-rafted material may take place.

That "axes" of deposition may occur has already been shown for the 50°N latitude (Ruddiman, 1977; Fig. 1). There are, as yet, insufficient data to extend Ruddiman's work to the south. It appears, however, that more southerly fronts like the Azores front (Gould, in press) may have caused similarly "axial" deposition. This process may be enhanced by the bottom topography. Gould discusses the influence of bottom topography upon the generation of meanders and eddies. It appears likely from his work that both the King's Trough and Great Meteor "shallows" are capable of affecting surface water circulation patterns. These areas are, therefore, likely to have experienced higher inputs of ice-rafted material than other areas away from fronts and topographic highs. Though this process cannot be quantified with the available data, it should be borne in mind for site selection purposes.

Boulder burial

Studies of the hydrodynamics of boulders sinking through the water column have shown that boulders larger than 25 cm fall through the water column with turbulent rather than laminar flow. This means that boulders larger than 25 cm

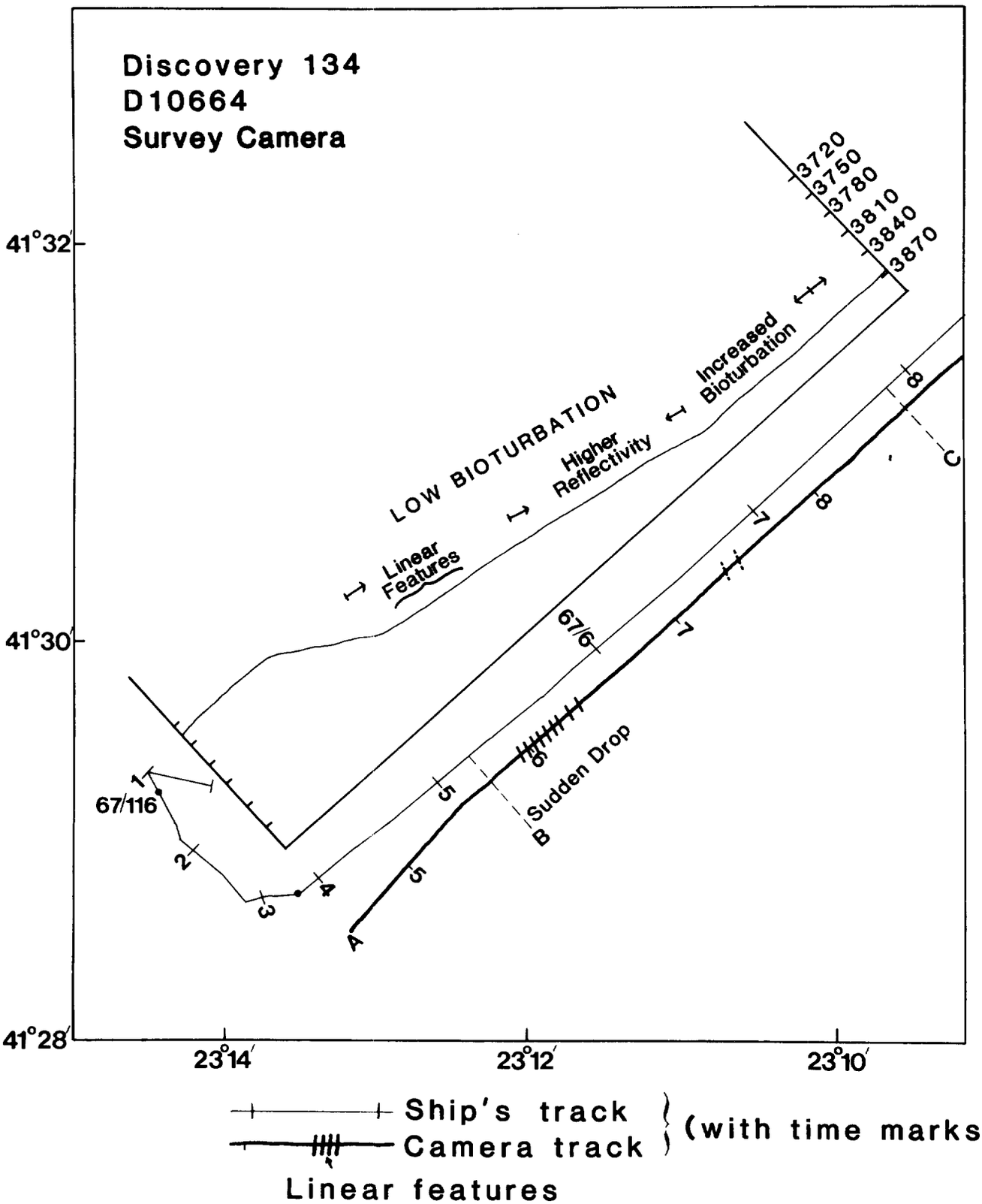

Figure 24 Chart and cross-section showing some of the features observed during a WASP camera run on the King's Trough Flanks (43°N, 23°W).

(diameter) may fall fast enough to penetrate the sediment and become completely obscured (Nicholson, pers. comm.). According to all the grain size observations made so far, even on rock outcrop, erratic boulders larger than 25 cm should only rarely be recovered as the areas sampled are too small. The effect of boulder burial on the direct sampling programme is, therefore, slight. Results from the camera may be affected, however, as, firstly, it samples large areas and, secondly, it is only suitable for observing larger objects (larger than 10 cm). It is interesting to note here that a boulder 26 cm in diameter was photographed in the King's Trough Flank region (D10656). However, since this boulder is close to the calculated limit for turbulent flow, this should not be taken as evidence that the predictions of boulder burial are false (Nicholson, pers. comm.).

Seafloor processes themselves may cause burial to occur. The most straightforward is natural sedimentation. The lowest sedimentation rates observed during this work were at 25°N in an area of pelagic clay (Table 1a). The burial rates for boulders on these clays and pelagic oozes can be estimated fairly accurately. In GME, however, sedimentation varies between normal pelagic sedimentation to geologically instantaneous turbidity current events. In the GME area major turbidites occur on average every 40,000 years (Weaver & Kuijpers, 1983). In Table 1a the boulder count is not only affected by a recent turbidite cover, but also by the fact that the turbidite at the surface will still be soupy and have a much lower shear strength, so making boulder penetration more likely.

The effect of bioturbation on boulder burial is not clearly understood as yet. Evidence from the Porcupine Seabight (50°N) indicates that benthic organisms may be causing the burial of coarse clastic material (Kidd & Huggett, 1981). Other workers, however, have cited benthic organisms as being responsible for the maintenance of manganese nodules at the surface (Paul, 1976; Menard, 1976; Glasby, 1977; Piper & Fowler, 1980). Therefore, the role of the benthic community in pebble burial/exhumation is not understood and, for the present, will not be considered in this study.

Sediment winnowing

Figure 24 is a chart showing the track of a camera run (Station No. D10664), together with a bathymetric profile along the same line. Two anomalous features were observed by this camera run. The first was a series of nine parallel bands, 1-m wide approximately 75 m apart, seen on the steepest part of the slope

(gradient = 1/52). The bands appeared to consist of ice-rafted pebble material in random orientation. The second was that the occurrence of the benthic holothurian Pseudostichopus (D. Billett, pers. comm.) appeared to be restricted to the flat-lying seafloor at the foot of the slope. These two phenomena are best explained by current activity which may winnow sediment from the slope, so concentrating glacial erratics at the surface and starving the benthic foraging community of its food supply. A maximum bottom current of 18.8 cm/sec has been recorded in the KTF area (R. Dickson, pers. comm.); however, precise direction is unknown and may be altered by the bottom topography anyway. These linear and biological features may, therefore, represent either contour following currents or slope-related migration of fine sediment. A more detailed study of these features is to be undertaken in the future.

Although sediment winnowing is common on seamounts and hills it has only been observed in this one case on flat-lying ocean floors. It has also been observed on low abyssal hills and seamounts. It is felt, however, that winnowing has not affected the distributions of ice-rafted material over the areas where the quantitative studies were carried out.

Downcore variations in ice rafting

Clearly, the main problem with this work is that it only covers the upper 1.7 m of sediment (or 100,000 years), whereas in the base case scenario for disposal burial to a depth of 30 m is envisaged (Anderson, 1981). In addition, as shown by Ruddiman (1977), deposition rates of ice-rafted material have varied over many glacial/interglacial cycles as well as within the cycles themselves. He wrote that, of the 200,000 km^3 of ice-rafted detritus deposited in the North Atlantic in the past three million years, 120,000 km^3 were deposited in the past 1.2 million years. If we are to consider using any sites within the southern limits of ice rafting, therefore, a deep core must be obtained in order to calcuate accurately down-core variations in ice rafting. For the upper 1.7 m of sediment, however, Figures 15 and 16 provide a good basis for estimating downcore fluctuations and Figure 18 provides a rough guide for deeper sediments. Ruddiman's work (Fig. 11), though complicated by the occurrence of carbonate erratics, may be used for comparison.

CONCLUSIONS

(1) The maximum cumulative risk of encountering ice-rafted material is 0.5% down to oxygen isotope stage 5 (approximately 127,000 years BP) (at 42° latitude). By comparison, the risk is 0.46% at 50°and 0.02% at 31°N.

(2) The southernmost limit of ice-rafting is at 26°N.

(3) This study has covered material deposited during the last glacial/interglacial cycle (127,000 years). Estimates of impacts down to 30 m require deep core data to cover the whole of the Pleistocene (2.4 m.y.).

(4) Only in the KTF and GME areas are there sufficient data to provide estimates of impact risk. Lateral inhomogeneities in the deposition of ice-rafted material make interpolated estimates of ice-rafted material between data points unreliable. Sufficient data to cover the KTF and GME area have been recovered, however.

ACKNOWLEDGEMENTS

I would like to thank Professor W. Feld (Hamburg) and Projessor J. Cann (Newcastle), Dr. F. McCoy (Lamont), Jim Brodie (Woods Hole) and Nicole Lenotre (Brest) for their help in providing me with the rock dredge data for this project. I would like to thank Peter Challenor for his invaluable help with the mathematics used here. I would also like to thank the officers and crews of the research ships Challenger, Shackleton and Discovery for their help in collecting my own dredge and photographic data.

I would like to thank Gabrielle Mabley for typing this manuscript and Dr. Whitmarsh and Dr. Weaver for their constructive reviews.

REFERENCES

Aldred, R.G., Thurston, M.H., Rice, A.L. & Morley, D.R., 1976. An acoustically monitored opening and closing epibenthic sledge. Deep Sea Research, 23, pp. 167-174.

Anderson, D.R., 1981. Proceedings of the sixth annual NEA-Seabed Working Group Meeting, Paris, France, 2-5 February 1981. SANDIA Report, SAND 81-7427.

Barndorff-Nielsen, O., 1977. Exponentially decreasing distributions for the logarithm of particle size. Proc. Roy. Soc. Lond., A353, pp. 401-419.

Belderson, R.H., Kenyon, N.H. & Wilson, J.B., 1973. Iceberg ploughmarks in the North East Atlantic. Palaeo. Palaeo. Palaeo., 13, pp. 215-224.

Davies, T.A., Laughton, A.S., 1972. Sedimentary processes in the North Atlantic. Init. Rep. DSDP, XII, pp. 905-933.

Glasby, G.P., 1977. Why manganese nodules remain at the sediment/water interface. New Zealand Journ. Sci., 20, pp. 187-200.

Gould, W.J., in press. Physical oceanography of the Azores Front. Swallow festschrift volume of progress in oceanography. Pergamon Press.

Harland, W.B., Herod, K.N. & Krinsley, D.H., 1966. The definition and identification of tills and tillites. Earth Sci. Rev., 2, pp. 225-256.

Heezen, B.C. & Hollister, C.D., 1971. The Face of the Deep. Oxford University Press, New York, 659 pp.

Hessler, R.R. & Sanders, H.L., 1967. Faunal diversity in the deep sea. Deep Sea Research, 14, pp. 65-78.

Huggett, Q.J. & Kidd, R.B., 1984. The identification of ice-rafted and other exotic material in deep-sea dredge hauls. Geomarine letters, 23, pp. 23-29.

Il'In, A.V. & Shurko, I.I., 1968. Petrographic regionalisation of the coarse clastic deposits of the North east Atlantic. Izvestiya Akademii Navk SSR, Seriya Geologicheskaya, 9, pp. 126-129. Translated by N.C.P. Holland, IOS translation A3.

Kidd, R.B., Huggett, Q.J., Crease, S., 1980. The distribution of pebble material on the northeast Atlantic seabed: preliminary results. IOS Internal Document No. 84, 11 pp.

Kidd, R.B. & Huggett, Q.J., 1981. Rock debris on abyssal plains in the NE Atlantic: a comparison of epibenthic sledge hauls and photographic surveys. Oceanologica Acta, 4(1), pp. 99-104.

Kidd, R.B., Searle, R.C., Ramsay, A.T.S., Pritchard, H. & Mitchell, J., 1982.

The geology and formation of King's Trough, North East Atlantic Ocean. Marine Geology, 48, pp. 1-30.

Kidd, R.B., Searle, R.C., Weaver, P.P.E., Jacobs, C.L., Huggett, Q.J., Noel, M.J. & Schultheiss, P.J., 1983. King's Trough Flank: geological and geophysical investigations of its suitability for high-level radioactive waste disposal. IOS Report No. 166, 93 pp.

Kidd, R.B., Ruddiman, W. et al., in press. Init. Repts. DSDP Leg 94. Washington, U.S. Govt. Printing Office.

Menard, H.W., 1976. Time, chance and the origin of manganese nodules. Am. Sci., 64, pp. 519-525.

Nalwalk, A.J., Hersey, J.B., Reitzel, J.S. & Edgerton, H.E., 1961. Improved techniques of deep-sea dredging. Deep Sea Research, 8, pp. 301-302.

Ovenshine, A.T., 1966. Observations of iceberg-rafting in Glacier Bay, Alaska, and the identification of ancient ice-rafted deposits. Geol. Soc. Am. Bull., 81, pp. 891-894.

Paul, A.Z., 1976. Deep bottom photographs show that benthic organisms remove sediment cover from manganese nodules. Nature, 236, pp. 50-51.

Piper, D.Z. & Fowler, B., 1980. New constraints on the maintenance of manganese nodules at the sediment surface. Nature, 286, pp. 880-883.

Pisias, N.G. & Moss, T.C., Jr., 1980. The evolution of Pleistocene climate: A time series approach. Earth Planet. Sci. Lett., 52, pp. 450-458.

Rawson, M.D., Ryan, W.B.F., et al., 1978. Ocean floor and polymetallic nodules. Office of the Geographer, Washing D.C. (Map at scale 1:23,230,300).

Ruddiman, W.F., 1977. Late Quaternary deposition of ice-rafted sand in the sub-polar North Atlantic (Latitude 40°N to 65°N). Bull. Geol. Soc. Am., 88, pp. 1813-1827.

Searle, R.C., 1979. Guidelines for the selection of sites for the disposal of radioactive wastes on or beneath the ocean floor. IOS Internal Report No. 91.

Shackleton, N.J., Backman, J., Zimmeran, H., Kent, D.V., Hall, M.A., Roberts, D.G., Schnitker, D., Baldauf, J.G., Desprairies, A., Homrighausen, R., Huddlestun, P., Keene, J.B., Kaltenback, A.J., Krumsiek, K.A.O., Morton, A.C., Murray, S.W. & Westberg-Smith, J., 1984. Oxygen isotope calibration of the onset of ice-rafting and history of glaciation in the North Atlantic region. Nature, 307, (5952), pp. 620-623.

Somerville, B.T., 1950. Ocean passages for the world. Hydrographic Department

of the Admiralty. London, 367 pp., 7 charts.

Sukhov, B.P., 1977. Measurement of iceberg draft. Proc. 1st International Conference on Iceberg Utilisation, pp. 265-275.

Tchernia, P. & Jeanin, P.F., 1983. Quelques aspects de la circulation oceanique Antarctique reveles par l'observation de la derive d'icebergs (1972-1983). Toulouse: Centre National d'Etudes Spatiales/Expeditions Polaires Françaises (CNRS)/Museum National d'Histoire Naturelle.

United States Navy Oceanographic Office, 1968. Publication No. 700, ICE.

Weaver, P.P.E. & Kuijpers, A., 1983. Climatic control of turbidite deposition on the Madeira Abyssal Plain. Nature, 306 (5941), pp. 360-363.

FIGURE CAPTIONS

Figure 1. Occurrence of ice-rafted material in the North Atlantic reported in literature prior to this project on glacial erratics. Black squares indicate erratics in dredges and dots and triangles indicate erratics in DSDP and Lamont cores respectively. Contours indicate maximum rate of deposition of glacial sands in milligrams per square centimetre per thousand years (from Ruddiman, 1977); also shown are inferred limits of ice rafting (from Davies & Laughton, 1971).

Figure 2. Chart showing the locations of the dredge hauls examined. Asterisks indicate that the dredge hauls contained ice-rafted material.

Figure 3. Chart showing the locations of the cores examined in the literature survey. Asterisks indicate that exotic pebbles were reported in the core descriptions. The cores used in Ruddiman's study (1977) and D10333 are indicated with triangles and an asterisk respectively.

Figure 4. Chart showing the locations of all the camera stations examined. The asterisks indicate the stations at which exotic material was observed.

Figure 5. (i) Pipe dredge. A type of rock dredge used until the early 1960s by many institutions. The mouth opening is 15 cm in diameter.

(ii) Rock dredge. A generalised picture of a rock dredge for use on rock outcrops. These, in various modified forms are used by most institutes and universities of the world. The mouth opening is usually around 1 m wide.

Figure 6. (i) IOS Epibenthic Sledge. A sampling device used by the IOS benthic biology group for sampling sedimented sea floors. It is an acoustically-monitored device which relays information to the ship on camera operation, sledge attitude, distance travelled over the sea floor and absolute water depth. The mouth opening is 1.2 m wide.

(ii) WHOI sampling sledge. Also used by marine biologists for sampling sedimented surfaces, this device has no camera or positive monitoring system and may be used either way up. It

has a mouth opening of 1.2 m.

(iii) Agassiz trawl. This is the simplest dredge used on sediment surfaces. It has no positive monitoring system and may be used either way up. The mouth opening is adjustable and is usually set from 1-4 m wide.

Figure 7. Linear plot of cumulative size data from Station G21.

Figure 8. Log-linear plot of cumulative size data from Station G21.

Figure 9. Log-normal plot of cumulative size data from Station G21.

Figure 10. Log-normal plot of all stations from which size data could be obtained.

Figure 11. Downcore estimates of ice-rafted input taken from two of Ruddiman's (1977) cores: V29-177 (at 41.5°N) and V29-179 (at 44°N).

Figure 12. Downcore variations in ice-rafted input for core D10333. The estimates have been made at 8 cm intervals and have been normalised to produce numbers of ice-rafted particles per 100 cc.

Figure 13. WASP (Wide Area Survey Photography) camera system. This system has six flash units illuminating an area of the seafloor from approximately 10m which is photographed by one or two cameras. At least 1600 frames may be photographed per run, covering a maximum area of 100,000 m^2 of seafloor per run. The height of the camera from the seafloor is monitored using a near-bottom echo sounder, the output of which is displayed both on board the ship and in the corner of the frame being photographed.

Figure 14. Downcore graph of D10333 showing correction factors to be applied to impact risk data at surface when accumulating the risk downcore.

Figure 15. Graph showing risk of encountering ice-rafted material for all material between 1.5 and 7800 cm diameter downcore. Three lines have been drawn to show the differences between the risks calculated in the three areas for which there are data.

Figure 16. Graph showing risk of encountering ice-rafted material at 42°N. Three lines have been drawn to show the risk for different ranges of grain sizes.

Figure 17. Graph showing effect of turbidite sedimentation on risk of encountering ice-rafted material between 1.5 cm and 7,800 cm

diameter. This graph is based upon Line A (Fig. 15) and core 82PCS13 from the Great Meteor East area.

Figure 18. Graph illustrating possible risks of encountering ice-rafted material down to a depth of 20 m. TO BE USED AS A ROUGH GUIDE ONLY.

Figure 19. Chart showing rock-type distribution for all the IOS sediment surface dredges.

Figure 20. Coal briquette dredged from sediments at 46°N, 17°W with its provenance clearly marked! [PATENTS CARDIFF].

Figure 21. Chart showing major steamship routes where deposits of clinker are likely to be found (taken from Somerville, 1950).

Figure 22. Pie chart showing the distribution of rock types in ice-rafted material in the King's Trough region (44°N, 22°W) (dredge hauls D9561-D9566).

Figure 23. Chart showing 500 m isobath.

Figure 24. Chart and cross-section showing some of the features observed during a WASP camera run on the King's Trough Flanks (43°N, 23°W).

TABLE LIST

TABLE 1 - Unprocessed Grain-size Data from Dredge Hauls

SIZE CLASSES (cm diameter)	TABLE OF FREQUENCIES								COMBINED STATIONS (excluding D9825
	..... (Station Numbers)								
	G3	G5	G21	G32	G47	#1 51109	#9 + 14 D9756	D9825	
1.5-2.5	1508	2515	2130	560	620	88	60	656	7481
2.5-3.5	361	348	557	217	308	22	29	355	1842
3.5-4.5	62	81	129	86	101	10	9	104	478
4.5-5.5	12	33	85	17	40	5	4	33	196
5.5-6.5	1	5	30	6	21	2	1	8	66
6.5-7.5	1	2	10	5	1	1	-	4	20
7.5-8.5	0	1	5	1	-	0	-	6	7
8.5-9.5	1	1	4	0	-	2	-	3	8
9.5-10.5	-	0	2	0	-	-	-	5	2
10.5-11.5	-	0	1	0	-	-	-	2	1
11.5-12.5	-	1	1	1	-	-	-	2	-
12.5 <	-	-	-	1	-	-	-	6	-
TOTALS	1946	2987	2954	794	1091	130	103	1184	10101
Least squares fit to log-normal distribution — Log mean	0.29	0.20	0.50	0.55	0.68	0.41	0.55	0.62	
Least squares fit to log-normal distribution — Variance	0.48	0.52	0.46	0.47	0.41	0.64	0.54	0.43	
AREA OF SEAFLOOR COVERED (m^2)	32,060	28,840	35,320	34,120	20,620	2,266	2,521		
No. of ERRATICS/km^2 (empirical)	60,699	120,250	83,635	23,271	52,910	57,370	40,857		

TABLE 2 - Photographic data on non-biogenic material

(a) WASP Data

	26°N PELAGIC CLAYS	31°N TURBIDITES	42°N PELAGIC OOZES
Sedimentation Rate	0.2 cm/1000 yrs	10 cm/1000 yrs	3 cm/1000 yrs
No. of erratics/km^2	60/km^2*	10/km^2**	94/km^2 > 10 m dia.
(corrected) "	60/km^2	50/km^2	1567/km^2

* based on one erratic only

** most recent turbidite deposited within the last 10,000 years

(b) Benthic Sledge Data

			> 10 cm dia.	
			DREDGED	PHOTOGRAPHED
STATION	POSITION	ROCK TYPE*	Debris/km^2	Debris/km^2
9775#3	50°57'N 12°22'W	90% clinker	40/km^2	0
9756#14	50°04'N 13°56'W	48% clinker	20/km^2	10/km^2
9756#9	49°47'N 14°02'W	68% clinker	38/km^2	30/km^2

* only two rock types were considered: clinker, glacial erratics.

TABLE 3 - Data from Station G21

SIZE CLASSES		No. RECOVERED IN RUN	FREQUENCY x AREA
DIAMETER (cm)	EQUIVALENT CROSS SECTIONAL AREA (cm^2)	Frequency	(cm^2)
1.5-2.5	3.14	2130	6688
2.5-3.5	7.07	557	3938
3.5-4.5	12.57	129	1622
4.5-5.5	19.63	85	1669
5.5-6.5	28.27	30	848
6.5-7.5	38.48	10	385
7.5-8.5	50.27	5	251
8.5-9.5	63.62	4	254
9.5-10.5	78.54	2	157
10.5-11.5	95.03	1	95
11.5-12.5	113.10	1	113
12.5 <	(122.72)		16,020 cm^2

Total projected area of glacial erratics - 1,602 m^2

Area covered by dredge - 35,320 m^2

Therefore, probability of encountering an erratic in top 3 cm = 0.0045%

TABLE 4 - Downcore Correction Factors based upon core No. D10333

Depth (i)	Correction Factor $\frac{E_i}{E_1}$
0-8	1
8-16	2.63
16-24	6.35
24-32	13.01
32-40	9.59
40-48	5.21
48-56	9.22
56-64	9.28
64-72	4.09
72-80	1.2
80-88	2.62
88-96	1.13
96-104	0.342
104-112	0.32
112-120	0.68
120-128	0.5
128-136	0.39
136-144	0.16
144-152	0.07
152-160	0
*160-164	0.02
**164-174	0.15

* This was a narrow sample so

$$R_i = \frac{4}{3} r \cdot \frac{E_i}{E_1}$$

** This was a thick sample so

$$R_i = \frac{10}{3} r \cdot \frac{E_i}{E_1}$$

TABLE 5

LATITUDE	DREDGE STATIONS	TOTAL AREA COVERED	No. of PARTICLES 1.5-7.5 cm ($P(p_1, p_2)$
50°N	51109#1 D9756 #9 & 14	4,724 m^2	233
42°N	G3 G5 G21 G47	112,840 m^2	8967
30°N	D10328	4,444 m^2	6

ζ = 0.48 mean

σ = 0.49 variance

TABLE 6 - Percentage (by count) of soluble sand-sized (> 65 n) material in three cores

S8-79-1

Soluble 10.3%
Insoluble 89.7% average for whole core

A maximum of 100% soluble material was recorded at 198 cm.

S8-79-2

Soluble 12%
Insoluble 88% average for whole core

A maximum of 14% soluble material was recorded at 15 cm.

S8-79-3

Soluble 18%
Insoluble 78% average for whole core

A maximum of 26% soluble material was recorded at 21 x 146 cm.

APPENDIX LIST AND LEGEND

Appendix 1: Positions of all dredge stations examined.
Appendix 2: Positions of all cores examined.
Appendix 3: Positions of all camera stations examined.

Explanation of symbols

Example	D3817	4341.5N 1239.4W	3
		Position (degrees and decimal minutes)	Result

Station No. Codes

Code	Vessel	Source
A	Atlantis	Woods Hole Oceanographic Institute
ALB	Albatross	Swedish Deep Sea Expedition
CA	Caryn	Woods Hole Oceanographic Institute
CHN	Chain	Woods Hole Oceanographic Institute
C	Challenger	Institute of Oceanographic Sciences
D	Discovery	Institute of Oceanographic Sciences
DSDP	Glomar Challenger	Deep Sea Drilling Project
EKV	Ekvator	USSR Hydrographic Service
G	Not Known	Hamburg Isotopen Laboratorium
H	Hudson	Bedford Institute of Oceanography
JC	Jean Charcot	Centre Oceanologique de Bretagne
K	Kane	US Navy Hydrographic Office
KNR	Knorr	Woods Hole Oceanographic Institute
LK	Lord Kelvin	Cable-laying ship
MB	Not Known	University College of North Wales
ML	Michail Lomonojov	USSR Marine Hydrographic Institute
PL	Peter Lebedev	USSR Academy of Science
REH	Rehobath	US Naval Hydrographic Office
RC	Robert D. Conrad	Lamont-Doherty Geological Observatory
S	Shackleton	Institute of Oceanographic Sciences
SED	Sedov	USSR Hydrographic Service
SMBA	Not Known	Scottish Marine Biological Association
SP	San Pablo	US Navy Hydrographic Office
TRI	Trident	University of Rhode Island
V	Vema	Lamont-Doherty Geological Observatory
ALBAT) GMA) GIB)	Not Known	Centre Oceanologique de Bretagne
NORAT) NEST)		
HHP	-----	From Heezen and Hollister (1971)
NL	Not Known	Rijks Geologische Dienst, Holland

Results Code (last column)

3 = No pebbles found
1 = Erratics (positively identified)
7 = Pebbles found (possibly erratics)

Positions of the dredge stations examined.

D7709	72	6006.9 N 1942.4 W	1
D7709	73	6007.1 N 1930.3 W	3
D7709	62	5958.8 N 1959.4 W	3
D7709	66	5958.7 N 1953.5 W	3
D7711	52	5253.3 N 1952.4 W	3
D7711	57	5248.7 N 2003.7 W	3
D7711	58	5247.7 N 2005.0 W	3
D7711	62	5250.0 N 2002.8 W	3
D7711	85	5305.8 N 1955.7 W	3
D9756	14	5004.0 N 1355.6 W	1
C51408	1	5103.6 N 1255.0 W	1
C51408	1	5103.6 N 1255.0 W	1
C51405	1	5201.8 N 1331.0 W	1
C51405	1	5201.8 N 1331.0 W	1
C51412	1	5016.9 N 1329.3 W	1
C51412	1	5016.9 N 1329.3 W	1
C51411	2	5022.3 N 1301.2 W	1
C51411	2	5022.3 N 1301.2 W	1
C51407	1	5119.5 N 1305.0 W	3
C51407	1	5119.5 N 1305.0 W	3
C51403	3	5136.8 N 1259.1 W	3
C51403	3	5136.8 N 1259.1 W	3
C51403	1	5137.7 N 1259.8 W	3
C51403	1	5137.7 N 1259.8 W	3
C51406	1	5123.3 N 1322.4 W	3
C51406	1	5123.3 N 1322.4 W	3
C51403	6	5137.8 N 1258.9 W	3
C51403	6	5137.8 N 1258.9 W	3
C51403	2	5137.4 N 1259.2 W	3
C51403	2	5137.4 N 1259.2 W	3
C51403	4	5136.7 N 1259.6 W	3
C51403	4	5136.7 N 1259.6 W	3
C50902	1	5117.4 N 1245.2 W	1
C50902	1	5117.4 N 1245.2 W	1
C50913	1	5011.9 N 1339.8 W	1
C50913	1	5011.9 N 1339.8 W	1
C50914	1	5017.2 N 1329.4 W	1
C50914	1	5017.2 N 1329.4 W	1
C50915	1	5028.9 N 1310.5 W	1
C50915	1	5028.9 N 1310.5 W	1
C51110	4	5014.2 N 1327.0 W	1
C51110	4	5014.2 N 1327.0 W	1
C51102	1	5201.9 N 1327.0 W	1
C51102	1	5201.9 N 1327.0 W	1
C51103	4	5147.9 N 1309.5 W	3
C51103	4	5147.9 N 1309.5 W	3
C51106	1	5028.9 N 1305.8 W	1
C51106	1	5028.9 N 1305.8 W	1
C51112	4	5125.5 N 1356.9 W	1
C51112	4	5125.5 N 1356.9 W	1
C51110	3	5016.4 N 1330.9 W	3
C51110	3	5016.4 N 1330.9 W	3

C51105	3	5104.4 N 1253.7 W	1
C51105	3	5104.4 N 1253.7 W	1
C51110	4	5014.2 N 1327.0 W	1
C51110	4	5014.2 N 1327.0 W	1
D9046	0	4658.5 N 1100.6 W	3
D9638	2	4950.2 N 1407.3 W	1
C51414	2	4947.2 N 1410.2 W	1
C50910	1	4949.6 N 1440.5 W	1
C50907	1	4953.7 N 1330.4 W	1
C50907	1	4953.7 N 1330.4 W	1
C51216	1	4948.1 N 1410.3 W	1
C51216	3	4950.1 N 1407.1 W	1
C51216	5	4948.7 N 1404.7 W	1
C51109	1	4950.7 N 1402.1 W	1
D10604		5222.0 N03143.0 W	3
D10605		5221.0 N03142.0 W	1
D10608		5220.0 N03141.0 W	1
D10609		5221.0 N03146.0 W	1
GMA2/07		4759.8 N01208.4 W	1
GMA2/08		4759.8 N01207.7 W	1
GMA2/09		4758.9 N01206.1 W	1
GMA2/10		4759.2 N01207.1 W	1
GMA2/12		4747.5 N01216.2 W	1
GMA2/13		4746.0 N01219.6 W	1
GMA2/18		4834.8 N01234.3 W	1
GMA2/20		4826.6 N01119.9 W	1
GMA2/21		4836.3 N01110.1 W	1
V27/6		4809.1 N01555.9 W	3
V28/8		4820.0 N01100.0 W	3
CHN13/08		4846.0 N01002.2 W	3
CHN13/09		4847.0 N01001.5 W	3
CHN43/37		4511.0 N02758.0 W	1
SMBA/6		5503.0 N01229.0 W	3
SMBA/26		5635.0 N00908.0 W	1
SMBA/128		5531.0 N01024.0 W	1
SMBA/139		5535.0 N01025.0 W	3
SMBA/144		5713.0 N01020.0 W	1
D7709.72		6009.0 N01942.0 W	3
SMBA/27		5440.0 N01216.0 W	1
SMBA/55		5440.0 N01216.0 W	3
SMBA/56		5440.0 N01216.0 W	3
SMBA/59		5440.0 N01220.0 W	3
SMBA/111		5440.0 N01216.0 W	3
SMBA/118		5439.0 N01214.0 W	3
SMBA/129		5439.0 N01217.0 W	3
SMBA/135		5439.0 N01216.0 W	3
SMBA/137		5434.0 N01219.0 W	3
SMBA/140		5440.0 N01216.0 W	1
SMBA/141		5444.0 N01214.0 W	3
SMBA/143		5441.0 N01214.0 W	3
SMBA/142		5439.0 N01216.0 W	3
SMBA/161		5052.0 N01227.0 W	1

SMBA/164	5437.0	N01222.0 W	3
D9775.3	5057.0	N01222.0 W	1
D9640.1	5003.0	N01351.0 W	1
D9638.2	4950.0	N01407.0 W	1
D9560	4350.7	N02156.7 W	3
D9561	4350.2	N02152.9 W	1
D9562	4354.8	N02156.5 W	1
D9563	4353.7	N02157.6 W	1
D9564	4359.1	N02154.0 W	1
D9565	4352.9	N02157.9 W	1
D9566	4402.6	N02148.7 W	3
D9572	4353.9	N02207.2 W	3
D5610	4251.0	N02016.5 W	1
D5614	4253.5	N02016.0 W	1
D5623	4307.5	N01939.5 W	3
D5626	4250.8	N01959.5 W	1
D5627	4251.5	N01956.0 W	1
D5636	4242.5	N02014.9 W	3
D5951	4235.8	N01157.5 W	1
D5975	4254.2	N02012.8 W	3
D5976	4253.6	N02015.7 W	3
D5978	4254.6	N02011.2 W	1
D5979	4250.7	N02016.2 W	1
D5981	4251.5	N02016.5 W	3
D5983	4254.4	N02013.4 W	3
D5607	4254.0	N02008.5 W	1
V27/7	4336.8	N01541.4 W	3
V27/8	4344.7	N02151.6 W	1
V27/9	4359.6	N02212.5 W	3
V27/10	4229.5	N02900.5 W	3
V27/11	4219.9	N02709.3 W	3
V27/12	4220.5	N02552.6 W	3
V27/17	4035.0	N01355.0 W	3
CHN43/38	4434.0	N02809.2 W	1
CHN43/40	4239.3	N02859.1 W	3
CHN43/41	4242.4	N02901.5 W	1
CHN82/6	4255.4	N02855.0 W	3
CHN82/1	4155.0	N02913.0 W	3
ATL13/1(75)	4229.0	N02856.0 W	1
ALBAT/5	4437.6	N01327.7 W	3
ALBAT/7	4311.0	N01200.0 W	1
ALBAT/8	4057.0	N01134.4 W	3
CHN82/2	4228.5	N02841.1 W	3
CHN82/3	4231.0	N02915.0 W	3
G3	4324.0	N01506.0 W	1
G5	4257.4	N01453.4 W	1
G7	4243.3	N01442.0 W	1
G12	4228.0	N01423.8 W	1
G13	4211.2	N01407.0 W	1
G16	4149.2	N01354.7 W	1
G21	4147.4	N01425.7 W	1
G24	4224.9	N01432.0 W	1

	G29	4239.7	NO1412.7 W	1
	G32	4548.6	NO1715.8 W	1
	G47	4549.8	NO1714.2 W	1
	G52	4557.5	NO1658.9 W	1
	G60	4309.3	NO1926.5 W	1
	G64	4313.8	NO1929.9 W	1
	G65	4308.9	NO1925.8 W	1
	G66	4320.5	NO1921.1 W	1
	HUD 1	4539.0	NO2809.0 W	1
	THET 5	4514.0	NO2948.0 W	3
	THET 6	4514.0	NO2950.0 W	3
	THET 8	4545.0	NO2914.0 W	3
	HUD 9	4521.0	NO2802.0 W	1
	HUD 14	4517.0	NO2857.0 W	3
	HUD 33	4517.0	NO2856.0 W	3
	HUD 35	4515.0	NO2858.0 W	3
	HUD 47	4522.0	NO2813.0 W	1
	HUD 48	4522.0	NO2806.0 W	1
	HUD 56	4513.0	NO2800.0 W	1
	HUD 103	4552.0	NO2805.0 W	3
	HUD 106	4522.0	NO2812.0 W	1
	HUD 108	4550.0	NO2818.0 W	3
	HUD 112	4529.0	NO2817.0 W	3
	HUD 116	4566.0	NO2758.0 W	3
	HUD 118	4544.0	NO2856.0 W	1
	HUD 120	4542.0	NO2856.0 W	3
	HUD 123	4545.0	NO2856.0 W	1
	HUD 128	4544.0	NO2814.0 W	3
	HUD 133	4531.0	NO2934.0 W	3
	HUD 134	4516.0	NO2926.0 W	3
	HUD 143	4530.0	NO2836.0 W	3
	HUD 147	4529.0	NO2836.0 W	1
	HUD 156	4548.0	NO2907.0 W	3
	HUD 159	4546.0	NO2859.0 W	3
	HUD 165	4513.0	NO2952.0 W	3
	HUD 168	4523.0	NO2735.0 W	3
	HUD 173	4537.0	NO2743.0 W	3
	HUD 182	4518.0	NO2723.0 W	3
	HUD 187	4530.0	NO2720.0 W	1
	HUD 190	4521.0	NO2710.0 W	1
	HUD 192	4535.0	NO2703.0 W	3
	HUD 193	4536.0	NO2715.0 W	3
	HUD 197	4541.0	NO2748.0 W	1
	HUD 198	4540.0	NO2742.0 W	1
D9817		4530.0	NO2717.0 W	1
D9818		4533.0	NO2717.0 W	1
D9822		4533.0	NO2717.0 W	1
D9825		4558.0	NO1957.5 W	1
D9827		4557.5	NO1956.5 W	1
D8511	2	4149.6	N 1105.9 W	3
D8514	1	4307.6	N 1110.0 W	3
D9041	0	4155.4	N 1114.5 W	3

D7423	1	3750.8 N 2704.0 W	3
D7424	1	3727.4 N 2651.8 W	3
D7476	1	3720.2 N 2521.2 W	3
GIB/2		3501.1 NO1255.6 W	3
GIB/4		3635.5 NO1143.0 W	3
GIB/5		3648.6 NO1112.4 W	3
GIB/6		3643.2 NO1121.5 W	3
GIB/7		3730.5 NO1350.4 W	3
GIB/8		3640.5 NO1542.1 W	3
GIB/10		3656.4 NO1846.8 W	3
GIB/11		3730.6 NO1849.9 W	3
GIB/12		3702.5 NO2005.3 W	3
GIB/14		3633.1 NO2652.3 W	3
GIB/25		3809.5 NO2707.9 W	3
CYA/2		3625.0 NO1129.0 W	3
CYA/4		3625.7 NO1136.7 W	3
CYA/5		3631.7 NO1123.1 W	1
CYA/6		3634.2 NO1125.3 W	3
CYA/7		3632.5 NO1105.6 W	3
CYA/8		3638.4 NO1109.9 W	3
CYA/9		3636.8 NO1140.7 W	3
CYA/10		3637.2 NO1142.6 W	3
CYA/11		3633.5 NO1135.7 W	3
CYA/12		3636.5 NO1140.2 W	3
CYA/13		3640.8 NO1103.2 W	3
CYA/14		3642.1 NO1105.2 W	3
CYA/15		3640.9 NO1106.9 W	3
GOR/14		3644.2 NO1103.7 W	3
NORAT/6		3636.5 NO2638.1 W	3
NESTL/15		3645.0 NO1124.0 W	3
V27/13		3843.7 NO1806.3 W	3
V27/14		3637.1 NO1409.8 W	3
V27/15		3647.0 NO1415.6 W	3
V27/16		3645.8 NO1415.7 W	3
V30/12		3508.0 NO3536.0 W	1
ATL13/2		3751.0 NO2552.0 W	3
ATL13/3		3935.0 NO3112.0 W	3
ATL77/10		3635.0 NO3331.5 W	1
ATL73/12		3630.6 NO3325.3 W	3
KNR42/24		3636.4 NO3328.5 W	3
KNR42/27		3650.9 NO3332.5 W	3
KNR42/30		3631.9 NO3329.4 W	3
CHN7/19		3505.0 NO1213.0 W	3
CHN7/20		3505.0 NO1213.0 W	3
D7424.1		3727.0 NO2652.0 W	3
D7423.1		3751.0 NO2704.0 W	3
GIB/1		3459.3 NO1257.2 W	3
KNR42/33		3448.6 NO5713.4 W	1
CHN7/1		3002.0 NO2834.0 W	1
CHN7/2		3002.0 NO2833.0 W	3
CHN7/21		3344.0 NO1420.0 W	3
CHN7/22		3344.0 NO1420.0 W	3

CHN7/23	3344.0	N01420.0 W	3
CHN7/24	3000.0	N02825.0 W	3
CHN7/25	3000.0	N02823.0 W	3
CHN7/26	3000.0	N02833.0 W	1
CHN7/27	3000.0	N02830.0 W	3
CHN21/8	2949.0	N02840.0 W	3
CHN21/10	2949.0	N02840.0 W	3
CHN21/11	2949.0	N02840.0 W	3
CHN21/13	2947.0	N02819.0 W	3
CHN21/14	2947.0	N02820.0 W	3
CHN21/15	2946.3	N02819.0 W	3
D9035.1	3406.0	N01156.0 W	3
D8682.5	2534.0	N01640.0 W	3
D8519.7	2402.0	N01659.0 W	3
D8933.3	2456.0	N01801.0 W	1
D8933.4	2458.0	N01757.0 W	3
D9128.10	2418.0	N03028.0 W	3
D9129.1	2306.0	N02759.0 W	3
D9128.6	2411.0	N03027.0 W	3
D8524.1	2046.0	N02243.0 W	3
D8524.6	2044.0	N02244.0 W	3
D8521.6	2048.0	N01853.0 W	3
D9131.10	2015.0	N02136.0 W	3
D8532.6	1348.0	N01808.0 W	3
D8540.1	1116.0	N01823.0 W	3
D10315	2612.0	N02559.0 W	3
D10328	3025.0	N02405.0 W	1
D10978	3238.0	N02419.0 W	3

Positions of the core stations examined.

A152	88	3905.0 N 2325.0 W	3
A180	31	2926.0 N 2702.0 W	3
A180	33	2907.0 N 2615.0 W	3
A180	35	2905.0 N 2608.0 W	3
ALB	215	2955.0 N 1732.0 W	3
ALB	288	4108.0 N 3150.0 W	3
ALB	289	4112.0 N 3130.0 W	3
ALB	290	4135.0 N 2937.0 W	3
ALB	292	4216.0 N 2636.0 W	3
ALB	293	4223.0 N 2602.0 W	3
ALB	296	4227.0 N 2108.0 W	3
ALB	297	4304.0 N 1940.0 W	3
ALB	299	4741.0 N 1243.0 W	3
C67	14	4528.06N 425.05W	3
CA	10	3757.0 N 2415.0 W	3
CA	15	3706.0 N 1137.0 W	3
CHN13	4/4P	5353.0 N 2412.0 W	3
CHN21	14/14G	3332.0 N 1811.0 W	3
CHN21	15/15G	3400.0 N 1551.0 W	3
CHN43	102/28	4530.0 N 2750.0 W	7
CHN43	106/30	4436.0 N 2810.0 W	3
CHN43	109/32	4237.1 N 2844.8 W	3
CHN43	115/33	4238.1 N 2848.4 W	3
CHN82	21/1PG	3609.5 N 716.3 W	3
CHN82	22/2PG	3539.0 N 1342.0 W	3
CHN82	23/3PG	4138.0 N 2720.0 W	3
CHN82	24/4PG	4142.5 N 3251.0 W	3
CHN82	25/5PG	4218.7 N 2834.5 W	7
CHN82	26/6PG	4210.0 N 3138.0 W	7
CHN82	27/7PG	4206.0 N 2816.0 W	7
CHN82	28/8PG	4200.0 N 2957.0 W	3
CHN82	30-1/9	4150.6 N 2627.0 W	3
CHN82	30-2/1	4048.2 N 2627.0 W	3
CHN82	31/11P	4223.0 N 3147.5 W	7
CHN82	32/12P	4345.0 N 2746.5 W	7
CHN82	33/13P	4228.5 N 2840.0 W	7
CHN82	36/14P	4233.3 N 2918.5 W	3
CHN82	41/15P	4322.3 N 2813.9 W	7
CHN82	42/16P	4319.6 N 2804.6 W	7
CHN82	44/17P	4057.7 N 2712.5 W	7
CHN82	45/18P	4135.9 N 2727.8 W	7
CHN82	49/19P	4329.3 N 2934.4 W	7
CHN82	50/20P	4329.9 N 2952.0 W	7
CHN82	51/21P	4317.3 N 2949.8 W	7
CHN82	54/22P	4350.0 N 2757.9 W	7
CHN82	56/23P	4335.1 N 3137.5 W	7
CHN82	57/24P	4327.9 N 3037.8 W	7
CHN82	58/25P	4329.5 N 3013.0 W	7
CHN82	59/26P	4320.1 N 3000.0 W	7
CHN96	98/8G	3031.3 N 2019.7 W	3
CHN96	6-10/1	3236.1 N 2126.2 W	3
D3738		4100.0 N 1508.0 W	3

D3815	4343.0 N 1239.0 W	3
D3816	4342.0 N 1239.3 W	3
D3817	4341.5 N 1239.4 W	3
D3819	4335.0 N 1247.0 W	3
D3820	4337.0 N 1249.5 W	3
D4774	2902.25N 2526.0 W	3
D4775	2901.75N 2526.5 W	3
D4777	2859.5 N 2525.75W	3
D4778	2902.75N 2533.0 W	3
D4784	2903.5 N 2516.75W	3
D4790	2710.0 N 2106.0 W	3
D4795	2712.5 N 2105.5 W	3
D4805	2935.0 N 2336.0 W	3
D4813	2852.25N 2526.0 W	3
D4817	2934.0 N 2518.0 W	3
D4821	2935.0 N 2523.5 W	3
D4822	2903.5 N 2422.5 W	3
D4824	4303.0 N 1948.0 W	3
D5591	4112.0 N 1252.0 W	3
D5592	4110.0 N 1253.0 W	3
D5593	4107.0 N 1254.0 W	3
D5594	4103.0 N 1258.0 W	3
D5595	4057.0 N 1306.0 W	3
D5596	4053.0 N 1308.0 W	3
D5597	4050.0 N 1310.0 W	3
D5598	4047.0 N 1314.0 W	3
D5599	4036.0 N 1323.0 W	3
D5600	4034.0 N 1327.0 W	3
D5601	4031.5 N 1328.0 W	3
D5602	4029.0 N 1330.0 W	3
D5603	4101.0 N 1357.0 W	3
D5613	4247.5 N 2017.0 W	3
D5615	4306.0 N 2007.0 W	3
D5620	4249.5 N 2016.0 W	3
D5621	4246.5 N 2017.0 W	3
D5622	4250.0 N 2017.0 W	3
D5635	4250.5 N 2015.0 W	7
D5638	4226.0 N 2028.0 W	3
D5642	4152.0 N 1430.0 W	3
D5643	4153.0 N 1421.5 W	3
D5644	4154.0 N 1414.0 W	3
D5646	4215.0 N 1404.0 W	3
D5648	4215.5 N 1401.0 W	3
D5980	4248.2 N 2014.3 W	3
D9567	4402.12N 2148.79W	7
D9571	4402.8 N 2147.03W	7
D9574	4333.5 N 2223.9 W	7
D9806	4332.5 N 1753.3 W	7
D9812	4514.4 N 2225.8 W	7
DSDP 114	5956.0 N 2648.0 W	3
DSDP 115	5854.4 N 2107.0 W	3
DSDP 116	5729.76N 1555.46W	3

DSDP	117	5720.17N 1523.97W	3
DSDP	118	4502.65N 900.63W	3
DSDP	119	4501.9 N 758.49W	3
DSDP	120	3641.19N 1125.94W	3
DSDP	135	3520.8 N 1025.46W	3
DSDP	136	3410.13N 1618.19W	3
DSDP	137	2555.53N 2703.64W	3
DSDP	332	3652.72N 3338.46W	3
DSDP	333	3650.45N 3340.05W	3
DSDP	334	3702.13N 3424.87W	3
DSDP	335	3717.74N 3511.92W	3
DSDP	370	3250.2 N 1046.6 W	3
DSDP	399	4723.4 N 913.3 W	3
DSDP	400,A	4722.9 N 911.9 W	3
DSDP	410	4530.51N 2928.56W	3
DSDP	410A	4530.53N 2958.56W	3
DSDP	411,A	3645.97N 3323.3 W	3
DSDP	412,A	3633.74N 3309.96W	3
DSDP	413	3632.59N 3310.5 W	3
EKV	133	5939.2 N 427.8 W	3
EKV	134	5940.2 N 322.8 W	3
EKV	135	5941.0 N 219.80E	3
EKV	136	5940.7 N 24.30E	3
EKV	137	5942.6 N 111.3 W	3
EKV	138	5940.4 N 258.5 W	3
EKV	139	5940.5 N 423.0 W	3
EKV	140a	5942.3 N 619.0 W	3
EKV	140b	5943.4 N 619.0 W	3
EKV	144	6101.7 N 1252.0 W	3
EKV	145	6122.8 N 1427.5 W	3
EKV	146	6143.2 N 1601.2 W	3
EKV	148	6215.4 N18340.6 W	3
EKV	150	6154.6 N 2139.0 W	3
EKV	151	6118.3 N 2313.0 W	3
EKV	152	6043.2 N 2119.5 W	3
EKV	153	6020.4 N 2000.2 W	3
EKV	154	5958.0 N 1825.9 W	3
EKV	155	5924.2 N 1657.9 W	3
EKV	156	5850.0 N 1519.5 W	3
EKV	158	5509.8 N 1243.0 W	3
EKV	159	5538.3 N 1348.0 W	3
EKV	160	5617.5 N 1526.3 W	3
EKV	163	5753.5 N 1958.0 W	3
EKV	164	5824.0 N 2133.4 W	3
EKV	165	5858.0 N 2318.0 W	3
EKV	166	5933.4 N 2416.0 W	3
EKV	167	6003.4 N 2627.5 W	3
EKV	168	5925.1 N 2820.7 W	3
EKV	170	5758.0 N 2839.1 W	3
EKV	171	5719.8 N 2716.2 W	3
EKV	173	5553.3 N 2427.4 W	3
EKV	174	5513.7 N 2305.6 W	3

EKV	176	5410.7	N	2031.1	W	3
EKV	177	5326.4	N	1946.5	W	3
EKV	183	4959.0	N	1146.9	W	3
EKV	184	4941.9	N	1033.1	W	3
K708	1	5000.0	N	2345.0	W	1
K708	4	4959.0	N	2501.0	W	1
K708	6	5134.0	N	2934.0	W	1
K708	7	5356.0	N	2405.0	W	1
K708	8	5245.0	N	2233.0	W	1
K714	3	5730.0	N	2732.0	W	1
K714	14	5857.0	N	2830.0	W	1
K714	15	5846.0	N	2557.0	W	1
K5	50	3458.0	N	1300.0	W	3
K28	C5	3708.0	N	3015.0	W	3
K28	07	3742.0	N	3035.0	W	3
KNR31	1/1PG	3626.5	N	3200.0	W	3
KNR51	21/1FF	6142.4	N	2051.4	W	3
KNR51	22/2FF	6138.4	N	2032.8	W	3
KNR51	23/3FF	6138.6	N	2034.4	W	3
KNR51	36/13G	5428.5	N	1517.9	W	7
KNR51	39/17G	5616.5	N	1230.2	W	3
KNR51	41/19G	5617.9	N	1231.3	W	3
KNR51	41/22,	5616.8	N	1232.3	W	3
KNR51	41/24F	5616.6	N	1233.3	W	3
KNR51	41/25F	5616.5	N	1233.8	W	3
KNR51	41/26F	5616.6	N	1234.0	W	3
KNR51	42/31G	5613.4	N	1238.0	W	3
KNR54	19/5B	5826.0	N	2.80	E	3
KNR54	22/6B	5826.7	N	19.10	E	3
KNR54	30A/7B	5854.9	N	408.20	E	3
KNR54	32/8B	5850.3	N	41.40	E	3
KNR54	44/9B	5958.0	N	8.90	E	3
KNR54	48/10B	6021.3	N	158.70	E	3
KNR54	59/13B	5825.5	N	140.00	E	3
KNR54	76/18B	5930.6	N	20.00	E	3
KNR54	91/21B	5941.2	N	657.2	W	3
KNR54	92/22B	5911.7	N	857.5	W	3
KNR54	94/24B	5926.0	N	1306.4	W	7
KNR54	96/25B	6008.6	N	1501.4	W	3
KNR54	98/26B	6059.7	N	1605.5	W	3
LK	4	4829.0	N	3554.0	W	1
LK	6	4903.5	N	3244.0	W	1
LK	7	4932.0	N	2921.0	W	1
LK	8	4936.0	N	2854.0	W	7
LK	9	4940.0	N	2829.0	W	7
LK	10	4945.0	N	2330.5	W	7
LK	11	4838.0	N	1709.0	W	3
LK	12	4937.0	N	1334.0	W	7
LK	13	4938.0	N	1328.0	W	7
MB	F7	2511.0	N	1944.0	W	3
MB	G1	2810.0	N	2442.0	W	3
MB	H6	3053.0	N	2308.0	W	7

MB	I1	3352.0 N 1256.0 W	3
MB	I2	3352.0 N 1917.0 W	3
MB	J5	3715.0 N 2740.0 W	3
MB	J6B	3709.0 N 1423.0 W	3
MB	K1A	3957.0 N 1033.0 W	3
MB	K1	4002.0 N 1052.0 W	3
MB	K2	4001.0 N 2254.0 W	3
MB	L3	4304.0 N 3235.0 W	3
MB	L4	4304.0 N 2316.0 W	3
MB	L5	4301.0 N 1714.0 W	3
MB	M2	4609.0 N 1904.0 W	7
MB	M3	4559.0 N 3211.0 W	7
MB	N2	4852.0 N 3412.0 W	3
MB	N3	4840.0 N 2431.0 W	3
MB	N4	4855.0 N 1712.0 W	3
MB	O1	5201.0 N 1240.0 W	3
MB	O2	5200.0 N 1750.0 W	3
MB	P1	5500.0 N 1110.0 W	3
MB	P2	5509.0 N 2245.0 W	3
MB	Q1	5759.0 N 1004.0 W	3
MB	Q3	5756.0 N 2908.0 W	3
MB	R1	6100.0 N 2908.0 W	3
MB	R2	6054.0 N 1305.0 W	3
MB	R3	6058.0 N 2058.0 W	3
MB	R4	6104.0 N 3230.0 W	3
MB	BALEN	3456.0 N 809.0 W	3
MB	PALMAS	3017.0 N 1433.0 W	3
ML1	2	5755.8 N 1045.70E	3
ML1	3	5742.7 N 734.80E	3
ML1	4	5757.0 N 632.50E	3
ML1	5	5813.5 N 510.30E	3
ML1	10	5848.4 N 632.0 W	3
ML1	19	6223.1 N 1323.5 W	3
ML1	23	6339.1 N 1625.0 W	3
ML1	24	6322.0 N 1718.0 W	3
ML1	25	6244.3 N 1841.8 W	3
ML1	26	6207.0 N 2024.8 W	3
ML1	27	6148.7 N 2124.0 W	7
ML1	34	5931.2 N 1552.0 W	3
ML1	36	5839.5 N 1433.9 W	7
ML1	39	5747.9 N 1212.8 W	3
ML1	41	5656.0 N 1050.2 W	3
ML1	43	5734.2 N 908.0 W	3
ML1	46	5955.9 N 848.0 W	7
ML1	47	5955.9 N 848.0 W	7
ML1	47	6035.2 N 730.3 W	7
ML1	50	6025.1 N 401.2 W	7
ML4	215	4652.1 N 745.0 W	3
ML4	217	4303.6 N 933.3 W	3
ML4	218	4314.6 N 951.2 W	3
ML4	221	4512.1 N 1253.0 W	3
ML4	227	4903.0 N 2027.0 W	7

ML4	231	5143.3 N 2428.3 W	7
ML4	233	5259.6 N 2716.3 W	7
ML4	237	5536.6 N 3242.9 W	7
ML4	238	5559.9 N 3358.0 W	7
ML4	242	5317.8 N 3323.3 W	8
ML4	243	5242.8 N 3231.0 W	3
ML4	244	5151.8 N 3139.3 W	3
ML4	246	5006.7 N 2942.8 W	7
ML4	248	4829.0 N 2746.1 W	3
ML4	249	4748.5 N 2655.6 W	3
ML4	254	4347.3 N 2236.0 W	7
ML4	255	4304.5 N 2140.2 W	7
ML4	256	4238.0 N 2115.0 W	3
ML4	257	4128.5 N 2123.2 W	3
ML4	260	4013.8 N 2422.3 W	7
ML4	262	3942.1 N 2648.2 W	3
ML4	263a	3850.4 N 2837.5 W	7
ML4	263b	3855.6 N 2834.3 W	3
ML4	265	3959.3 N 3059.0 W	7
ML4	270	4426.8 N 3407.0 W	7
ML4	271	4606.9 N 3517.0 W	3
ML4	273	4756.1 N 3656.6 W	3
ML4	275	4944.0 N 2754.8 W	3
ML4	276	5107.9 N 3800.0 W	3
ML4	283	5206.0 N 4457.7 W	3
ML4	287	4949.0 N 4727.0 W	3
ML4	289	4959.0 N 5038.0 W	3
ML4	295	4750.4 N 4949.6 W	3
ML4	296	4659.2 N 4924.3 W	3
ML4	297	4602.5 N 4823.7 W	3
ML4	305	3819.0 N 4507.3 W	3
ML4	307	3900.5 N 4306.9 W	3
ML4	311	4141.4 N 4112.0 W	3
ML4	317	4656.0 N 4506.0 W	3
ML4	318	4800.0 N 4457.5 W	3
ML4	319	4857.2 N 4455.9 W	3
ML4	331	5009.4 N 1653.0 W	7
ML4	333	4959.4 N 1140.4 W	3
PL	901	6204.0 N 203.0 W	3
PL	902	6302.0 N 229.0 W	3
PL	903	6511.0 N 7.0 W	3
PL	904	6652.0 N 154.00E	3
PL	908	1607.0 N 3330.0 W	3
PL	909	1558.0 N 3359.0 W	3
PL	914	1635.0 N 3507.0 W	3
PL	915	1631.0 N 3323.0 W	3
PL	916	1638.0 N 2913.0 W	3
PL	919	1620.0 N 3355.0 W	3
PL	920	1617.0 N 3415.0 W	3
PL	1004	1317.0 N 6342.0 W	3
PL	1005	1338.0 N 6443.0 W	3
PL	1006	1439.0 N 6548.0 W	3

PL	1007	1020.0 N 5516.0 W	3
PL	1008	838.0 N 5452.0 W	3
PL	1012	4030.0 N 610.00E	3
PL	1013	3855.0 N 453.00E	3
PL	1017	4740.0 N 1610.0 W	3
R5	50	3458.0 N 1311.0 W	7
R10	2	5659.0 N 1228.0 W	3
RE5	34	4223.0 N 2158.0 W	1
RE5	36	4655.0 N 1835.0 W	1
RC9	225	5459.0 N 1524.0 W	1
RC9	211	4209.0 N 1431.0 W	3
RC9	212	4412.0 N 1455.0 W	3
RC9	213	4334.0 N 1547.0 W	3
RC9	214	4347.0 N 1544.0 W	3
RC9	215	4416.0 N 1547.0 W	3
RC9	216	4421.0 N 1525.0 W	3
RC9	217	4431.0 N 1528.0 W	3
S8	79-1	4104.3 N 2144.2 W	7
S8	79-2	4128.5 N 2141.4 W	7
S8	79-3	4208.7 N 2123.6 W	7
S8	79-4	4222.6 N 2203.1 W	7
S8	79-5	4213.5 N 2233.9 W	7
S8	79-6	4151.9 N 2244.2 W	3
S8	79-7	4219.9 N 2303.5 W	3
S8	79-8	4249.6 N 2303.8 W	7
SED'59	2	5213.7 N 1328.7 W	3
SED'59	3	5243.8 N 1453.0 W	3
SED'59	4	5310.4 N 1632.2 W	3
SED'59	5	5340.3 N 1804.2 W	3
SED'59	14	6025.0 N 3512.0 W	3
SED'59	16	6140.4 N 3906.6 W	3
SED'59	20	5606.5 N 4527.6 W	3
SED'59	21	5432.3 N 4658.5 W	3
SED'59	22	5325.1 N 4328.5 W	3
SED'59	23	5208.6 N 4052.4 W	3
SED'59	24	5049.3 N 3758.5 W	3
SED'59	27	4710.3 N 2927.1 W	3
SED'59	28	4609.0 N 2712.9 W	3
SED'59	29	4503.8 N 2515.6 W	3
SED'59	30	4402.0 N 2309.5 W	3
SED'59	31	4254.5 N 2102.7 W	3
SED'59	35	3904.8 N 1315.7 W	3
SED'59	37	3740.1 N 1020.5 W	3
SED'59	38	3717.5 N 938.2 W	3
SED'59	39	3644.9 N 849.9 W	3
SED'59	40	3623.2 N 755.6 W	3
SED'60	4	2959.8 N 2335.1 W	3
SED'60	7	3010.7 N 3035.0 W	3
SED'60	8	3013.8 N 3248.2 W	3
SED'60	9	3026.3 N 3514.4 W	3
SED'60	10	3030.4 N 3730.0 W	3
SED'60	11	3053.2 N 3945.3 W	3

SED'60	12	3052.2 N	4213.3 W	3
SED'60	13	3051.2 N	4325.4 W	3
SED'60	14	3105.2 N	4417.7 W	3
SED'60	15	3110.8 N	4653.8 W	3
SED'60	16	3120.8 N	4909.2 W	3
SED'60	17	3130.1 N	5140.6 W	3
SED'60	18	3139.2 N	5400.0 W	3
SED'60	19	3142.8 N	5619.0 W	3
SED'60	20	3155.8 N	5835.2 W	3
SED'60	21	3203.3 N	6100.3 W	3
SED'60	22	3307.9 N	6328.8 W	3
SED'60	25	3935.5 N	6708.4 W	3
SED'60	26	4102.0 N	6625.5 W	3
SED'60	29	4021.8 N	6016.5 W	3
SED'61	2	2656.1 N	2717.5 W	3
SED'61	3	2658.6 N	3325.7 W	3
SED'61	4	2658.1 N	3857.2 W	3
SED'61	7	2705.3 N	5323.1 W	3
SED'61	8	2704.5 N	5526.7 W	3
SED'61	9	2849.3 N	6008.2 W	3
SED'61	12	3243.6 N	6930.5 W	3
SED'61	13	3324.0 N	6853.0 W	3
SED'61	15	3507.0 N	6622.0 W	3
SED'61	16	3540.1 N	6504.9 W	3
SED'61	19	3656.0 N	6112.0 W	3
SED'62	1	1709.3 N	2750.0 W	3
SED'62	2	1647.9 N	3210.8 W	3
SED'62	3	1626.3 N	4026.2 W	3
SED'62	4	1612.7 N	4421.8 W	3
SED'62	6	1506.8 N	5301.3 W	3
SED'62	7	1451.2 N	5607.3 W	3
SED'62	8	1629.0 N	5108.8 W	3
SED'62	10	1954.0 N	6205.5 W	3
SED'62	13	2337.5 N	7305.2 W	3
SED'62	14	2451.0 N	7207.6 W	3
SED'62	15	2602.3 N	7301.3 W	3
SED'62	18	3305.2 N	7301.3 W	3
SED'62	19	3501.3 N	7257.3 W	3
SED'62	22	2847.8 N	6407.1 W	3
SED'62	29	4108.0 N	4338.0 W	3
SP3	33	4718.8 N	1125.5 W	3
SP3	38	5206.0 N	2021.0 W	3
SP8	3	3024.0 N	3047.0 W	3
TR121	2	3828.2 N	2622.8 W	3
TR121	6	3847.4 N	2359.4 W	3
TR121	7	3953.7 N	2320.[illegible]	3
TR121	8	3858.0 N	2224.0 W	3
TR121	9	3853.0 N	2244.0 W	3
TR121	10	3918.0 N	2034.2 W	3
TR121	12	3933.0 N	1919.8 W	3
TR121	13	3939.0 N	1842.6 W	3
TR121	14	3853.0 N	1753.1 W	3

TR121	15	3857.0	N	1758.8	W	3
TR121	17	3224.0	N	2001.8	W	3
TR121	18	3824.0	N	2034.8	W	3
TR121	19	3815.6	N	2118.0	W	3
TR121	21	3810.2	N	2216.8	W	3
TR121	22	3806.9	N	2248.6	W	3
TR121	24	3801.0	N	2319.0	W	3
TR121	26	3753.4	N	2351.0	W	3
TR121	30	3819.9	N	2518.0	W	3
TR121	31	3814.6	N	2542.1	W	3
V4	8	3713.5	N	3308.2	W	3
V4	13	3636.0	N	1834.5	W	3
V4	14	3543.2	N	1721.0	W	3
V4	15	3511.0	N	1520.5	W	3
V4	19	3414.0	N	1512.0	W	3
V4	20	3507.5	N	1304.0	W	7
V4	22	3508.0	N	1300.0	W	7
V4	23	3500.5	N	1257.0	W	3
V4	24	3500.0	N	1257.0	W	3
V4	25	3501.0	N	1257.0	W	3
V4	27	3503.0	N	1257.5	W	3
V4	32	3503.0	N	1137.0	W	3
V4	33	3435.0	N	841.0	W	3
V4	34	3410.0	N	816.0	W	3
V4	35	3404.0	N	802.5	W	3
V4	39	3812.3	N	923.8	W	3
V4	40	3817.4	N	923.0	W	3
V4	41	3812.0	N	945.0	W	3
V4	42	3812.0	N	1005.0	W	3
V4	44	3740.0	N	1107.5	W	3
V4	46	3805.0	N	1154.0	W	3
V4	47	3713.9	N	1216.0	W	3
V4	48	3702.0	N	1236.2	W	3
V4	51	3309.0	N	2849.0	W	3
V4	53	3305.0	N	2918.5	W	3
V4	54	3313.8	N	2931.0	W	3
V12	9	654.4	N	3601.0	W	3
V14	5	51.0	N	3251.0	W	3
V14	143	4139.0	N	500.00	E	3
V14	144	4058.0	N	149.00	E	3
V14	145	3601.0	N	214.0	W	3
V14	146	3617.0	N	209.0	W	3
V14	147	3613.0	N	447.0	W	3
V14	149	3557.0	N	730.0	W	3
V14	151	3836.5	N	2850.5	W	3
V16	24	818.0	N	3803.0	W	3
V16	25	504.0	N	3648.0	W	3
V16	26	247.0	N	3542.0	W	3
V16	200	158.0	N	3704.0	W	3
V16	201	201.0	N	3709.0	W	3
V16	202	432.0	N	3750.0	W	3
V16	203	921.0	N	3952.0	W	3

V17	154	23.0 N 1758.0 W	3
V17	155	20.0 N 1759.0 W	3
V17	156	328.0 N 1831.0 W	3
V17	157	921.0 N 1838.0 W	3
V17	158	1223.0 N 1855.0 W	3
V17	159	1659.0 N 2003.0 W	3
V17	160	2122.0 N 2402.0 W	3
V17	161	2316.0 N 2643.0 W	3
V17	162	2458.0 N 2856.0 W	3
V17	163	2758.0 N 3408.0 W	3
V17	164	2937.0 N 3655.0 W	3
V19	284	16.0 N 436.00E	3
V19	285	39.0 N 342.00E	3
V19	286	41.0 N 19.00E	3
V19	287	126.0 N 240.0 W	3
V19	288	133.0 N 515.0 W	3
V19	289	126.0 N 557.0 W	3
V19	290	139.0 N 537.0 W	3
V19	291	20.0 N 513.0 W	3
V19	292	209.0 N 509.0 W	3
V19	293	219.0 N 447.0 W	3
V19	294	453.0 N 401.0 W	3
V19	295	257.0 N 607.0 W	3
V19	296	125.0 N 905.0 W	3
V19	297	237.0 N 1200.0 W	3
V19	298	339.0 N 1503.0 W	3
V19	299	439.0 N 1729.0 W	3
V19	300	653.0 N 1928.0 W	3
V19	301	818.0 N 2245.0 W	3
V19	302	1015.0 N 2522.0 W	3
V19	303	1247.0 N 2247.0 W	3
V19	304	1532.0 N 3002.0 W	3
V19	305	1754.0 N 3157.0 W	3
V19	306	2028.0 N 3407.0 W	3
V19	307	2622.0 N 3850.0 W	3
V20	232	34.0 N 3706.0 W	3
V20	233	200.5 N 3536.0 W	3
V20	234	519.0 N 3302.0 W	3
V20	235	828.0 N 3008.0 W	3
V20	236	1159.0 N 3236.0 W	3
V20	237	1412.0 N 3427.0 W	3
V20	238	1628.0 N 3619.0 W	3
V20	239	1904.0 N 3812.0 W	3
V20	240	2104.0 N 3951.0 W	3
V22	27	623.0 N 3758.0 W	3
V22	28	549.0 N 3916.0 W	3
V22	29	409.0 N 3521.0 W	3
V22	30	315.0 N 3415.0 W	3
V22	31	151.0 N 3228.0 W	3
V22	32	55.0 N 3146.0 W	3
V22	184	21.0 N 1731.0 W	3
V22	185	234.0 N 1914.0 W	3

V22	186	323.0 N 2007.0 W	3
V22	187	426.0 N 2048.0 W	3
V22	188	440.0 N 2055.0 W	3
V22	189	456.0 N 2107.0 W	3
V22	190	602.0 N 2116.0 W	3
V22	191	655.0 N 2122.0 W	3
V22	192	748.0 N 2124.0 W	3
V22	193	955.0 N 2058.0 W	3
V22	194	1140.0 N 2019.0 W	3
V22	195	1325.0 N 1927.0 W	3
V22	196	1350.0 N 1857.0 W	3
V22	197	1410.0 N 1835.0 W	3
V22	198	1435.0 N 1739.0 W	3
V22	199	1434.0 N 1740.5 W	3
V22	200	1429.0 N 1747.0 W	3
V22	201	1422.0 N 1803.0 W	3
V22	202	1424.0 N 2109.0 W	3
V22	203	1502.0 N 2305.0 W	3
V22	204	1501.0 N 2314.0 W	3
V22	205	1555.0 N 2414.0 W	3
V22	206	1625.0 N 2405.0 W	3
V22	207	1716.0 N 2618.0 W	3
V22	208	1737.0 N 2702.0 W	3
V22	209	1901.5 N 2909.0 W	3
V22	210	1940.0 N 3007.0 W	3
V22	211	2042.0 N 3127.0 W	3
V22	212	2302.0 N 3429.0 W	3
V22	213	2504.0 N 3746.0 W	3
V22	214	2600.5 N 3931.0 W	3
V23	23	5604.0 N 4433.0 W	1
V23	27	5946.0 N 3925.0 W	3
V23	28	5948.0 N 3752.0 W	3
V23	29	5957.0 N 3251.0 W	3
V23	30	6007.0 N 2909.0 W	3
V23	31	6010.0 N 2437.0 W	3
V23	32	6124.5 N 2601.0 W	3
V23	33	6153.0 N 2623.0 W	3
V23	34	6235.0 N 2657.0 W	3
V23	35	6200.2 N 2841.0 W	3
V23	36	6213.1 N 2824.0 W	3
V23	37	6230.5 N 2758.0 W	3
V23	38	6939.6 N 2732.0 W	3
V23	39	6235.4 N 2744.4 W	3
V23	40	6144.7 N 2837.6 W	3
V23	41	6159.8 N 2804.0 W	3
V23	42	6210.8 N 2755.6 W	1
V23	43	6123.1 N 2803.3 W	3
V23	44	6128.8 N 2751.6 W	3
V23	45	6138.3 N 2735.0 W	3
V23	46	6153.2 N 2742.0 W	3
V23	47	6135.7 N 2812.6 W	3
V23	48	6213.2 N 2712.9 W	3

V23	49	6010.2 N 2928.3 W	3
V23	50	6024.4 N 2908.0 W	3
V23	51	6032.3 N 2853.8 W	3
V23	52	5958.4 N 2931.8 W	3
V23	53	5948.8 N 2948.5 W	3
V23	54	5949.7 N 2916.3 W	3
V23	55	6251.8 N 2713.5 W	3
V23	56	6248.8 N 2523.7 W	3
V23	57	6247.0 N 1508.0 W	3
V23	75	6448.0 N 119.0 W	3
V23	76	6339.0 N 122.00E	3
V23	77	6239.0 N 558.0 W	3
V23	78	6231.0 N 1112.0 W	3
V23	79	6056.0 N 1734.0 W	3
V23	80	5609.7 N 1118.9 W	3
V23	81	5415.0 N 1650.0 W	3
V23	82	5235.1 N 2156.0 W	3
V23	83	4952.3 N 2415.0 W	3
V23	84	4600.3 N 1655.0 W	3
V23	85	4109.9 N 1442.2 W	3
V23	86	3723.7 N 1702.0 W	3
V23	87	3404.5 N 1942.0 W	3
V23	88	3106.5 N 2157.5 W	3
V23	89	2952.4 N 2405.7 W	3
V23	90	2950.5 N 2503.0 W	3
V23	91	2935.0 N 2834.0 W	3
V23	92	3003.5 N 2815.0 W	3
V23	93	3026.5 N 2323.5 W	3
V23	94	3037.3 N 2008.6 W	3
V23	95	3024.2 N 1823.0 W	3
V23	96	2948.0 N 1505.5 W	3
V23	97	2407.0 N 1726.0 W	3
V23	98	2307.0 N 1918.0 W	3
V23	99	2228.0 N 2026.0 W	3
V23	100	2118.0 N 2241.0 W	3
V23	101	1953.0 N 2532.0 W	3
V23	102	1833.0 N 2809.0 W	3
V23	103	1742.0 N 2952.0 W	3
V23	104	1713.0 N 3221.0 W	3
V23	105	1712.0 N 3550.0 W	3
V23	106	1725.0 N 3901.0 W	3
V24	257	4.0 N 3503.0 W	3
V25	58	4.0 N 3247.8 W	3
V25	59	122.4 N 3328.9 W	3
V25	60	316.8 N 3449.7 W	3
V25	61	321.5 N 3706.7 W	3
V26	34	1951.2 N 3654.5 W	3
V26	35	1742.4 N 3414.1 W	3
V26	36	1632.2 N 3132.5 W	3
V26	37	1637.8 N 3105.0 W	3
V26	38	1621.8 N 3100.2 W	3
V26	39	1633.0 N 3134.3 W	3

V26	40	1940.1	N	2607.3	W	3
V26	41	1919.9	N	2606.8	W	3
V26	42	2004.9	N	2605.9	W	3
V26	43	1917.3	N	2606.7	W	3
V26	44	1850.3	N	2428.5	W	3
V26	45	1717.0	N	2202.1	W	3
V26	46	933.8	N	1810.8	W	3
V26	47	635.7	N	1808.0	W	3
V26	48	608.3	N	1804.9	W	3
V26	49	549.9	N	1751.5	W	3
V26	50	616.0	N	1754.8	W	3
V26	51	601.9	N	1814.5	W	3
V26	52	550.4	N	1805.0	W	3
V26	53	18.0	N	1448.0	W	3
V27	16	4409.7	N	3952.1	W	3
V27	17	5005.5	N	3718.1	W	1
V27	18	5112.3	N	3658.6	W	3
V27	19	5205.6	N	3848.0	W	1
V27	20	5400.0	N	4612.0	W	1
V27	31	5940.7	N	3947.9	W	3
V27	32	6042.2	N	3716.5	W	3
V27	33	6156.0	N	3316.3	W	3
V27	34	6301.2	N	3057.3	W	3
V27	35	6403.4	N	2816.0	W	3
V27	36	6226.1	N	1906.2	W	3
V27	37	6035.5	N	1256.2	W	3
V27	38	6122.2	N	1129.7	W	3
V27	39	6251.5	N	805.2	W	3
V27	40	6326.9	N	607.8	W	3
V27	41	6229.5	N	315.8	W	3
V27	42	6150.5	N	127.8	W	3
V27	43	6300.6	N	129.4	W	3
V27	93	6256.1	N	416.8	W	3
V27	96	6100.6	N	420.3	W	3
V27	97	6016.9	N	711.9	W	3
V27	98	6039.2	N	725.5	W	3
V27	99	6111.9	N	757.7	W	3
V27	100	6141.8	N	919.5	W	3
V27	101	6252.5	N	1118.1	W	3
V27	102	6207.7	N	1412.3	W	3
V27	103	6221.6	N	1628.0	W	3
V27	104	6251.7	N	1755.5	W	3
V27	105	6221.2	N	1843.0	W	3
V27	106	6113.7	N	2251.5	W	3
V27	107	5927.4	N	2357.5	W	3
V27	108	5832.8	N	2212.3	W	3
V27	110	5653.6	N	1829.6	W	1
V27	111	5603.9	N	2405.2	W	3
V27	112	5607.6	N	2530.9	W	3
V27	113	5609.8	N	2737.4	W	3
V27	114	5502.9	N	3304.2	W	3
V27	115	5334.7	N	3122.4	W	3

V27	116	5250.2 N 3020.4 W	1
V27	117	5328.8 N 2527.4 W	3
V27	118	5345.3 N 2436.5 W	3
V27	119	5143.8 N 2010.5 W	3
V27	120	5058.1 N 1913.4 W	3
V27	121	4948.1 N 1753.5 W	3
V27	122	4817.7 N 1658.4 W	3
V27	123	4628.8 N 1655.2 W	3
V27	124	4422.9 N 1626.9 W	3
V27	125	4322.1 N 1540.5 W	3
V27	126	4347.9 N 1441.2 W	3
V27	127	4437.3 N 1457.6 W	3
V27	129	4511.6 N 935.5 W	3
V27	130	4503.9 N 759.1 W	3
V27	132	4505.2 N 757.8 W	3
V27	133	4505.4 N 756.9 W	3
V27	134	4800.1 N 1206.3 W	3
V27	135	4803.6 N 1609.6 W	3
V27	136	4358.1 N 1548.7 W	3
V27	137	4241.5 N 1704.1 W	1
V27	138	4256.7 N 2504.4 W	7
V27	139	4202.7 N 2717.0 W	3
V27	140	4103.8 N 2449.8 W	3
V27	141	3528.7 N 2456.4 W	7
V27	142	3659.9 N 2254.1 W	3
V27	143	3942.8 N 2009.4 W	3
V27	144	3935.6 N 1333.4 W	3
V27	145	3902.6 N 1159.2 W	3
V27	146	3809.2 N 1142.3 W	3
V27	147	3701.9 N 1114.7 W	3
V27	148	3545.6 N 1326.7 W	3
V27	149	3520.0 N 1401.9 W	3
V27	150	3626.9 N 1259.2 W	3
V27	151	3552.9 N 1223.3 W	3
V27	152	3532.0 N 1204.4 W	3
V27	153	3550.9 N 1138.0 W	3
V27	154	3537.2 N 1050.6 W	3
V27	157	3415.0 N 1040.2 W	3
V27	155	3603.2 N 1033.7 W	3
V27	156	3607.7 N 1013.3 W	3
V27	158	3416.7 N 1146.4 W	3
V27	159	3358.9 N 1319.6 W	3
V27	160	3326.3 N 1253.4 W	3
V27	161	3334.7 N 1358.3 W	3
V27	162	3411.9 N 1651.5 W	3
V27	163	3129.7 N 1721.8 W	3
V27	164	2929.3 N 1936.8 W	3
V27	166	2550.9 N 2242.9 W	3
V27	167	2556.2 N 2635.1 W	3
V27	168	2551.6 N 3019.2 W	3
V27	169	2550.0 N 3226.2 W	3
V27	170	2425.8 N 3402.3 W	3

V27	171	2144.2	N	3233.5	W	3
V27	172	1632.0	N	2851.0	W	3
V27	173	1456.7	N	2713.0	W	3
V27	174	1250.7	N	2500.4	W	3
V27	175	848.2	N	2206.9	W	3
V27	176	710.9	N	2522.2	W	3
V27	177	552.3	N	2839.8	W	3
V27	178	506.1	N	2639.0	W	3
V27	179	412.0	N	2334.2	W	3
V27	180	320.3	N	2059.8	W	3
V27	234	59.8	N	159.1	W	3
V27	235	227.4	N	14.9	W	3
V27	236	116.7	N	504.2	W	3
V27	237	113.4	N	309.5	W	3
V27	242	17.1	N	633.9	W	3
V27	244	254.1	N	824.1	W	3
V27	245	144.3	N	904.4	W	3
V27	246	353.7	N	933.3	W	3
V27	247	129.5	N	1036.0	W	3
V27	248	303.1	N	1148.9	W	3
V27	249	113.6	N	1222.0	W	3
V27	251	322.5	N	1433.0	W	3
V27	252	546.0	N	1531.9	W	3
V27	253	808.7	N	1734.4	W	3
V27	254	2010.9	N	2637.4	W	3
V27	255	2236.1	N	2800.3	W	3
V27	256	2625.1	N	2958.6	W	3
V27	257	2746.1	N	3643.9	W	3
V27	258	2606.6	N	3047.6	W	3
V27	259	2646.1	N	3453.2	W	3
V27	260	2555.8	N	3106.2	W	3
V27	261	3122.2	N	3559.1	W	3
V28	5	5248.3	N	3905.4	W	3
V28	6	5249.0	N	3955.1	W	3
V28	11	6025.0	N	3550.0	W	3
V28	12	6102.0	N	3248.0	W	3
V28	13	6345.0	N	2834.0	W	3
V28	14	6447.0	N	2934.0	W	1
V28	32	6447.0	N	418.00E		3
V28	33	6254.0	N	35.00E		3
V28	34	6450.0	N	335.0	W	3
V28	57	6438.0	N	1109.0	W	3
V28	58	6500.0	N	749.0	W	3
V28	59	6452.0	N	752.0	W	3
V28	60	6405.0	N	402.0	W	3
V28	60A	6425.0	N	402.0	W	3
V28	61	6204.0	N	310.0	W	3
V28	62	6149.0	N	300.0	W	3
V28	63	5930.0	N	953.0	W	3
V28	64	6136.0	N	840.0	W	3
V28	65	6033.0	N	1127.0	W	3
V28	66	6037.0	N	1511.0	W	3

V28	67	6052.0 N 1844.0 W	3
V28	68	6124.0 N 2354.0 W	3
V28	69	6013.0 N 2222.0 W	3
V28	70	5905.0 N 1741.0 W	3
V28	71	5900.0 N 1741.0 W	3
V28	72	5744.0 N 1153.0 W	3
V28	73	5711.0 N 2052.0 W	3
V28	74	5523.0 N 2210.0 W	3
V28	75	5230.0 N 2027.0 W	3
V28	76	5450.0 N 1654.0 W	3
V28	77	5257.0 N 1646.0 W	3
V28	78	5226.0 N 1948.0 W	3
V28	79	5214.0 N 2248.0 W	3
V28	80	5329.0 N 2532.0 W	3
V28	81	5221.0 N 2555.0 W	3
V28	82	4927.0 N 2216.0 W	3
V28	83	4728.0 N 1959.0 W	3
V28	84	4655.0 N 1927.0 W	1
V28	85	4455.0 N 1702.0 W	3
V28	86	4555.0 N 1916.0 W	3
V28	87	4549.0 N 2018.0 W	3
V28	88	4515.0 N 2754.0 W	3
V28	89	4432.0 N 3235.0 W	1
V29	145	231.0 N 428.00E	3
V29	146	343.0 N 331.00E	3
V29	147	553.0 N 257.00E	3
V29	148	415.0 N 240.00E	3
V29	149	242.3 N 224.00E	3
V29	150	357.0 N 51.00E	3
V29	151	252.0 N 14.00E	3
V29	152	108.0 N 4.00E	3
V29	153	58.0 N 10.00E	3
V29	154	346.0 N 547.0 W	3
V29	155	128.3 N 801.4 W	3
V29	156	257.0 N 846.0 W	3
V29	157	304.0 N 932.0 W	3
V29	158	210.0 N 1105.0 W	3
V29	159	616.4 N 1236.4 W	3
V29	160	557.6 N 1627.2 W	3
V29	162	654.0 N 1545.0 W	3
V29	163	744.0 N 1456.0 W	3
V29	164	809.0 N 1419.0 W	3
V29	165	1203.0 N 1930.0 W	3
V29	166	1458.5 N 2056.9 W	3
V29	167	1622.9 N 1755.3 W	3
V29	169	2004.0 N 2000.0 W	3
V29	170	2228.0 N 2004.0 W	3
V29	171	2939.0 N 1621.0 W	3
V29	172	3342.0 N 2923.0 W	3
V29	173K	3342.0 N 2923.0 W	3
V29	174	3617.8 N 2921.7 W	3
V29	175	3730.0 N 2817.0 W	3

V29	176	4033.3	N	2600.3	W	3
V29	177	4132.2	N	2542.5	W	1
V29	178	4250.9	N	2509.1	W	1
V29	179	4400.6	N	2432.4	W	1
V29	180	4618.2	N	2352.4	W	1
V29	181	4801.5	N	2502.3	W	3
V29	182	4908.3	N	2530.1	W	3
V29	183K	4908.3	N	2530.1	W	3
V29	184	4908.3	N	2530.1	W	3
V29	185	5236.9	N	2152.9	W	3
V29	187K	5236.9	N	2152.9	W	3
V29	188	5236.9	N	2152.9	W	3
V29	189	5222.0	N	1732.0	W	3
V29	190	5240.0	N	1510.0	W	3
V29	191	5416.0	N	1647.0	W	3
V29	192K	5416.0	N	1647.0	W	3
V29	193	5524.0	N	1647.0	W	3
V29	194	5700.2	N	2119.3	W	3
V29	195	5807.2	N	2110.8	W	3
V29	196	5808.8	N	1738.9	W	3
V29	197	5808.8	N	1738.9	W	3
V29	198	5843.5	N	1533.8	W	3
V29	199	5919.0	N	1630.0	W	3
V29	200	5957.0	N	1912.0	W	3
V29	201	5958.0	N	1927.0	W	3
V29	202	6023.0	N	2058.0	W	3
V29	203	6048.4	N	2226.5	W	3
V29	204	6111.2	N	2300.5	W	3
V29	205	6133.1	N	2507.2	W	3
V29	206	6454.3	N	2917.4	W	3
V29	208	6358.0	N	812.0	W	3
V29	221	6256.0	N	1155.0	W	3
V29	222	6251.0	N	1432.0	W	3
V29	223	6155.0	N	2403.0	W	3
V29	224	6040.0	N	2644.0	W	3
V29	225	6041.0	N	2718.0	W	3
V29	226	6041.0	N	2748.0	W	3
V29	227K	5922.0	N	3442.0	W	3
V29	228	5922.0	N	3442.0	W	3
V30	27	334.0	N	3911.0	W	3
V30	28	354.0	N	3847.0	W	3
V30	29	141.0	N	3356.0	W	3
V30	34	106.0	N	2951.0	W	3
V30	35	144.0	N	2748.0	W	3
V30	36	521.0	N	2719.0	W	3
V30	37	151.0	N	2645.0	W	3
V30	39	149.0	N	2332.0	W	3
V30	41K	13.0	N	2304.0	W	3
V30	42	237.0	N	2211.0	W	3
V30	43	451.0	N	2134.0	W	3
V30	44	106.0	N	1933.0	W	3
V30	45	618.0	N	1956.0	W	3

V30	46	1226.0 N 1805.0 W	3
V30	47	1352.0 N 1836.0 W	3
V30	48	1707.0 N 1920.0 W	3
V30	49	1826.0 N 2105.0 W	3
V30	50	1952.0 N 1955.0 W	3
V30	51K	1952.0 N 1955.0 W	3
V30	52	2114.0 N 2119.0 W	3
V30	53	2202.0 N 1804.0 W	3
V30	54	2239.0 N 1912.0 W	3
V30	55	2311.0 N 1740.0 W	3
V30	56	2407.0 N 1906.0 W	3
V30	57	2440.0 N 1640.0 W	3
V30	58	2543.0 N 2053.0 W	3
V30	59	2543.0 N 1931.0 W	3
V30	60	2541.0 N 1827.0 W	3
V30	61	2534.0 N 1650.0 W	3
V30	62	2550.0 N 1655.0 W	3
V30	63	2550.0 N 1718.0 W	3
V30	64	2553.0 N 1733.0 W	3
V30	65	2555.0 N 1903.0 W	3
V30	66	2616.0 N 1642.0 W	3
V30	67	2636.0 N 1509.0 W	3
V30	68	2655.0 N 1908.0 W	3
V30	69	3212.0 N 1849.0 W	3
V30	70	3219.0 N 1955.0 W	3
V30	71	3218.0 N 1950.0 W	3
V30	72	3408.0 N 2219.0 W	3
V30	73	3243.0 N 2413.0 W	3
V30	74	3353.0 N 2534.0 W	3
V30	75	3258.0 N 2908.0 W	3
V30	76	3336.0 N 3129.0 W	3
V30	77	3504.2 N 3426.4 W	3
V30	78	3459.0 N 3409.0 W	3
V30	79	3459.0 N 3542.0 W	3
V30	80	3444.0 N 3541.0 W	3
V30	81	3454.0 N 3541.0 W	3
V30	82	3508.5 N 3432.2 W	3
V30	83	3456.0 N 3419.0 W	3
V30	84	3520.1 N 3421.5 W	3
V30	85	3511.0 N 3428.5 W	3
V30	86	3507.0 N 3401.5 W	3
V30	87	3502.0 N 3536.0 W	3
V30	88	3459.0 N 3515.0 W	3
V30	93	3540.0 N 3837.0 W	3
V30	94	3522.0 N 3750.0 W	3
V30	96	3956.0 N 3308.0 W	1
V30	97	4100.0 N 3756.0 W	1
V30	98	4202.0 N 3248.0 W	3
V30	99	4309.0 N 3227.0 W	3
V30	100	4406.0 N 3230.0 W	1
V30	101K	4406.0 N 3230.0 W	3
V30	102	4923.0 N 3419.0 W	3

V30	103	5246.0 N 3635.0 W	3
V30	104	5306.0 N 3742.0 W	3
V30	105	5431.0 N 3630.0 W	3
V30	106	5448.0 N 3853.0 W	3
V30	107	5542.0 N 3940.0 W	3
V30	108	5606.0 N 3844.0 W	3
V30	110	5722.0 N 3912.0 W	3
V30	122	5648.0 N 3833.0 W	3
V30	125	5752.0 N 3530.0 W	3
V30	126	5834.0 N 3530.0 W	3
V30	127	6309.0 N 3532.0 W	3
V30	128	6409.0 N 3013.0 W	3
V30	134	6428.0 N 457.0 W	3
V30	177	5404.0 N 2411.0 W	3
V30	178	5155.0 N 2759.0 W	3
V30	179	5246.0 N 3259.0 W	3
V30	180	5238.0 N 3140.0 W	3
V30	181	5208.0 N 3122.0 W	3
V30	182	5225.0 N 3025.0 W	3
V30	183	5225.0 N 2940.0 W	3
V30	184	5234.0 N 2927.0 W	3
V30	185	5223.0 N 2740.0 W	3
V30	186	4101.0 N 1804.0 W	3
V30	187	4107.0 N 1004.0 W	7
V30	188	3954.0 N 1033.0 W	3
V30	189	3825.0 N 1129.0 W	3
V30	190	3755.0 N 1406.0 W	3
V30	191	3659.0 N 1543.0 W	3
V30	192	3521.0 N 1707.0 W	3
V30	193	3507.0 N 1634.0 W	3
V30	194	3402.0 N 1357.0 W	3
V30	195	3322.0 N 1201.0 W	3
V30	196	3257.0 N 1107.0 W	3
V30	197	3238.0 N 1012.0 W	3
V30	198	3308.0 N 933.0 W	3
V30	199	3356.0 N 955.0 W	3
V30	200	3418.0 N 925.0 W	3
V30	201	3443.0 N 753.0 W	3
V30	202	3533.0 N 759.0 W	3
V30	203	3607.0 N 810.0 W	3
V30	204	3619.0 N 806.0 W	3
V30	205	3618.0 N 849.0 W	3
V30	206	3602.0 N 902.0 W	3
V30	207	3628.0 N 908.0 W	3
V30	208	3436.0 N 817.0 W	3
V30	209	3620.0 N 444.0 W	3
V30	210	3639.0 N 743.0 W	3
V30	211	3624.0 N 726.0 W	3
V30	215	3558.0 N 528.0 W	3
V30	216	3526.0 N 707.0 W	3
V30	217	3442.0 N 719.0 W	3
V30	218	3436.0 N 902.0 W	3

V30	219	3427.0 N 1016.0 W	3
V30	220	3336.0 N 931.0 W	3
V30	221	3328.0 N 919.0 W	3
V30	222	3328.0 N 918.0 W	3
V30	223	3336.0 N 925.0 W	3
V30	224	3336.0 N 933.0 W	3
V30	225	3346.0 N 925.0 W	3
V30	226	3346.0 N 924.0 W	3
V30	228	3151.0 N 1226.0 W	3
V30	229	3108.0 N 1138.0 W	3
V30	230	3108.0 N 1138.0 W	3
V30	231	3018.0 N 1052.0 W	3
V30	232	2913.0 N 2218.0 W	3
V30	233	2527.0 N 2029.0 W	3
V30	234	2600.0 N 1943.0 W	3
V30	235	2529.0 N 1710.0 W	3
V30	236	2519.0 N 1659.0 W	3
V30	237	2509.0 N 1720.0 W	3
V30	238	2453.0 N 1712.0 W	3
V30	239	2334.0 N 2004.0 W	3
V30	241	2324.0 N 1938.0 W	3
V30	242	2321.0 N 1928.0 W	3
V30	243	2134.0 N 2210.0 W	3
V30	244	1844.0 N 1636.0 W	3
V30	245	1632.0 N 1718.0 W	3
V30	246	1629.0 N 1719.0 W	3
V31	1	1413.0 N 1901.0 W	3
V31	2	919.3 N 2411.6 W	3
ML1	46	5955.9 N 848.0 W	7
DSDP	1	2551.5 N 9211.0 W	3
DSDP	2	2327.3 N 9235.2 W	3
DSDP	3	2301.0 N 9201.4 W	3
DSDP	4,A	2428.68N 7347.52W	3
DSDP	5,A	2443.59N 7338.46W	3
DSDP	6,A	3050.39N 6738.86W	3
DSDP	7,A	3008.04N 6817.8 W	3
DSDP	8,A	3523.0 N 6733.2 W	3
DSDP	9	3246.4 N 5911.7 W	3
DSDP	10	3237.0 N 5219.92W	3
DSDP	11,A	2956.58N 4444.8 W	3
DSDP	12B,C,D	1941.73N 2600.03W	3
DSDP	13,A	0602.4 N 1813.71W	3
DSDP	26,A	1053.55N 4402.57W	3
DSDP	27,A	1551.59N 5652.76W	3
DSDP	28	2035.19N 6537.33W	3
DSDP	29,A,B,C	1447.11N 6919.36W	3
DSDP	30	1252.92N 6223.0 W	3
DSDP	31	1456.6 N 7201.63W	3
DSDP	85,A	2250.49N 9125.37W	3
DSDP	86	2252.48N 9057.75W	3
DSDP	87	2300.9 N 9205.16W	3
DSDP	88	2122.93N 9400.21W	3

DSDP	89	2053.41N 9506.73W	3
DSDP	90	2347.8 N 9446.09W	3
DSDP	91	2346.4 N 9320.77W	3
DSDP	92	2550.69N 9149.29W	3
DSDP	93	2237.25N 9128.78W	3
DSDP	94	2431.64N 8828.16W	3
DSDP	95	2409.0 N 8623.85W	3
DSDP	96	2344.56N 8545.8 W	3
DSDP	97	2553.05N 8426.74W	3
DSDP	98	2522.95N 7718.68W	3
DSDP	99,A	2341.14N 7750.99W	3
DSDP	100	2441.28N 7347.95W	3
DSDP	101,A	2511.93N 7426.31W	3
DSDP	102	3043.93N 7427.14W	3
DSDP	103	3027.08N 7434.99W	3
DSDP	104	3049.65N 7419.64W	3
DSDP	105	3453.72N 6910.4 W	3
DSDP	106,A	3626.01N 6927.69W	3
DSDP	106B	3625.28N 6925.81W	3
DSDP	107	3839.59N 7228.52W	3
DSDP	108	3848.27N 7239.21W	3
DSDP	111	5025.57N 4622.05W	3
DSDP	112	5401.0 N 4636.24W	3
DSDP	113	5647.4 N 4818.91W	3
DSDP	121	3609.65N 0422.43W	3
DSDP	122	4026.87N 0237.46E	7
DSDP	123	4037.83N 0250.27E	7
DSDP	124	3852.38N 0459.69E	7
DSDP	125,A	3437.49N 2025.76E	7
DSDP	126,A	3509.72N 2125.63E	7
DSDP	127,A,B	3543.9 N 2229.81E	7
DSDP	128	3542.58N 2228.10E	7
DSDP	129,A,B	3420.96N 2704.92E	7
DSDP	130,A	3336.31N 2751.99E	7
DSDP	131,A	3306.39N 2830.69E	7
DSDP	132A	4015.7 N 1126.47E	7
DSDP	133	3911.99N 0720.13E	7
DSDP	134,A-C	3911.7 N 0718.25E	7
DSDP	138	2555.37N 2533.79W	3
DSDP	139	2331.14N 1842.26W	3
DSDP	140,A	2144.97N 2147.52W	3
DSDP	141	1925.16N 2359.91W	3
DSDP	142	032215 N 4223.49W	3
DSDP	143,A-D	0928.45N 5418.71W	3
DSDP	144,A,B	0927.23N 5420.52W	3
DSDP	145	1634.74N 6803.37W	3
DSDP	146	1506.99N 6922.67W	3
DSDP	146A	1506.99N 6922.74W	3
DSDP	147	1042.48N 6510.48W	3
DSDP	147A,B	1042.68N 6543.45W	3
DSDP	148	1325.12N 6343.25W	3
DSDP	149	1506.25N 6921.85W	3

DSDP	150,A	1430.69N 6921.35W	3
DSDP	151,A	1501.02N 7324.58W	3
DSDP	152	1552.72N 7436.47W	3
DSDP	153	1358.33N 7226.08W	3
DSDP	154	1105.11N 8022.75W	3
DSDP	154A	1105.07N 8022.82W	3
DSDP	336	6321.06N 0747.27W	3
DSDP	337	6452.3 N 0521.51W	3
DSDP	338	6747.11N 0523.26E	7
DSDP	339	6712.65N 0617.05E	7
DSDP	340	6712.47N 0618.38E	7
DSDP	341	6720.1 N 0606.64E	7
DSDP	342	6757.04N 0456.02E	7
DSDP	343	6842.91N 0545.73E	7
DSDP	344	7609.98N 0752.52E	7
DSDP	345	6950.23N 0114.26W	3
DSDP	346	6953.35N 0841.14W	3
DSDP	347	6952.31N 0841.8 W	3
DSDP	348	6830.18N 1227.72W	3
DSDP	349	6912.41N 0805.8 W	3
DSDP	350	6703.34N 0817.18W	3
DSDP	351	6747.34N 1118.26W	3
DSDP	352,A	6338.97N 1228.26W	3
DSDP	353	1054.9 N 4402.25W	3
DSDP	353A	1055.39N 4402.21W	3
DSDP	353B	1055.49N 4402.29W	3
DSDP	354	0553.95N 4411.78W	3
DSDP	366,A	0540.7 N 1951.1 W	3
DSDP	367	1229.2 N 2002.8 W	3
DSDP	368	1730.4 N 2121.2 W	3
DSDP	369	2635.5 N 1459.0 W	3
DSDP	382	3425.04N 5632.25W	3
DSDP	383	3914.88N 5321.18W	3
DSDP	384	4021.65N 5139.8 W	3
DSDP	385	3722.17N 6009.45W	3
DSDP	386	3111.21N 6414.94W	3
DSDP	387	3219.2 N 6740.0 W	3
DSDP	395,A	2245.35N 4604.9 W	3
DSDP	396	2258.88N 4330.95W	3
DSDP	396A,B	2259.14N 4330.9 W	3
DSDP	397	2650.7 N 1510.8 W	3
DSDP	398	4057.6 N 1043.1 W	3
DSDP	401	4725.65N 0848.68W	3
DSDP	402,A	4752.48N 0850.44W	3
DSDP	403	5608.31N 2317.64W	3
DSDP	404	5603.13N 2314.95W	3
DSDP	405	5520.18N 2203.49W	3
DSDP	406	5515.5 N 2205.41W	3
DSDP	407	6356.32N 3034.56W	3
DSDP	408	6322.63N 2854.71W	3
DSDP	409	6236.98N 2557.17W	3
DSDP	414	3203.0 N 2730.1 W	3

DSDP 415,A	3101.72N 1139.11W	3
DSDP 416,A	3250.18N 1048.06W	3
DSDP 417,A-D	2506.63N 6802.48W	3
DSDP 418,A,B	2502.1 N 6803.44W	3
D10298	3624.7 N 1820.0 W	3
D10302	3420.0 N 2131.2 W	3
D10305	3144.97N 2949.13W	3
D10307	3012.8 N 2911.5 W	3
D10311	2539.2 N 3057.6 W	3
D10314	2538.3 N 3057.3 W	3
D10316	2613.2 N 2659.9 W	3
D10320	3105.2 N 2550.0 W	3
D10321	3104.8 N 2549.3 W	3
D10323	3021.7 N 2406.8 W	3
D10325	3022.9 N 2405.8 W	3
D10330	3649.0 N 2018.8 W	3
D10331	3708.0 N 2005.0 W	3
D10333	4107.3 N 2257.1 W	7
NL82PCS01	4205.9 N 2331.0 W	7
NL82PCS02	4133.1 N 2331.0 W	3
NL82PCS04	4140.0 N 2331.0 W	7
NL82PCS10	3209.1 N 2327.5 W	3
NL82PCS11	3156.5 N 2512.7 W	3
NL82PCM12	3136.6 N 2512.2 W	3
NL82PCS13	3109.5 N 2536.2 W	3
NL82PCL14	3110.0 N 2535.7 W	3

Positions of the camera stations examined.

D9128	6	2410.5	N03027.1	W	3
D9129	1	2305.7	N02758.7	W	7
D9131	9	2018.3	N02143.4	W	3
D9131	10	2015.1	N02135.5	W	7
D9131	11	2009.0	N02140.0	W	7
D9131	12	2007.0	N02126.0	W	7
D9134	0	2154.6	N01802.8	W	3
D9753	7	5054.5	N01210.9	W	3
D9754	3	5108.4	N01201.5	W	3
D9756	9	4947.1	N01401.5	W	7
D9756	14	5004.0	N01355.6	W	7
D9775	3	5056.8	N01222.4	W	3
D9779	1	4922.3	N01249.1	W	3
D10153	1	2906.3	N01229.0	W	3
D10138		2430.0	N01821.2	W	3
D10134		2423.7	N01757.4	W	3
D10113		5016.1	N01331.9	W	7
D10114		4945.3	N01408.1	W	7
C50304		5612.0	N01200.0	W	7
C50603		4943.3	N01401.0	W	7
C50605		5011.4	N01330.7	W	3
D10328		3025.0	N02405.0	W	7
D4526		4509	N02518	W	3
D4522		4543	N02746.5	W	3
D4521		4551	N02738	W	3
D4518		4544	N02730	W	3
D4286		4330.5	N01237.5	W	3
D4283		4331.5	N01236.1	W	3
D4277		4114.5	N01042	W	7
D4275		4330.5	N01238	W	3
D4263		4810	N00731	W	3
D3770		4117	N01423	W	3
D3723		4716.5	N00732	W	3
D3734		4122	N01424	W	3
D3737		4100	N01508	W	3
D3739		4120	N01429	W	3
D3743		4120	N01430	W	7
D3755		4112	N01514	W	3
D3757		4114	N01512.5	W	3
D3763		4240	N01135	W	7
D3766		4241	N01134	W	3
D3770		4118	N01423.5	W	3
D3467		4911	N00544	W	3
D3461		3636	N01713	W	3
D3456		3451	N01636	W	3
D3455		3453	N01632	W	3
D3452		3452	N01631	W	3
D3434		3445	N02552	W	3
D3433		3748	N02556.5	W	3
D3431		4024	N02627	W	3
D3430		4253	N02645	W	3
D3425		4634	N02714	W	3

D3430	4711	N02719	W	7
V4 19	3500	N01257	W	3
V4 18	3510	N01255	W	3
V4 16	3507	N01304	W	3
V4 14	3512	N01522	W	3
V4 13	3510.5	N01528	W	3
V4 12	3522.2	N01518	W	3
V4 11	3511	N01520.5	W	3
V4 10	3729	N02422	W	3
V4 9	3755	N02558	W	3
V4 8	3820	N02801	W	7
V4 7	3725	N03110	W	3
V4 6	3725	N03320	W	3
V4 5	3720	N03325	W	3
D5955	4235.8	N01157.1	W	7
D5945	4504.3	N00800.2	W	7
D5941	4519.0	N00523.2	W	7
D5938	4431.0	N00537.0	W	3
D5678	4739	N00804	W	7
D5676	4740.5	N00813	W	7
D5675	4740.5	N00807.5	W	7
D5639	4243.5	N02014.5	W	3
D5629	4250.5	N01956.0	W	7
D5616	4253.5	N02016.0	W	3
D5609	4254	N02016	W	3
HHP 24	4838	N02848	W	3
HHP 30	4515	N02855	W	7
HHP 32	2529	N01925	W	7
HHP 34	3408	N01254	W	3
HHP 38	4531	N02759	W	3
HHP 41	3500	N01257	W	3
HHP 57	4742	N00734	W	7
HHP 58	3400	N03009	W	3
HHP 59	3905	N06102	W	3
HHP 65	3755	N02558	W	3
HHP 67	2808	N01410	W	3
HHP 70	1214	N04548	W	3
HHP 80	4836	N02217	W	3
HHP 97	3206	N03041	W	3
HHP103	3511	N01528	W	3
HHP110	2807	N01409	W	3
HHP119	4829	N01419	W	3
HHP124	2807	N01409	W	3
HHP131	4836	N02217	W	3
HHP135	3051	N04429	W	3
HHP146	3512	N01522	W	3
HHP151	3820	N02807	W	3
HHP155	4542	N02038	W	3
HHP159	3437	N02805	W	3
HHP160	3237	N01706	W	3
HHP203	4829	N01419	W	3
HHP210	2807	N01409	W	3

HHP212	3729	N02422	W	3
HHP215	2807	N01402	W	3
HHP218	3720	N03315	W	3
HHP220	3112	N01340	W	3
HHP229	2515	N02545	W	3
HHP237	4821	N01735	W	3
HHP352	4650	N02858	W	3
HHP353	3507	N01304	W	7
HHP387	3636	N01010	W	3
HHP388	3615	N00746	W	3
HHP389	3558	N00657	W	3
HHP501	1525	N02154	W	3
HHP509	3507	N01304	W	3
HHP511	3112	N01340	W	3
HHP512	3510	N01255	W	3
HHP523	3408	N03012	W	3
HHP538	3200	N04000	W	3
HHP557	4512	N02759	W	3
HHP559	4520	N02802	W	3
HHP561	1045	N04030	W	3
HHP564	4650	N02858	W	3
HHP565	4529	N02832	W	3
HHP566	4836	N02217	W	3
HHP567	4542	N02038	W	3
HHP581	2639	N02008	W	3
RC9 197	4506.0	N01035.0	W	3
RC9 196	4452.0	N01051.0	W	3
RC9 195	4333.0	N01024.0	W	3
RC9 194	4239.0	N01109.0	W	7
RC9 187	4208.0	N01432.0	W	7
V27 70	4433.0	N01457.0	W	3
V27 71	4458.0	N01207.0	W	3
V27 72	4511.0	N00937.0	W	3
V27 74	4358.0	N01549.0	W	3
V27 69	4348.0	N01441.0	W	3
V30 129	4101.0	N01804.0	W	3
V30 172	2913.0	N02218.0	W	7
V30 57	3258.0	N02908.0	W	3
V30 132	3825.0	N01129.0	W	3
V30 70	3511.0	N03607.0	W	3
V30 54	3408.0	N02219.0	W	7
V30 136	3507.0	N01635.0	W	7
V30 135	3521.0	N01707.0	W	7
V23 66	3404.0	N01944.0	W	3
V27 101	3412.0	N01652.0	W	3
V23 72	3027.0	N02325.0	W	3
V23 71	3001.0	N02814.0	W	3
V23 70	2935.0	N02834.0	W	3
V23 69	2952.0	N02501.0	W	3
V23 68	2953.0	N02407.0	W	7
V30 58	3336.0	N03129.0	W	3
V32 10	3411.0	N03058.0	W	3

V4	29	3315.0	NO2932.0 W	3
V4	28	3308.0	NO2848.0 W	3
V4	27	3651.0	NO1418.0 W	3
V29	92	3618.0	NO2922.0 W	3
D10299		3625.4	NO1820.5 W	7
D10319		3115.6	NO2543.3 W	3
D10312		2542.0	NO3057.0 W	7
S126/6		3109.9	NO2348.5 W	7
S126/9		3050.0	NO2253.0 W	3
D10656		4152.5	NO2350.0 W	7
D10664		4129.0	NO2314.4 W	7
D10669		4203.0	NO2353.0 W	7
D10678		3123.8	NO2334.6 W	3
D10689		3239.5	NO2421.0 W	7
D10693		3139.9	NO2448.3 W	3